Determining the Effective PG Grade of Binder in RAP Mixes

Jo Sias Daniel, PI
Walaa S. Mogawer, co-PI

Prepared for
The New England Transportation Consortium
January 2010
NETCR78 **Project No. 04-4**

This report, prepared in cooperation with the New England Transportation Consortium, does not constitute a standard, specification, or regulation. The contents of this report reflect the views of the authors who are responsible for the facts and the accuracy of the data presented herein. The contents do not necessarily reflect the views of the New England Transportation Consortium or the Federal Highway Administration.

ACKNOWLEDGEMENTS

The following are the members of the Technical Committee that developed the scope of work for the project and provided technical oversight throughout the course of the research:

Denis Boisvert, New Hampshire Department of Transportation, Chairperson
Michael Byrne, Rhode Island Department of Transportation
Stephen Cooper, Federal Highway Administration, CT Division
Raffaele Donato, Connecticut Department of Transportation
Alan Lugg, New Hampshire Department of Transportation
Ed Mirka, Massachusetts Department of Transportation
Nelio Rodrigues, Connecticut Department of Transportation
Merlin Williams, Maine Department of Transportation

The research team would also like to acknowledge Tilcon Industries, Hudson Industries, Citgo, and Pike Industries, Inc. for material donations used in this research project. UNH students and interns Steven Hall, Aravind Krishna Swamy, and Carlos Acosta are acknowledged for their efforts in this research project.

Technical Report Documentation Page

1. Report No. NETCR78	2. Government Accession No. N/A	3. Recipient's Catalog No. N/A
4. Title and Subtitle Determining the Effective PG Grade of Binder in RAP Mixes		5. Report Date January 4, 2010 6. Performing Organization Code N/A
7. Author(s) Jo Sias Daniel Walaa S. Mogawer		8. Performing Organization Report No. NETCR78
9. Performing Organization Name and Address University of New Hampshire Department of Civil Engineering Kingsbury Hall 33 Academic Way Durham, NH 03824		10 Work Unit No. (TRAIS) N/A 11. Contract or Grant No. N/A
12. Sponsoring Agency Name and Address New England Transportation Consortium C/O Advanced Technology & Manufacturing Center University of Massachusetts Dartmouth 151 Martine Street Fall River, MA 02723		13. Type of Report and Period Covered Final Report 14. Sponsoring Agency Code NETC 04-4 A study conducted in cooperation with the U.S. DOT
15 Supplementary Notes N/A		

16. Abstract

This report presents the results of a research study to develop a method to determine or estimate the binder grade in mixtures designed with RAP from the properties of the mixture itself. A 12.5 mm Superpave mixture was used to evaluate mixtures containing 0% RAP, 10% RAP , 25% RAP, and 40% RAP with a virgin PG 64-28 binder. Virgin mixtures with PG 58-28, PG 70-22, and PG 76-22 binders were also evaluated. Testing included dynamic modulus, creep compliance, and strength tests in the indirect tensile mode. Partial |G*| master curves were measured on the extracted binder from each mixture and the recovered binder was also PG graded. Several methods of estimating the effective PG grade of the binder were evaluated. Empirically based methods of interpolating values of measured mixture properties are straightforward, but require an extensive amount of testing in the laboratory. The relationship between material properties and PG grade must be established for each type of mixture (gradation, asphalt content). The most promising methods for determining the effective PG grade of the mixture use the Hirsch model to back calculate binder |G*| from the measured mixture dynamic modulus. This report summarizes the research effort and provides a recommended procedure for estimating the effective PG grade of binders in RAP mixtures.

17. Key Words RAP, Dynamic Modulus, binder grade	18. Distribution Statement No restrictions. This document is available to the public through the National Technical Information Service, Springfield, Virginia 22161.		
19. Security Classif. (of this report) Unclassified	20. Security Classif. (of this page) Unclassified	21. No. of Pages 98	22. Price N/A

Form DOT F 1700.7 (8-72) Reproduction of completed page authorized

SI* (MODERN METRIC) CONVERSION FACTORS

APPROXIMATE CONVERSIONS TO SI UNITS

Symbol	When You Know	Multiply By	To Find	Symbol
		LENGTH		
in	inches	25.4	millimetres	mm
ft	feet	0.305	metres	m
yd	yards	0.914	metres	m
mi	miles	1.61	kilometres	km
		AREA		
in^2	square inches	645.2	millimetres squared	mm^2
ft^2	square feet	0.093	metres squared	m^2
yd^2	square yards	0.836	metres squared	m^2
ac	acres	0.405	hectares	ha
mi^2	square miles	2.59	kilometres squared	km^2
		VOLUME		
fl oz	fluid ounces	29.57	mililitres	mL
gal	gallons	3.785	Litres	L
ft^3	cubic feet	0.028	metres cubed	m^3
yd^3	cubic yards	0.765	metres cubed	m^3

NOTE: Volumes greater than 1000 L shall be shown in m^3

		MASS		
oz	ounces	28.35	grams	g
lb	pounds	0.454	kilograms	kg
T	short tons (2000 lb)	0.907	megagrams	Mg
		TEMPERATURE (exact)		
°F	Fahrenheit temperature	5(F-32)/9	Celcius temperature	°C

* SI is the symbol for the International System of Measurement

APPROXIMATE CONVERSIONS TO SI UNITS

Symbol	When You Know	Multiply By	To Find	Symbol
		LENGTH		
mm	millimetres	0.039	inches	in
m	metres	3.28	feet	ft
m	metres	1.09	yards	yd
km	kilometres	0.621	miles	mi
		AREA		
mm^2	millimetres squared	0.0016	square inches	in^2
m^2	metres squared	10.764	square feet	ft^2
ha	hectares	2.47	acres	ac
km^2	kilometres squared	0.386	square miles	mi^2
		VOLUME		
mL	millilitres	0.034	fluid ounces	fl oz
L	litres	0.264	gallons	gal
m^3	metres cubed	35.315	cubic feet	ft^3
m^3	metres cubed	1.308	cubic yards	yd^3
		MASS		
g	grams	0.035	ounces	oz
kg	kilograms	2.205	pounds	lb
Mg	megagrams	1.102	short tons (2000 lb)	T
		TEMPERATURE (exact)		
°C	Celcius temperature	1.8C+32	Fahrenheit temperature	°F

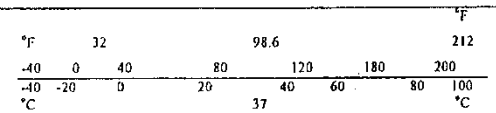

ABSTRACT

This report presents the results of a research study to develop a method to determine or estimate the binder grade in mixtures designed with RAP from the properties of the mixture itself. A 12.5 mm Superpave mixture was used to evaluate mixtures containing 0% RAP, 10% RAP , 25% RAP, and 40% RAP with a virgin PG 64-28 binder. Virgin mixtures with PG 58-28, PG 70-22, and PG 76-22 binders were also evaluated. Testing included dynamic modulus, creep compliance, and strength tests in the indirect tensile mode. Partial |G*| master curves were measured on the extracted binder from each mixture and the recovered binder was also PG graded. Several methods of estimating the effective PG grade of the binder were evaluated. Empirically based methods of interpolating values of measured mixture properties are straightforward, but require an extensive amount of testing in the laboratory. The relationship between material properties and PG grade must be established for each type of mixture (gradation, asphalt content). The most promising methods for determining the effective PG grade of the mixture use the Hirsch model to back calculate binder |G*| from the measured mixture dynamic modulus. This report summarizes the research effort and provides a recommended procedure for estimating the effective PG grade of binders in RAP mixtures.

TABLE OF CONTENTS

1.0 Introduction……. 1

1.1 Research Objective…… 1

1.2 Literature Review…….. 1

1.3 Report Organization…….. 3

2.0 Materials and Testing Program…… 4

2.1 Materials…… 4

2.1.1 Virgin Aggregates…… 4

2.1.2 Asphalt Binder……. 4

2.1.3 Reclaimed Asphalt Pavement (RAP)……... 4

2.1.4 Field Cores……... 5

2.2 Mix Designs…….. 5

2.3 Specimen Fabrication…… 7

2.4 Testing Setup and Equipment……... 9

2.5 Specimen Instrumentation……. 11

2.6 Dynamic Modulus Testing……. 14

2.7 Hirsch Model……. 17

2.8 Creep Compliance Testing……. 17

2.9 Indirect Tensile Strength Testing……... 19

3.0 Results…….. 21

3.1 Dynamic Modulus…….. 21

3.1.1 RAP Mixtures…… 21

3.1.2 Different PG Binder Grades……. 24

3.2 Binder Modulus…….. 27

3.2.1 RAP Mixtures…… 27

3.2.2 Different PG Binder Grades…….. 31

3.3 Creep Compliance…….. 34

3.4 Indirect Tensile…….. 37

4.0 Estimating Effective PG Grade…… 41

4.1 High Temperature Grade…… 41

4.1.1 Linear Blending Prediction……... 41
4.1.2 Empirical Method Using Measured Mixture Properties……... 41
4.1.3 Method Using the Hirsch Model…….. 43
4.2 Low Temperature Grade…… 47
4.2.1 Linear Blending Prediction……... 47
4.2.2 Empirical Method Using Measured Mixture Properties……... 47
4.2.3 Method Using the Hirsch Model…….. 48
4.2.4 Method Using Creep Compliance……. 49
5.0 Summary and Recommendations……. 54
5.1 Summary…… 54
5.2 Recommended Procedure for Estimating PG Grade……. 54
5.3 Recommendations for Further Research…… 55
6.0 References…… 56
7.0 Appendices……... 58
Appendix A: Mixture Designs……. 58
Appendix B: Dynamic Modulus Data……. 66
Appendix C: Strength Data…….. 74

LIST OF TABLES

Table 2.1 Virgin Aggregate Gradations……... 4
Table 2.2 Extracted RAP Aggregate Gradation…….. 5
Table 2.3 Mixture Gradations…….. 6
Table 2.4 Mix Design Summary…….. 7
Table 2.5 Specimen Volumetrics……. 8
Table 3.1 Dynamic Modulus T-Test Results for RAP Mixtures……. 24
Table 3.2 Dynamic Modulus T-Test Results for PG Mixtures…… 27
Table 3.3 Binder Modulus T-Test Results for RAP Mixtures……. 31
Table 3.4 Extracted PG Grade of RAP Mixtures…… 31
Table 3.5 Binder Modulus T-Test Results for PG Mixtures……... 34
Table 3.6 Summary of Indirect Tensile Strengths…….. 38
Table 3.7 IDT T-Test Results for RAP Mixtures…… 40
Table 3.8 IDT T-Test Results for PG Mixtures……... 40
Table 4.1 Estimated High PG Grade Using Linear Blending…….. 41
Table 4.2 Estimated Effective High PG Binder Grades from Empirical Analysis…….. 42
Table 4.3 Estimated High PG Grade Using Hirsch Model……. 46
Table 4.4 Estimated Low PG Grade Using Linear Blending…….. 47
Table 4.5 Estimated Effective Low PG Binder Grades from Empirical Analysis…….. 48
Table 4.6 Estimated Low PG Grade Using Hirsch Model…….. 48
Table 4.7 Power Law Coefficients for Binder-Mixture Stiffness Relationships……. 50
Table 4.8 S-values and m-values Determined from Binder Stiffness Curves……. 51
Table 4.9 Estimated Low PG Grade from m-value……. 53

LIST OF FIGURES

Figure 2.1 Mixture Gradation Curves…… 6

Figure 2.2 Compacted SGC Specimen Marked for Cutting…….. 9

Figure 2.3 ITC IDT Load Fixture in Environmental Chamber……. 10

Figure 2.4 Environmental Chamber…….. 10

Figure 2.5 Brass Gluing Jig……... 11

Figure 2.6 Brackets prepared for gluing…… 11

Figure 2.7 L Brackets and Rod…….. 12

Figure 2.8 Brackets and Brass Targets Curing…….. 13

Figure 2.9 LVDT's Mounted onto a Specimen…….. 13

Figure 2.10 Instrumented Specimen Ready for Testing…….. 14

Figure 2.11 Typical Dynamic Modulus Data…….. 15

Figure 2.12 Typical Dynamic Modulus Master Curve…… 16

Figure 2.13 Typical Shift Factors…… 16

Figure 2.14 Creep Compliance Curves at Individual Temperatures……... 18

Figure 2.15 Creep Compliance Master Curve……. 19

Figure 2.16 Typical Strength Loading Curve…….. 20

Figure 3.1 Control Mixture Dynamic Modulus Master Curve…….. 21

Figure 3.2 10% RAP Mixture Dynamic Modulus Master Curve…….. 22

Figure 3.3 25% RAP Mixture Dynamic Modulus Master Curve…….. 22

Figure 3.4 40% RAP Mixture Dynamic Modulus Master Curve…….. 23

Figure 3.5 Average Dynamic Modulus Master Curves……. 23

Figure 3.6 PG 58-28 Mixture Dynamic Modulus Master Curve……... 25

Figure 3.7 PG 70-22 Mixture Dynamic Modulus Master Curve……... 25

Figure 3.8 PG 76-22 Mixture Dynamic Modulus Master Curve……... 26

Figure 3.9 Average PG Mixture Dynamic Modulus Master Curves……. 26

Figure 3.10 Control Mixture Binder Modulus Curves…… 28

Figure 3.11 10% RAP Mixture Binder Modulus Curves…… 28

Figure 3.12 25% RAP Mixture Binder Modulus Curves…… 29

Figure 3.13 40% RAP Mixture Binder Modulus Curves…… 29
Figure 3.14 Average Binder Modulus Curves for All RAP Mixtures……. 30
Figure 3.15 Recovered Binder Modulus Curves for All RAP Mixtures……. 30
Figure 3.16 PG 58-28 Mixture Binder Modulus Curves……. 32
Figure 3.17 PG 70-22 Mixture Binder Modulus Curves……. 32
Figure 3.18 PG 76-22 Mixture Binder Modulus Curves……. 33
Figure 3.19 Average PG Mixture Binder Modulus Curves……. 33
Figure 3.20 Control Mixture Creep Compliance Master Curve…….. 34
Figure 3.21 10% RAP Mixture Creep Compliance Master Curve…….. 35
Figure 3.22 25% RAP Mixture Creep Compliance Master Curve…….. 35
Figure 3.23 40% RAP Mixture Creep Compliance Master Curve…….. 36
Figure 3.24 Average Mixture Creep Compliance Master Curves……... 36
Figure 3.25 Indirect Tensile Strengths for RAP Mixtures……... 39
Figure 3.26 Indirect Tensile Strengths for PG Mixtures by High Grade……. 39
Figure 3.27 Indirect Tensile Strengths for PG Mixtures by Low Grade……. 40
Figure 4.1 Relationship Between High Temperature PG Grade and IDT Strength…….. 42
Figure 4.2 Percent Difference in G* values for 10% RAP Mixture…….. 43
Figure 4.3 Percent Difference in G* values for 25% RAP Mixture…….. 44
Figure 4.4 Percent Difference in G* values for 40% RAP Mixture…….. 44
Figure 4.5 Comparison of 10% RAP Mixture with PG Mixtures……. 45
Figure 4.6 Comparison of 25% RAP Mixture with PG Mixtures……. 45
Figure 4.7 Comparison of 40% RAP Mixture with PG Mixtures……. 46
Figure 4.8 Relationship Between Low Temperature PG Grade and IDT Strength……... 48
Figure 4.9 Typical Creep Stiffness Curve……. 49
Figure 4.10 Binder-Mixture Stiffness Relationships Using Hirsch Model……. 50
Figure 4.11 Determination of S-value and m-value…… 51
Figure 4.12 Calculated S-values for RAP Mixtures…… 52
Figure 4.13 Calculated m-values for RAP Mixtures……... 52

1.0 INTRODUCTION

Use of reclaimed asphalt pavement (RAP) material in Hot Mix Asphalt (HMA) has become common in the New England region, and in many areas across the country. RAP material is generated when old, damaged pavement materials are milled and crushed for addition as a component to new mixtures placed in the pavement structure. RAP utilization is an efficient use of resources for local, state and federal transportation agencies as the RAP provides quality materials in the HMA mixture. As the cost of virgin materials, particularly asphalt cement, increases, the paving industry is looking to increase the amount of RAP that is used in HMA. The Federal Highway Administration (FHWA) has developed an Expert Task Group on RAP; the charge of this group is to coordinate, develop, and improve national guidance and recommendations for the FHWA asphalt pavement recycling program (1).

The addition of RAP to an asphalt mixture changes the mechanistic properties (i.e., strength) of the mixture and affects its performance (i.e., resistance to cracking and deformation) in the field. The mechanistic properties change as a result of the aged binder introduced to the mixture as part of the RAP. The binder in the RAP will have a different chemical composition and different properties than the virgin binder added during the mixing process. Various studies (2-8) have shown that these two binders will mix to some extent, changing the properties of the mixture containing RAP from one that contains only virgin material. The actual extent of the blending is unknown and may be different for various RAP sources and virgin binders. The actual, or effective, properties of the binder in mixtures containing RAP cannot be tested directly, as the process of extracting the binder for testing results in complete blending of the virgin and RAP binder. Therefore, testing must be performed on the mixtures to determine the effective binder properties.

1.1 Research Objective

The objective of this research project is to develop a method to determine or estimate the binder grade in mixtures designed with RAP from the properties of the mixture itself.

1.2 Literature Review

The earliest noted use of RAP was in Texas in 1915 (9). It wasn't until the 1970's that many agencies began using RAP more often for projects. Several factors may have contributed to the increased use of RAP, including the rise of environmental awareness in the US as well as increased costs associated with crude oil. A study published by the National Cooperative Highway Research Program Synthesis of Highway Practice noted that in 1978, 41 states were recycling asphalt pavement to some degree (9).

Recycling asphalt has rapidly gained popularity with state agencies for many reasons, including the high price of crude oil and subsequent cost of asphalt cement (ac). Another reason that RAP is gaining popularity is the ability to recycle quality aggregate, especially in locations where there is a shortage of virgin aggregate. The US produces 2 billion tons of aggregate annually and is expected to increase to 2.5 billion tons by 2020 (10). Additionally, the environmental benefits of recycling are well known; less material in landfills and reduced mining impact to name several. A goal of pavement engineers is to close the material loop, and build structurally sound roadways that are 100% recycled (10).

Recent research has focused on determining the amount of blending that occurs between the aged asphalt that is part of the RAP (RAP binder) and the virgin binder and how much of an impact the RAP binder has on the PG grade of the final product. Originally, there were two basic theories: 1) that the RAP acts as a black rock and no blending of the RAP binder and the virgin binder occurs, and 2) that total blending of the RAP binder and virgin binder takes place. Studies conducted to date have been mostly inconclusive regarding the extent of blending that takes place and this has led to discussion on the use of blending charts. NCHRP 9-12 was a major nationally supported study led by Dr. Rebecca McDaniel and conducted at the North Central Superpave Center at Purdue University. The research team investigated several aspects regarding RAP and Superpave design guidelines. Some of the issues examined included the effects of the RAP binder from the RAP on the PG grading, how much blending occurs with virgin binder, and the effects on volumetrics and performance of the aggregate in the RAP. The study used RAP sources from Arizona, Connecticut, and Florida. This study found that RAP acts neither as a 'black rock', nor does total blending occur. The extent to how much blending occurs though is still unknown. Results of the NCHRP study supports a tiered approach to RAP usage since at higher RAP percentages, the RAP binder has a greater effect. The research also demonstrated that at higher RAP contents, the mixture stiffens. This can affect the choice of virgin binder used in mix designs. A softer virgin binder will be needed at higher RAP contents to correct for the stiffer, aged RAP binder (5).

Another major study that also investigated RAP binder properties was FHWA/IN/JRTP-2002/6 that continued the research began with the NCHRP 9-12 study. This study was also conducted at the North Central Superpave Center at Purdue University and led by Dr McDaniel. The goals were to widen the range of RAP sources used in the NCHRP study and to specifically look at materials in the north central US, investigate higher proportions of RAP, and to examine how the RAP affects mix properties (11). Findings showed that Superpave mixes could be designed with up to 50% RAP content. The study also concluded that linear blending charts as presented in NCHRP 9-12 are acceptable for most RAP sources. The study agreed with results from NCHRP 9-12 in that a tiered approach to RAP design is acceptable, and when adding 20-25% RAP to a mix, the high temperature grade increased one increment. Finally the study showed that using RAP stiffens a mix, adding increased rutting resistance.

A study conducted at the Ohio State University in conjunction with Ohio Department of Transportation looked at RAP contents based on expected mix durability. The study showed that in general, the addition of RAP, affects the stiffness of the mix and the binder. Higher RAP contents also led to higher results in all tests. The study also showed a decrease in phase angle as the amount of binder recovered from RAP increased when mixed with virgin binder. Another result found that the values for the complex shear modulus and the fatigue cracking factor increase as the amount of RAP binder increases (12).

A study conducted by the University of Minnesota funded by the Minnesota Department of Transportation looked at classifying RAP stockpiles in Minnesota and developing a design procedure to be used by the Minnesota DOT. One method used was complex modulus testing in Indirect Tension (IDT) mode. One of the results they found was excess noise when tested at frequencies above 5 Hz. This is most likely an instrumentation or equipment issue, at the University of New Hampshire the research team has achieved consistent results up to 20 Hz. Testing was also done to find the resilient modulus of the mixtures at various RAP contents. The study found that as RAP increased, the effect of the stiffer binder also led to increases in both the resilient and the complex modulus (13).

The Asphalt Pavement Association of Oregon performed a study that attempted to determine the asphalt content of RAP using volumetrics and specific gravity as opposed to traditional oven methods. This is very important with regards to determining the desired asphalt content of the mix. Unfortunately this study found that it was hard to consistently deliver accurate results and therefore should not be used in the field (14).

An article published in the North Central Superpave Center news discussed the importance of VMA in the mix design. One of the things the researchers determined was that aggregate fines help to improve durability in mixes by limiting permeability. Aggregate fines also help to increase rut resistance. Based on this, researchers suggest putting a minimum requirement for aggregate fines in a mix. It is proposed that there be a minimum VMA of 16% and a minimum VBE of 12% to help reduce rutting and to increase durability (15).

The University of New Hampshire research team has been examining the properties of RAP and how RAP affects mix properties through several ongoing and completed projects. The completed study (16) investigated the effects of RAP on the volumetric properties, as well as how the RAP changed the stiffness of the mixtures. RAP contents of 0%, 15%, 25%, and 40% were used and results show that 15% RAP increased stiffness and lowered creep compliance over the control mix. The higher levels of RAP had unexpected results. The results showed that the values of dynamic modulus and creep compliance were similar to the control mix. Some possible explanations are the higher VFA and VMA values which would soften the mix. This is under investigation in other projects.

1.3 Report Organization

This report is organized into seven sections. Chapter 1 presents the introduction and literature review, Chapter 2 presents materials and testing program, Chapter 3 contains the testing results, Chapter 4 discusses the estimation of the effective PG grade, and Chapter 5 presents a summary and recommendations from the project. The references are in Chapter 6 and the Appendices are in Chapter 7.

2.0 MATERIALS AND TESTING PROGRAM

This chapter presents the materials, testing equipment, and methods used for testing as well as data analysis methods.

2.1 Materials

2.1.1 Virgin Aggregates

Virgin aggregates used in this project were obtained from the Tilcon plant in Newington, Connecticut. The 12.5 mm and 9.5 mm coarse aggregate stockpiles were from the Newington, Connecticut quarry. The crushed stone sand was from the Tilcon quarry in Wallingford, Connecticut and the natural sand was from the Tilcon quarry in Manchester, Connecticut. The gradations for each stockpile are shown in Table 2.1.

Table 2.1 Virgin Aggregate Gradations

Sieve Size (mm)	Percent Passing			
	12.5 mm	9.5 mm	Stone Sand	Natural Sand
19 (3/4”)	100	100	100	100
12.5 (1/2”)	84.0	100	100	100
9.5 (3/8”)	31.0	91.0	100	100
4.75 (# 4)	1.4	17.0	99.0	97.0
2.36 (# 8)	0.8	2.2	76.0	91.0
1.18 (# 16)	0.8	1.9	47.0	84.0
0.600 (# 30)	0.7	1.8	30.0	62.0
0.300 (# 50)	0.7	1.7	20.0	28.0
0.150 (# 100)	0.6	1.5	14.0	8.0
0.075 (# 200)	0.5	1.0	6.0	2.8

2.1.2 Asphalt Binder

Several different binders were used in this project. The primary binder was a PG 64-28 obtained from the Pike Industries plant in Farmington, New Hampshire. The mixing range was 160-165 and the compaction range was 152-157 ^{o}C. A PG 58-28 obtained from the Pike plant in Farmington, a PG 70-22 obtained from Citgo, and a PG 76-22 binder obtained from Hudson Industries in Rhode Island were also used.

2.1.3 Reclaimed Asphalt Pavement (RAP)

The RAP for this project was obtained from the Tilcon aggregate plant in Newington, Connecticut. The RAP was processed by screening and crushing. The extracted PG grade of the

RAP binder was PG 100-4 and the RAP had an asphalt content of 4.85%. The extracted gradation of the RAP material is shown in Table 2.2.

Table 2.2 Extracted RAP Aggregate Gradation

Sieve Size (mm)	Percent Passing
19 (3/4”)	100
12.5 (1/2”)	98.0
9.5 (3/8”)	84.0
4.75 (# 4)	54.0
2.36 (# 8)	40.0
1.18 (# 16)	33.0
0.600 (# 30)	26.0
0.300 (# 50)	18.0
0.150 (# 100)	10.0
0.075 (# 200)	5.0

2.1.4 Field Cores

Field cores were taken from a paving project in Newington, Connecticut. These specimens were taken to represent a 100% RAP condition. The field cores were tested for strength at low temperatures. Due to issues in testing, the strength results for only two cores are available for analysis. The air void content of the field cores (Table 2.5) is significantly higher than the laboratory fabricated specimens, so the results cannot be directly compared.

2.2 Mix Designs

The Tilcon 12.5 mm Superpave mix design with 10% RAP used for the paving project in Newington, Connecticut was used as a starting point for this research project. From this point, the mix was modified to produce 0%, 25%, and a 40% RAP mixtures. When designing the new mixtures, the aggregate stockpile proportions were kept constant. The gradations for each mixture are shown in Table 2.3 and Figure 2.1

Table 2.3 Mixture Gradations

Sieve Size (mm)	Control	10%	25%	40%
25.0	100.0	100.0	100.0	100.0
19.0	100.0	100.0	100.0	100.0
12.5	94.1	94.5	95.2	95.7
9.5	72.9	74.3	75.9	77.5
4.75 (# 4)	48.8	49.9	50.6	51.3
2.36 (# 8)	36.4	37.3	37.7	38.1
1.18 (# 16)	24.1	25.4	26.7	27.8
0.600 (# 30)	16.0	17.3	18.8	20.1
0.300 (# 50)	10.1	11.1	12.2	13.4
0.150 (# 100)	6.6	7.0	7.5	8.0
0.075 (# 200)	3.0	3.2	3.5	3.8
pan	0.0	0.0	0.0	0.0

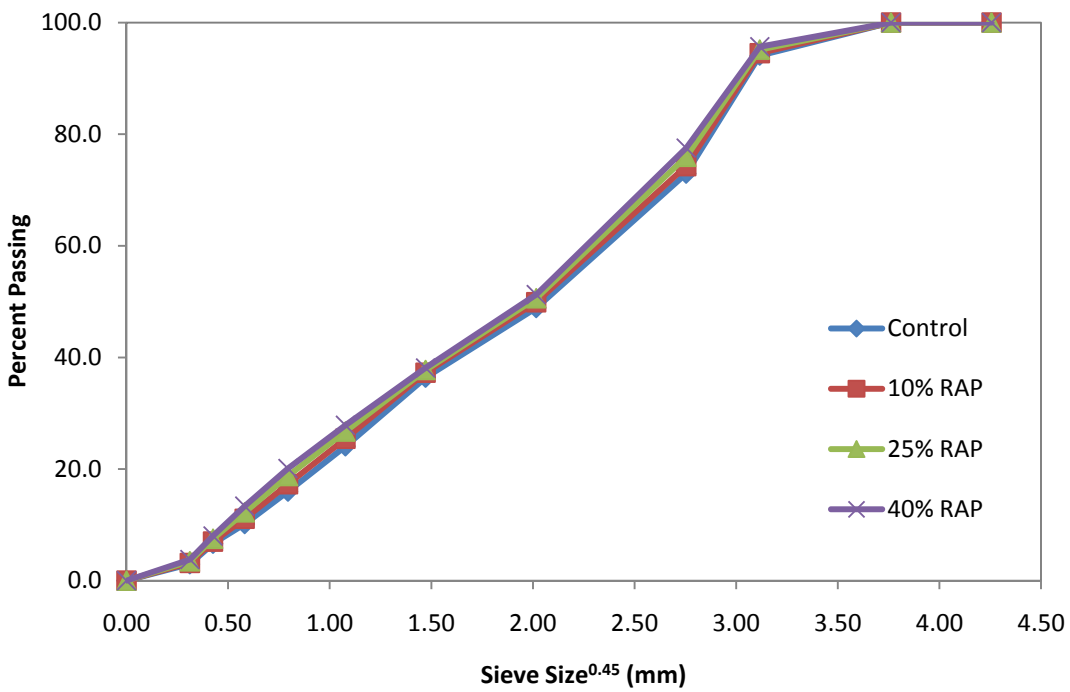

Figure 2.1 Mixture Gradation Curves

Table 2.4 shows a summary of the mix design parameters for each of the RAP contents. The design asphalt content decreased with the increased RAP percentages. The VMA remained fairly constant across all the RAP contents, while the VFA decreased.

Table 2.4 Mix Design Summary

	Asphalt Content	**VMA %**	**VFA %**
Criteria	N/A	13.0 min	65-78
Control Mix	6.0	17.4	77.0
10% RAP Mix	5.7	17.2	74.0
25% RAP Mix	5.3	16.3	75.9
40% RAP Mix	5.2	17.3	69.8

2.3 Specimen Fabrication

All virgin aggregate was sieved and stored in separate stockpiles by sieve size. The RAP was stored as a stockpile. Virgin aggregate for each specimen was batched by sieve size and heated overnight. The RAP was heated to mixing temperature for one hour and the asphalt binder was heated to mixing temperature. The aggregates, RAP, and binder were mixed using a bucket mixer and short term aged for two hours at the compaction temperature. The specimens were compacted using a Superpave Gyratory Compactor (SGC). After compaction, the cores were cooled and cut to testing dimensions (150 mm diameter, 38 mm thickness) using a diamond wet saw. Figure 2.2 shows an SGC specimen prior to cutting. The volumetric properties of all specimens were measured using a Corelok Vacuum Sealing system. Table 2.5 summarizes the air void content, VMA, and VFA values for the specimens tested in this study. All specimens fabricated in the laboratory were within the target air void range of 3.5% - 4.5%.

Table 2.5 Specimen Volumetrics

Mix Type	Sample Name	Air Voids (%)	Average % AV	VMA (%)	Average VMA	VFA (%)	Average VFA
Control	6000I	4.2	4.1	17.6	17.5	76.0	76.6
	6000J	3.6		17.1		78.6	
	6000K	4.4		17.7		75.3	
	6000L	4.2		17.6		76.0	
	6000M	4.0		17.4		77.0	
10% RAP	5710E	3.7	4.0	16.5	16.8	77.6	76.3
	5710F	4.2		17.0		75.0	
25% RAP	5325E	4.8	4.1	17.1	16.4	71.6	75.1
	5325F	3.6		16.0		77.4	
	5325G	4.0		16.3		75.6	
	5325I	3.9		16.3		75.8	
40% RAP	5240E	4.9	4.3	17.0	16.4	71.2	74.1
	5240F	3.6		15.9		77.1	
	5240G	4.5		16.6		73.1	
	5240H	4.2		16.4		74.3	
	5240I	4.1		16.3		74.9	
100% RAP	FC 3	5.6	5.6	n/a	n/a	n/a	n/a
	FC 5	5.7		n/a		n/a	
PG 58	6058A	4.0	4.3	16.4	16.7	75.6	74.0
	6058B	4.5		16.8		73.3	
	6058C	4.5		16.8		73.1	
	6058D	4.3		16.6		74.2	
PG 70	6070A	4.0	4.1	16.2	16.3	75.4	75.1
	6070B	3.8		16.0		76.6	
	6070C	3.8		16.1		76.2	
	6070D	4.6		16.8		72.4	
PG 76	6076A	3.9	3.9	16.1	16.2	76.0	75.9
	6076B	3.8		16.1		76.4	
	6076C	3.8		16.1		76.4	
	6076D	4.1		16.4		74.7	

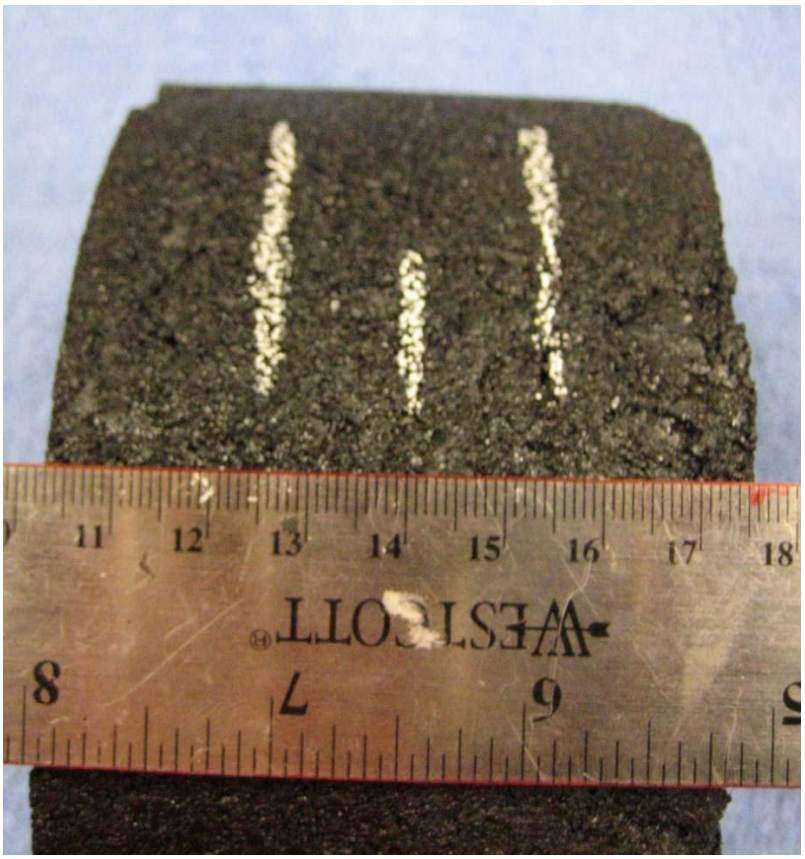

Figure 2.2 Compacted SGC Specimen Marked for Cutting

2.4 Testing Setup and Equipment

The strength and dynamic modulus testing performed in this study were conducted using a closed-loop servo-hydraulic system, manufactured by Instron ®. The testing apparatus included the loading frame (model 8800), a 20,000 pound hydraulic actuator (model IST 3690 Series 100kN Pedestal Mounted Actuator), a 5,000 pound load cell, a 20,000 pound load cell, control tower (model 8500) and control panel (model 8500 Plus), an environmental chamber (model 3119-407), testing specimen guide (Interlaken Technology Corporation (ITC), Indirect Tensile (IDT) Fixture), and personal computers running Instron's Fast Track 2 software (actuator control), LabVIEW 7.1 (data acquisition), Microsoft ® Excel and JMP (data and statistical analysis).

The ITC IDT load fixture was used to isolate the loading strips on the specimen. This allows for increased stability in the specimen and helps to minimize error induced by the specimen rocking. Figure 2.3 shows the load fixture installed in the environmental chamber.

Figure 2.3 ITC IDT Load Fixture in Environmental Chamber

The Envirotherm ® environmental chamber was used to set the testing environment desired using low pressure nitrogen. The chamber controlled the temperature within ± 0.1°C; the range of testing was between -10°C to 30°C. Figure 2.4 shows the environmental chamber with nitrogen hose in the lab.

Figure 2.4 Environmental Chamber

2.5 Specimen Instrumentation

Indirect tensile dynamic modulus testing requires measurement of both the horizontal and vertical strains. This was done by mounting two linearly variable differential transducers (LVDT's) in the horizontal and vertical axes on both faces of the specimen. L-shaped brackets were attached with screws to brass targets, which were used to hold the LVDT's during testing. To mount the brass targets, a gluing jig was used to set the 50 mm spacing for testing. This is shown in Figure 2.5.

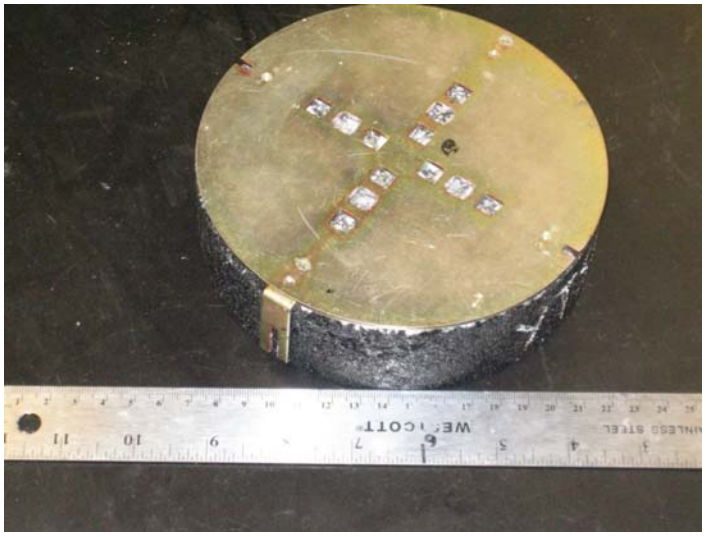

Figure 2.5 Brass Gluing Jig

To ensure that the testing distance is maintained, the brackets were attached to an aluminum rod and the spacing was checked again before they were glued to the specimen, as shown in Figure 2.6.

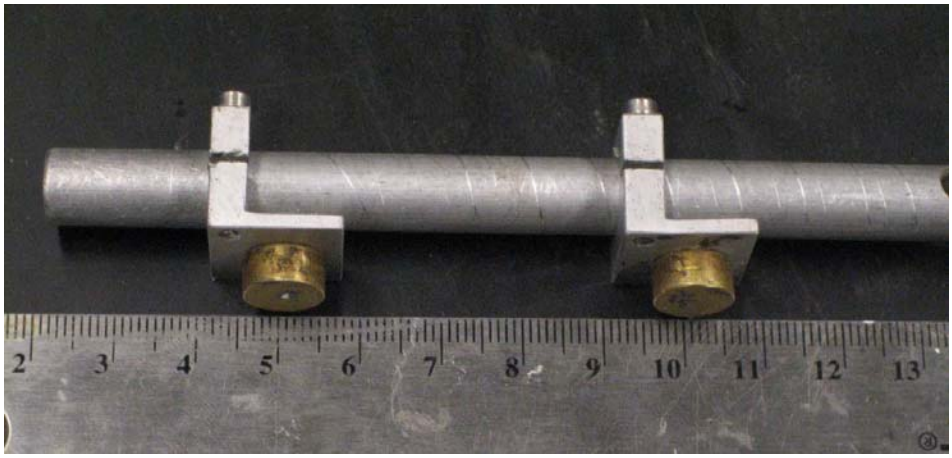

Figure 2.6 Brackets Prepared for Gluing

The brackets were then glued to each face of the specimen. The LVDT's must be at right angles to ensure that both strains are measured properly. To accomplish this, the LVDT's were glued to each face in the same orientation, then the rod was removed and the other LVDT rods were glued. This is shown in Figures 2.7 and 2.8.

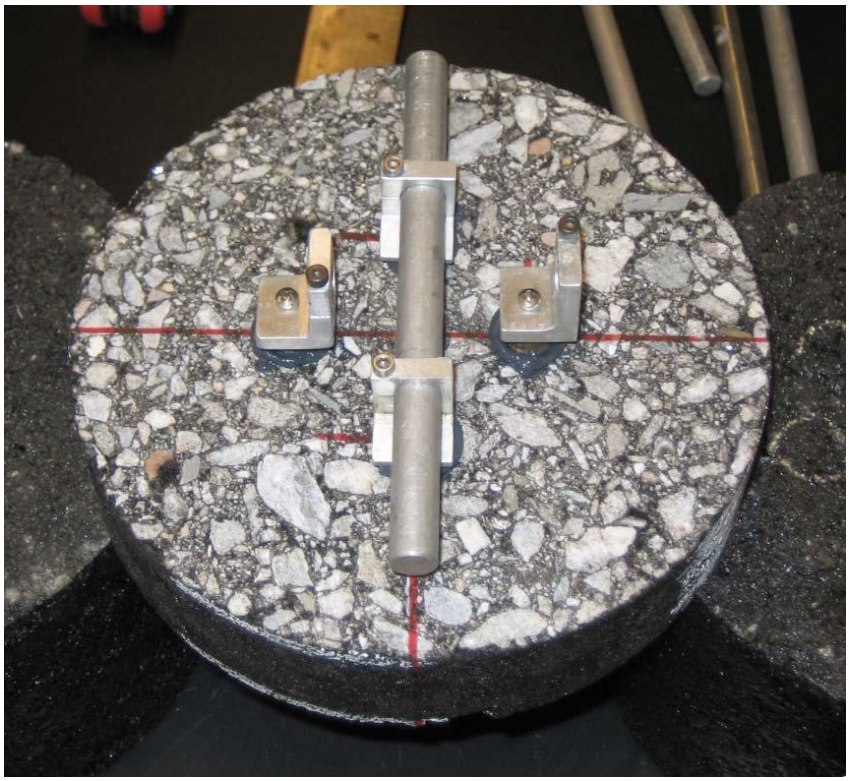

Figure 2.7 L Brackets and Rod

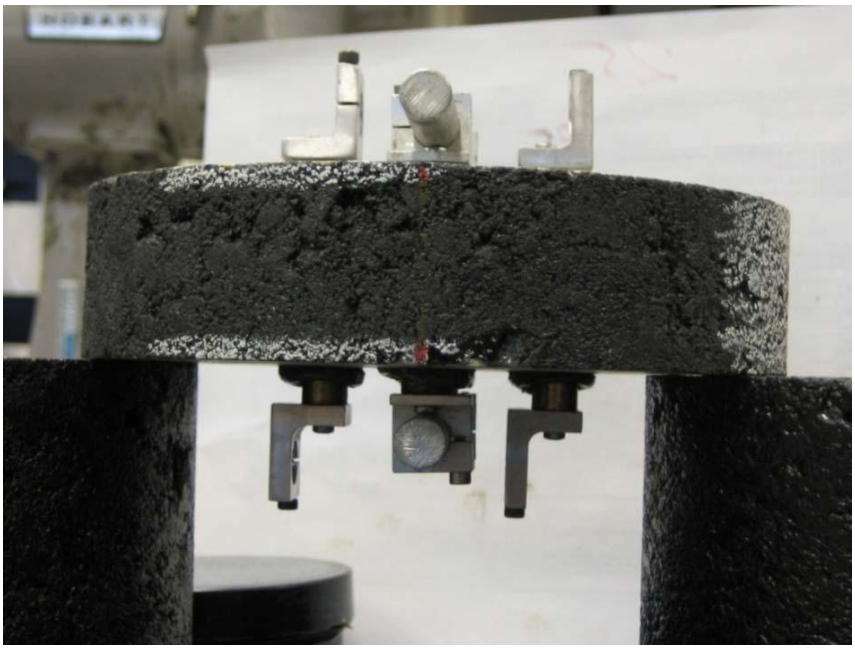

Figure 2.8 Brackets and Brass Targets Curing

The specimens were allowed to cure for at least 12 hours to ensure that the maximum bond was achieved. Once the specimens cured, the LVDT's were mounted into the L-shaped brackets. The specimen was then placed into the environmental chamber. Figure 2.9 shows a specimen with the LVDT's mounted and Figure 2.10 shows a completed specimen ready for testing in the environmental chamber.

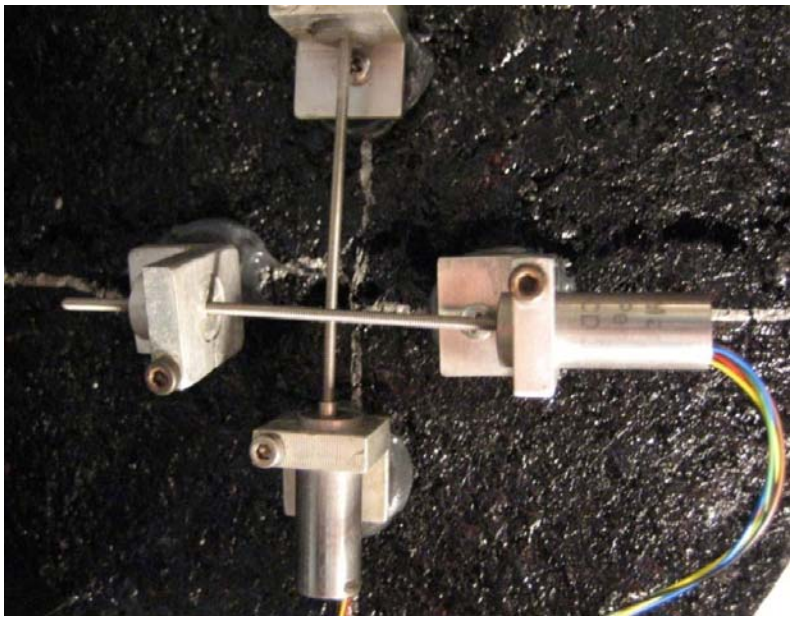

Figure 2.9 LVDT's Mounted onto a Specimen

Figure 2.10 Instrumented Specimen Ready for Testing

2.6 Dynamic Modulus Testing

Dynamic modulus testing in this study was done in the indirect tensile (IDT) mode, requiring the measurement of both horizontal and vertical strains. The dynamic modulus is calculated using the following equation developed by researchers at North Carolina State University (17):

$$|E*| = \left|\frac{2P_0}{\pi a d} \times \frac{\beta_1\gamma_2 - \beta_2\gamma_1}{\gamma_2 V_0 - \beta_2 U_0}\right| \tag{2.1}$$

Where, P_0 = applied load
a = loading strip width
d = thickness of specimen
U_0 = horizontal displacement
V_0 = vertical displacement
β_1, β_2, γ_1, γ_2 = constants
(-0.0134, -0.0042, 0.0037, 0.0116 respectively)

Frequency and temperature sweeps were conducted over a wide range of values. Testing was done at frequencies of 0.1, 0.2, 0.5, 1.0, 2.0, 5.0, 10.0, and 25.0 Hz and temperatures of -10°C, 0°C, 10°C, 20°C, and 30°C. A dummy specimen with an embedded thermocouple was used to ensure that the specimen reached test temperature prior to starting the test. A typical dynamic modulus data set is shown in Figure 2.11. There were some experimental difficulties in obtaining accurate results for the 25 Hz frequency at the lower testing temperatures.

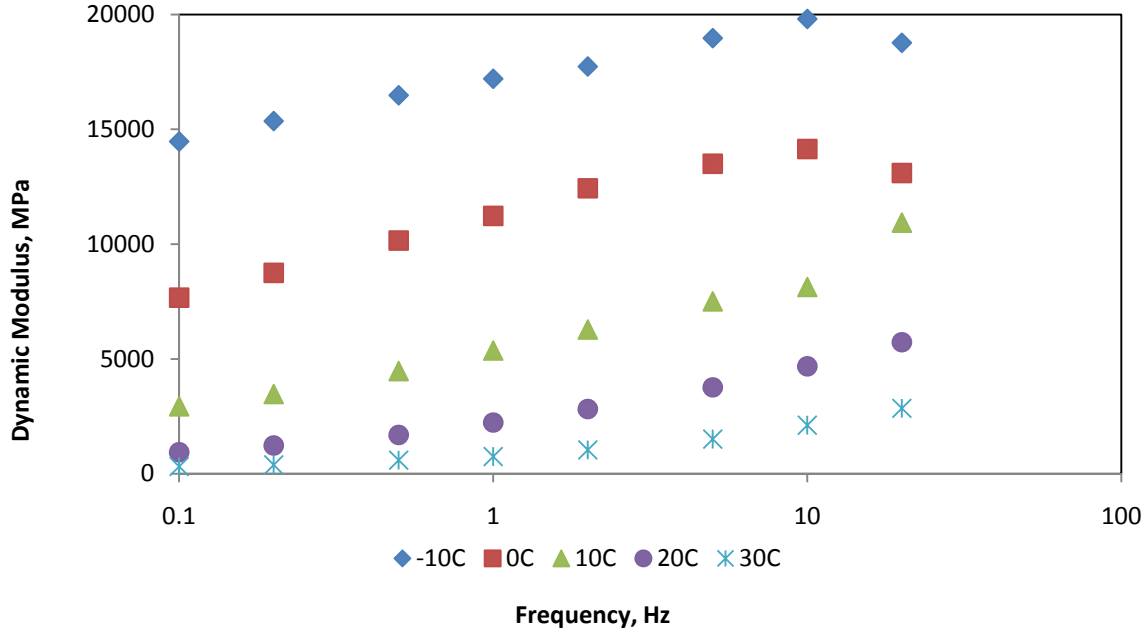

Figure 2.11 Typical Dynamic Modulus Data

The individual isotherms are then shifted horizontally along the frequency axis to a reference temperature of 20°C to create a master curve using the time-temperature superposition principle. The master curve is then fitted with a sigmoidal function which is shown in equation 2.2

$$\log\left|E^*\right| = a + \frac{b}{1+e^{c+d(\log \varpi_r)}} \tag{2.2}$$

Where |E*| = Dynamic Modulus
ω_r = reduced frequency
a,b,c,d = regression coefficients

A typical master curve is shown in Figure 2.12 and the associated shift factors are shown in Figure 2.13.

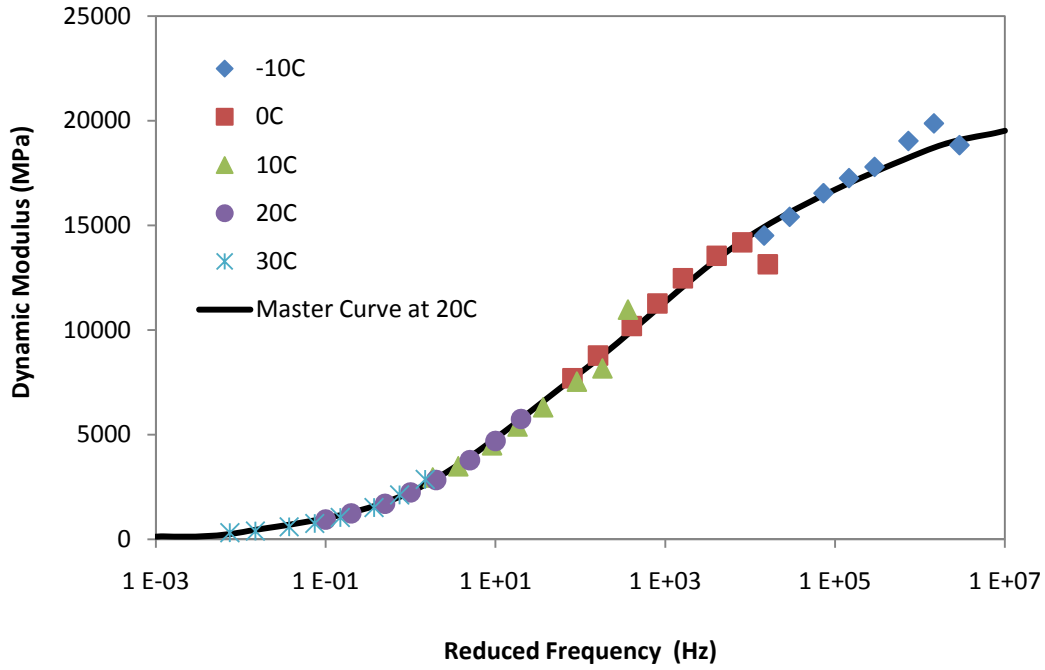

Figure 2.12 Typical Dynamic Modulus Master Curve

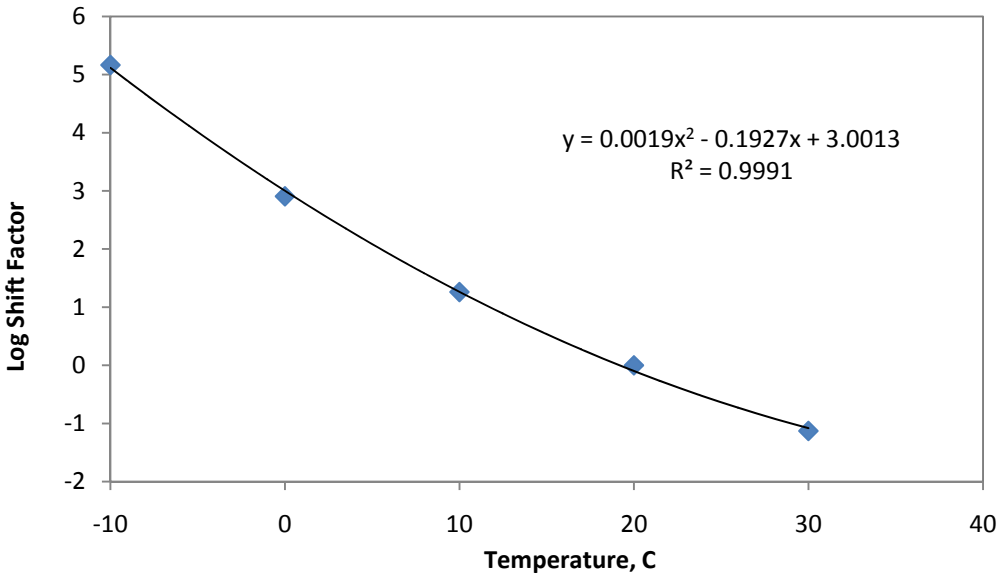

Figure 2.13 Typical Shift Factors

2.7 Hirsch Model

In this research project, the Hirsch model is used to back calculate the shear modulus, |G*| of the binder from the measured mixture properties. The Hirsch model was developed by T.J Hirsch in the late 1960's to calculate the modulus of elasticity of concrete. This model was refined by Christensen (18) to predict the |E*| of hot-mix asphalt using the |G*| of the binder used and volumetrics of the mix. The Hirsch model is shown below:

$$\left|E^*\right|_{mix} = Pc \cdot \left[4{,}200{,}000 \cdot \left(1 - \frac{VMA}{100}\right) + 3 \cdot \left|G^*\right|_{binder} \cdot \left(\frac{VFA \cdot VMA}{10{,}000}\right)\right] + (1 - Pc) \cdot \left[\frac{1 - \frac{VMA}{100}}{4{,}200{,}000} + \frac{VMA}{3 \cdot VFA \cdot \left|G^*\right|_{binder}}\right]^{-1}$$

$$Pc = \frac{\left(20 + \frac{VFA \cdot 3 \cdot \left|G^*\right|_{binder}}{VMA}\right)^{0.58}}{650 + \left(\frac{VFA \cdot 3 \cdot \left|G^*\right|_{binder}}{VMA}\right)^{0.58}}. \tag{2.3}$$

Where

VMA = Voids in mineral aggregate
VFA = Voids filled with asphalt
P_C = Contact area

It should be noted that the Hirsch model uses English units of measurement as opposed to metric and the dynamic modulus is reported in psi.

2.8 Creep Compliance Testing

Creep compliance testing at low temperatures was performed on indirect tensile specimens. Testing was done at -20°C, -10°C, and 0°C. A load was applied to the specimen to induce a horizontal deformation between 0.00125-0.00190 mm and held for 100 seconds. The horizontal deformation over time was recorded and the creep compliance was calculated as shown in Equation 2.4.

$$D(t) = \frac{\Delta X \times D_{avg} \times b_{avg}}{P_{avg} \times GL} \times C_{cmpl} \tag{2.4}$$

where:

D(t) = Creep compliance at time *t*
ΔX = Horizontal deformation of specimen

D_{avg} = Specimen diameter
b_{avg} = Specimen thickness
P_{avg} = Creep load applied
GL = Gage length in meters

C_{cmpl} is calculated as shown in equation 2.5:

$$C_{cmpl} = 0.6354 \times \left(\frac{X}{Y}\right)^{-1} - 0.332 \tag{2.5}$$

where:
X = Horizontal deformation of specimen
Y = Vertical deformation of specimen

Creep compliance data at the three different temperatures for a single specimen is shown in Figure 2.14. The time-temperature superposition principle is used to shift the individual temperature curves to create a master curve at a reference temperature of 0°C, as shown in Figure 2.15. The master curve is fit with a Generalized Power Law (GPL):

$$D(t) = D_0 + D_1 t^n \tag{2.6}$$

where D_0, D_1, and n are regression coefficients and t is reduced time in seconds.

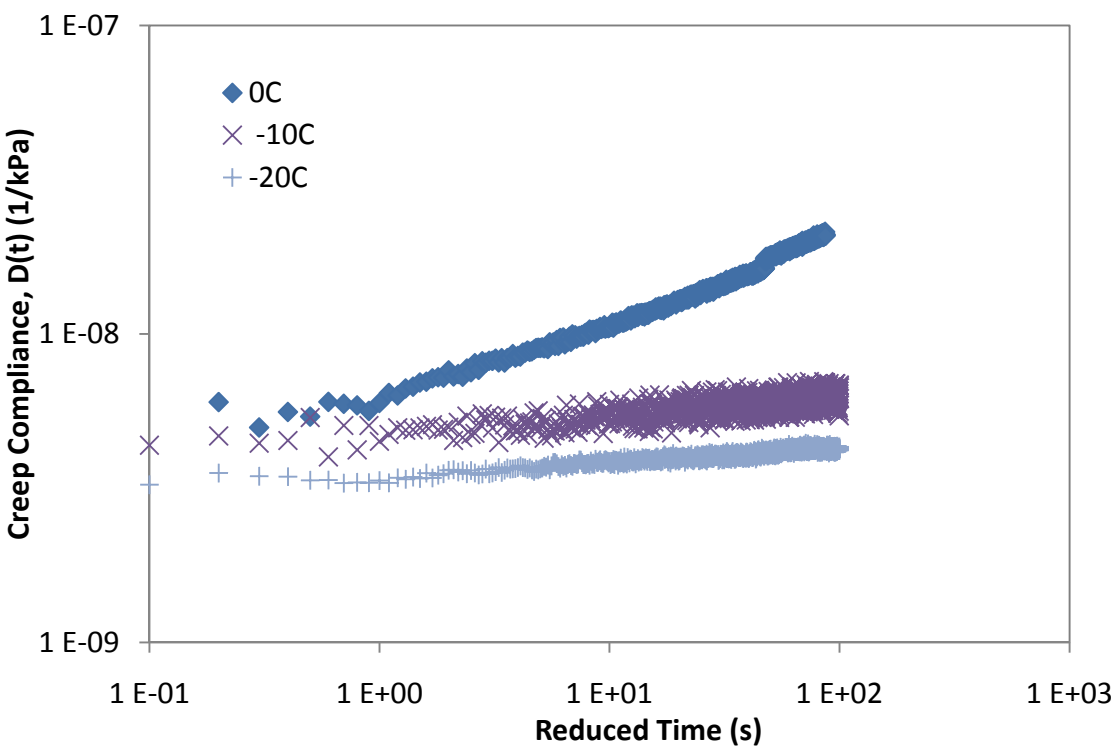

Figure 2.14 Creep Compliance Curves at Individual Temperatures

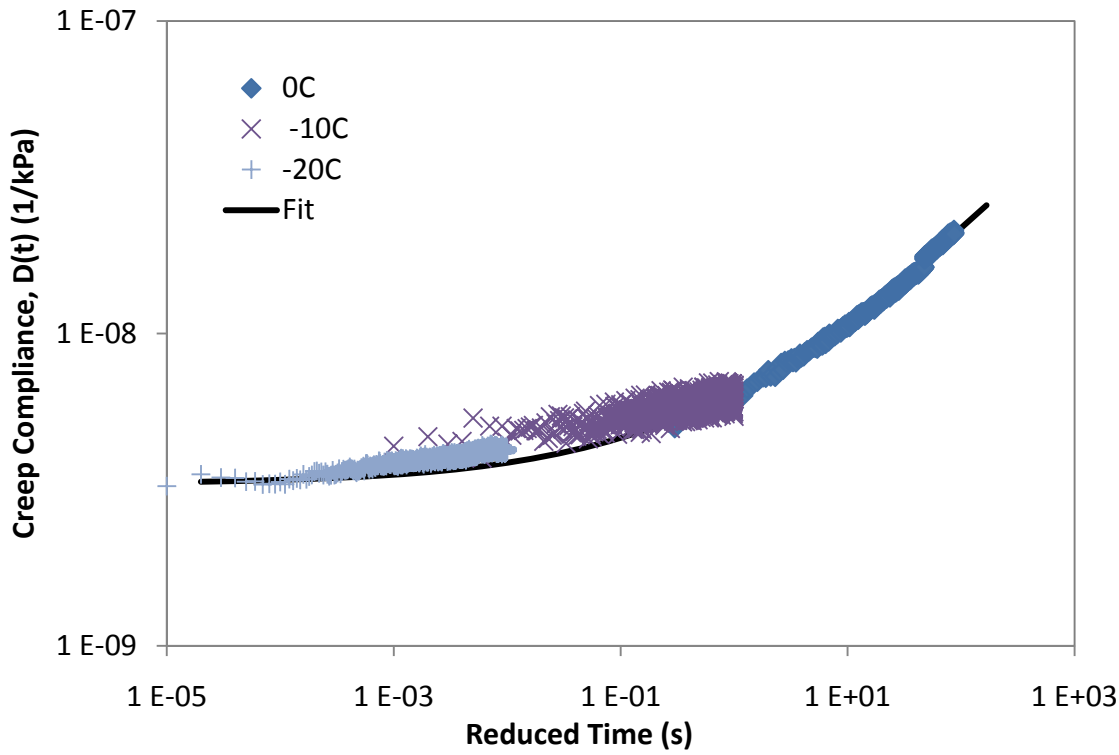

Figure 2.15 Creep Compliance Master Curve

2.9 Indirect Tensile Strength Testing

Indirect tensile strengths of the specimens were measured after the creep compliance testing was performed. The specimens were crushed at a constant rate of 50 mm per minute at a temperature of -10°C until the specimens failed. The strength was then calculated using Equation 2.7. A typical load curve is shown in Figure 2.16. The large break in the curve is due to a brittle failure of the specimen; all failures were brittle at the colder temperatures.

$$S = \frac{2 \times P_f}{\pi \times b \times D} \tag{2.7}$$

Where S = Strength of specimen
P_f = Load at failure
b = Thickness
D = Specimen diameter

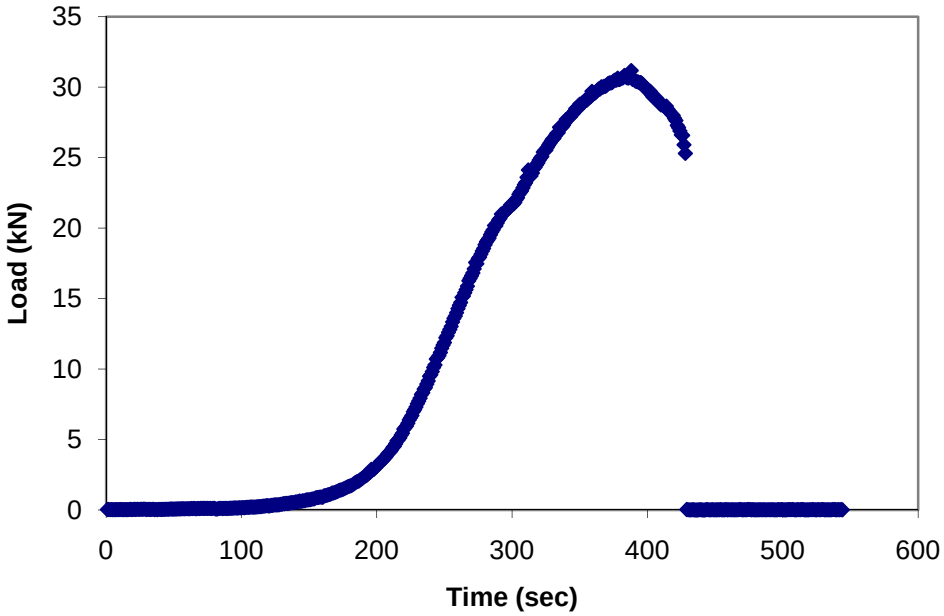

Figure 2.16 Typical Strength Loading Curve

3.0 RESULTS

This chapter will present the results of the dynamic modulus testing, strength testing, creep testing, binder shear modulus calculations and statistical analysis of all test results.

3.1 Dynamic Modulus

3.1.1 RAP Mixtures

The dynamic modulus master curves and individual data points for the control, 10%, 25% and 40% RAP are shown in Figures 3.1 through 3.4, respectively. Figure 3.5 shows a comparison among the average master curves for all four RAP mixtures. The dynamic modulus increases with increasing RAP content up to the 25% level. The dynamic modulus curves for the 25% and 40% RAP mixtures are almost identical.

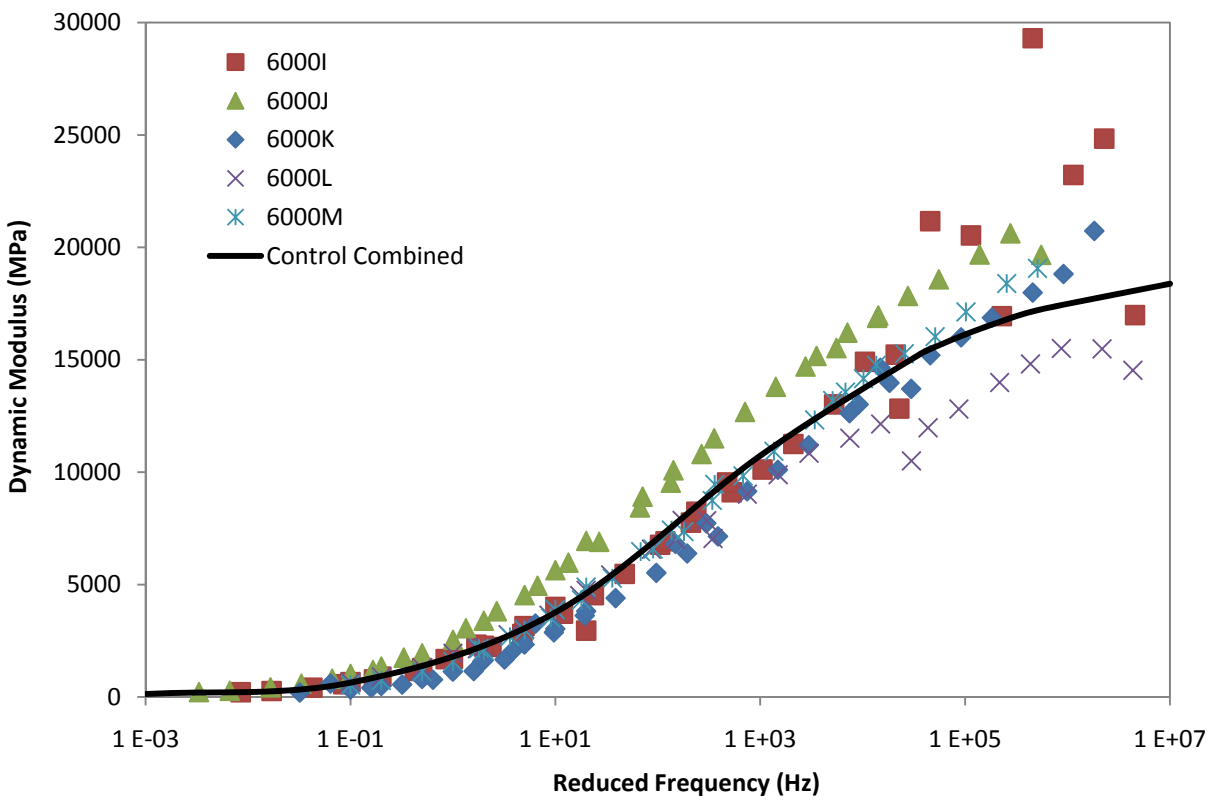

Figure 3.1 Control Mixture Dynamic Modulus Master Curve

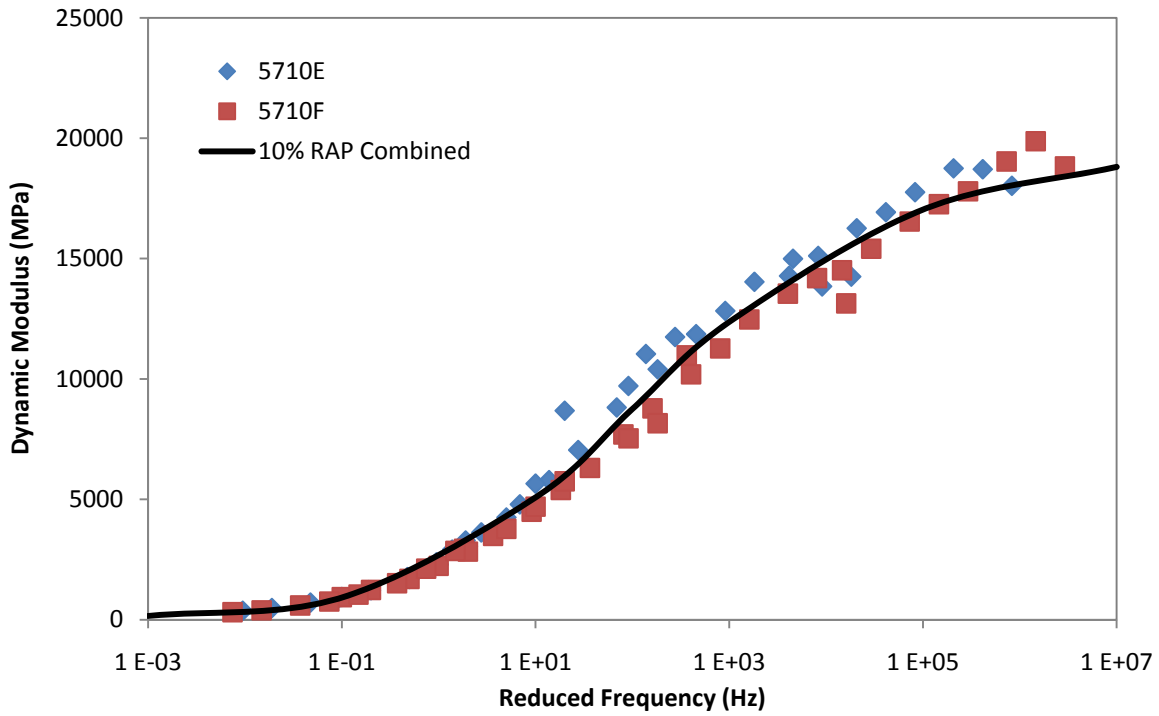

Figure 3.2 10% RAP Mixture Dynamic Modulus Master Curve

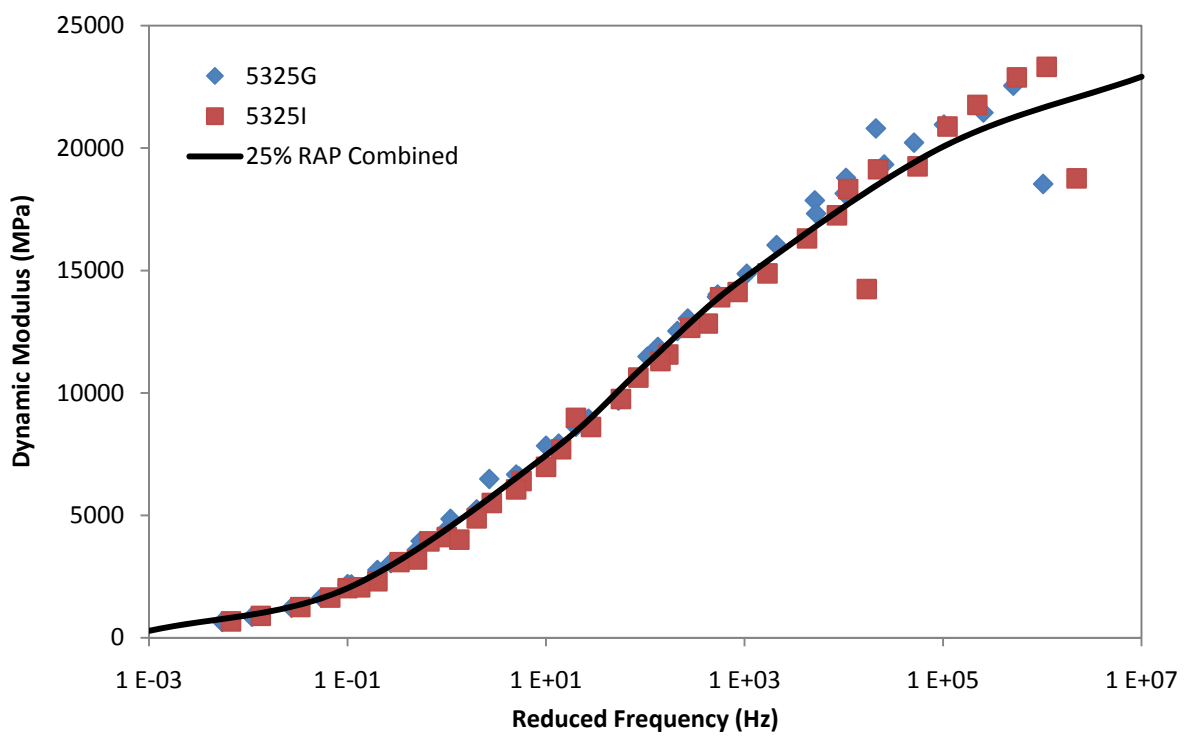

Figure 3.3 25% RAP Mixture Dynamic Modulus Master Curve

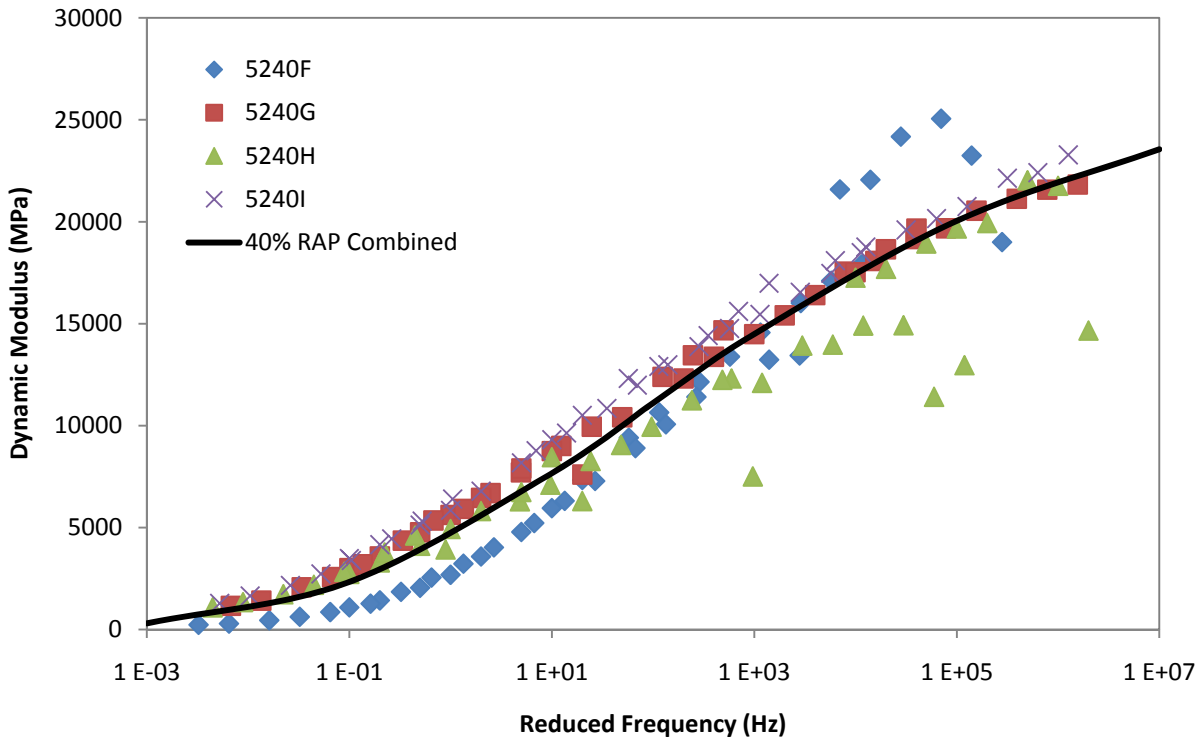

Figure 3.4 40% RAP Mixture Dynamic Modulus Master Curve

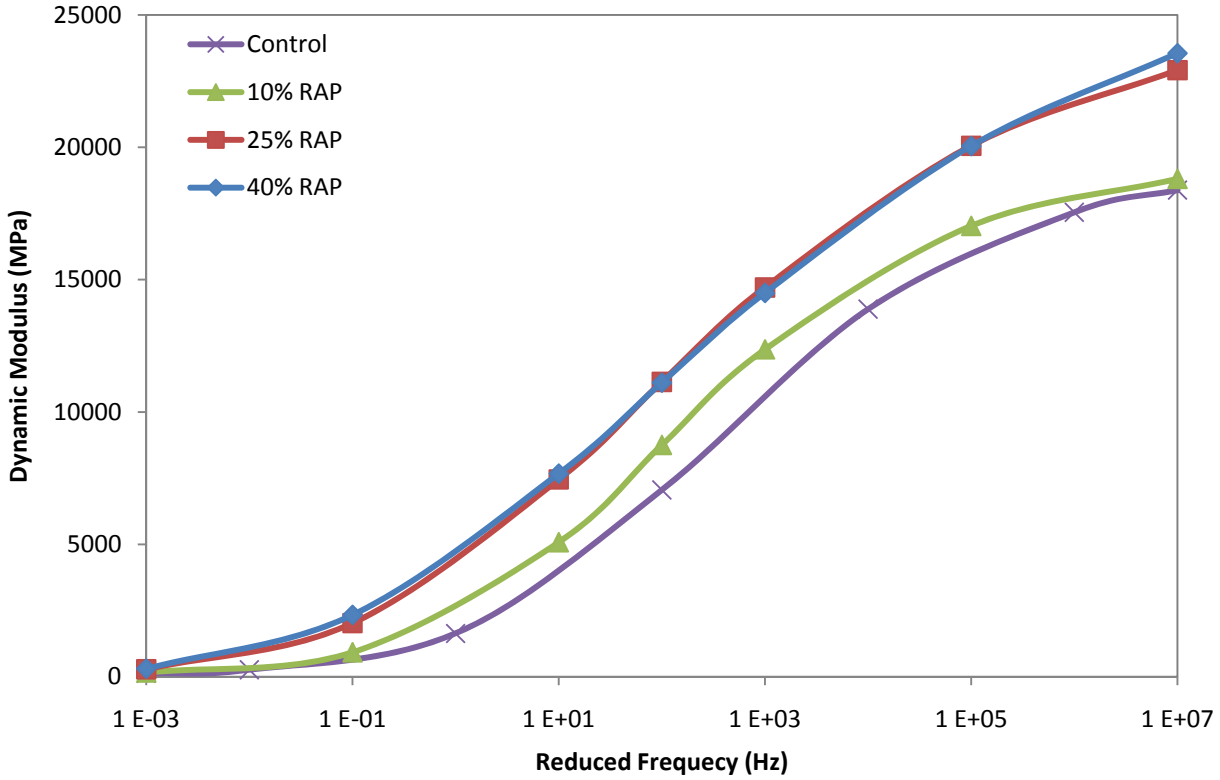

Figure 3.5 Average Dynamic Modulus Master Curves

Statistical analysis using two tailed t-test was performed on the dynamic modulus data at a range of frequencies to determine if there are significant differences between the mixtures. Table 3.1 shows the p-value results from this analysis. A p-value below 0.05 indicates a significant difference at a 95% confidence level. The control mixture is significantly different from the 25% RAP and 40% RAP mixtures, but the other mixtures are not statistically different.

Table 3.1 Dynamic Modulus T-Test Results for RAP Mixtures

Comparison	Reduced Frequency (Hz)				
	0.01	**10**	**100**	**1000**	**100000**
Control-10% RAP	0.23	0.24	0.23	0.23	0.68
Control-25% RAP	0.01	0.00	0.00	0.00	0.01
Control-40% RAP	0.03	0.01	0.00	0.01	0.10
10% RAP-25% RAP	0.11	0.20	0.21	0.15	0.02
10% RAP-40% RAP	0.06	0.12	0.16	0.14	0.12
25% RAP-40% RAP	0.35	0.63	0.87	0.81	0.56

3.1.2 Different PG Binder Grades

The dynamic modulus master curves and individual data points for the PG 58-28, PG 70-22, and PG 76-22 mixtures are shown in Figures 3.6 through 3.8, respectively. Figure 3.9 shows a comparison among the average master curves for all four different PG mixtures. The average curves show some differences at the high frequencies; however, the statistical analysis shown in Table 3.2 indicates that there are not any statistically significant differences between the different mixtures.

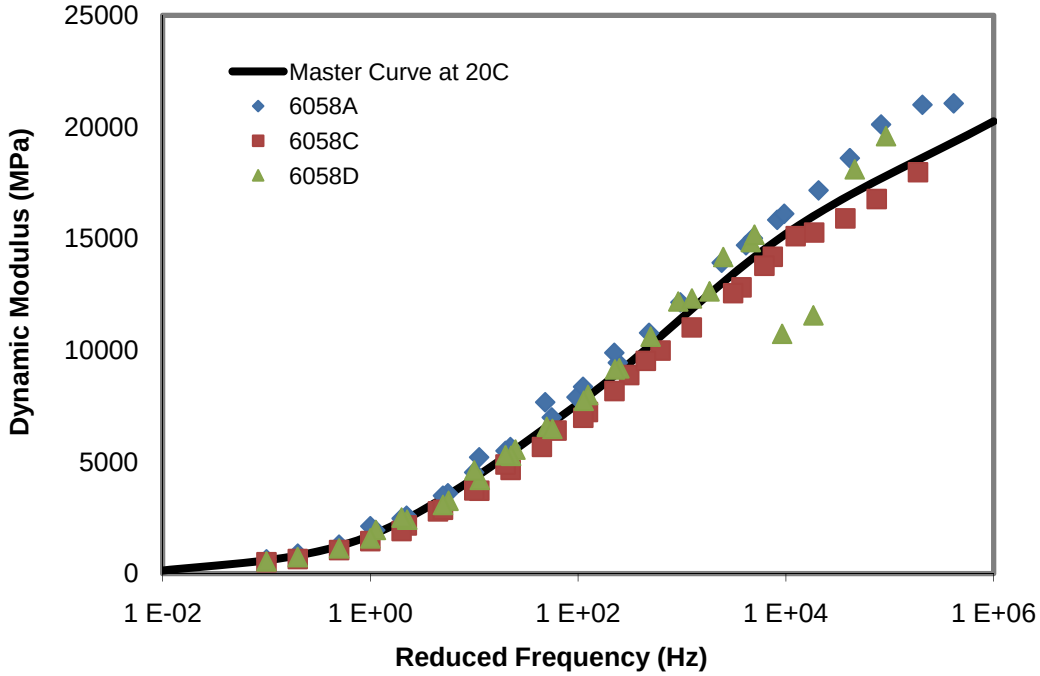

Figure 3.6 PG 58-28 Mixture Dynamic Modulus Master Curve

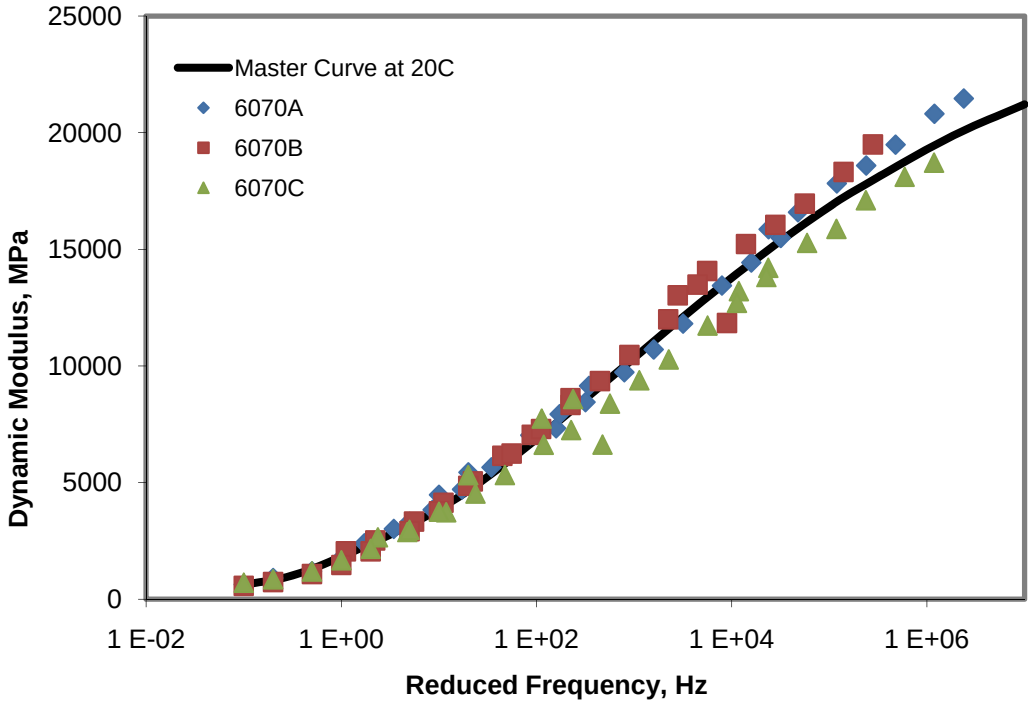

Figure 3.7 PG 70-22 Mixture Dynamic Modulus Master Curve

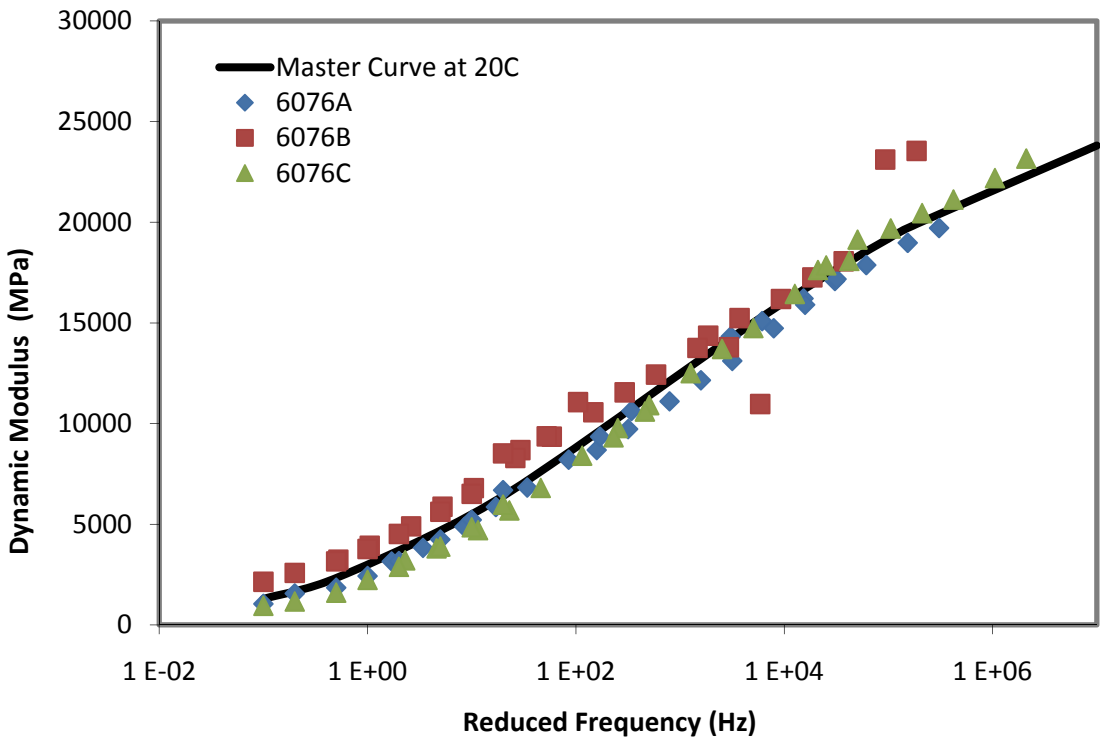

Figure 3.8 PG 76-22 Mixture Dynamic Modulus Master Curve

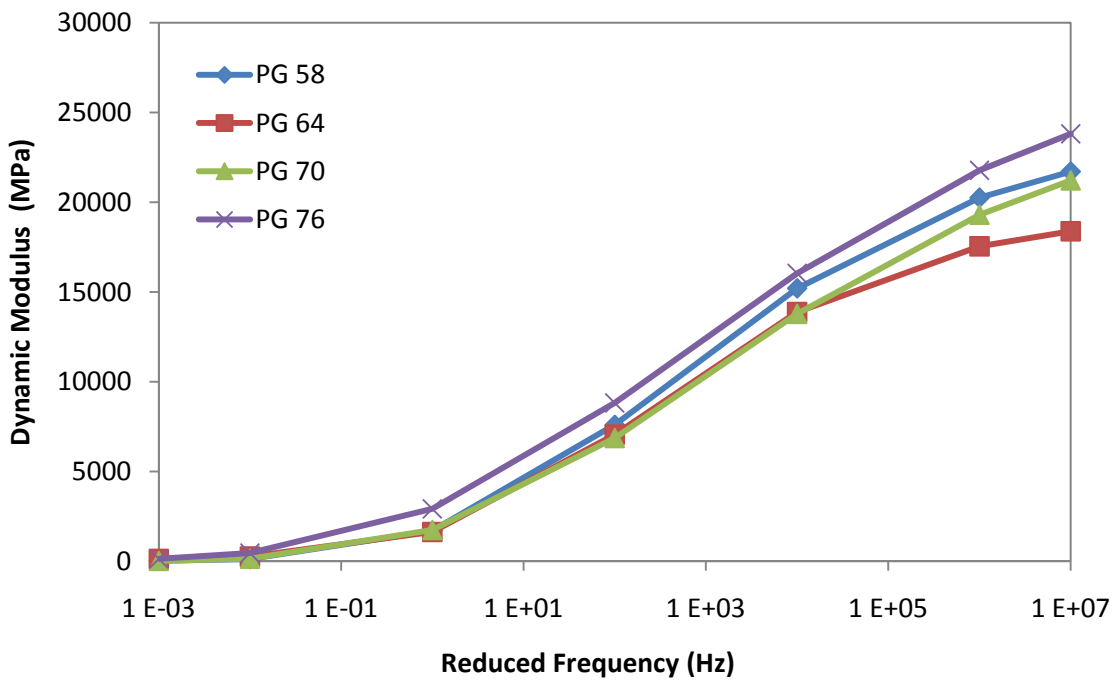

Figure 3.9 Average PG Mixture Dynamic Modulus Master Curves

Table 3.2 Dynamic Modulus T-Test Results for PG Mixtures

Comparison	Reduced Frequency (Hz)				
	0.01	**10**	**100**	**1000**	**100000**
PG 64-PG 58	0.17	0.82	0.42	0.16	0.22
PG 64-PG 70	0.31	0.77	0.97	0.86	0.64
PG 64-PG 76	0.23	0.14	0.07	0.06	0.09
PG 58-PG 70	0.80	0.93	0.25	0.18	0.27
PG 58-PG 76	0.17	0.13	0.15	0.51	0.65
PG 70-PG 76	0.18	0.13	0.06	0.08	0.03

3.2 Binder Modulus

3.2.1 RAP Mixtures

The Hirsch Model is used to back calculate the shear modulus of the asphalt binder, |G*|, from the measured dynamic modulus master curves. This was done for each individual specimen master curve and using the average master curve for each mixture. The back calculated |G*| master curves for the control, 10% RAP, 25% RAP, and 40% RAP mixtures are shown in Figures 3.10 through 3.13, respectively. The binder from each mixture was also extracted and tested directly to determine the recovered |G*| curves. The recovered binder represents a fully blended combination of the virgin asphalt binder and the RAP binder; these values are plotted on the graphs for each mixture. The recovered binder |G*| values are consistently higher than those back calculated from the mixture dynamic modulus curves. This indicates that in the mixture, the RAP binder does not fully blend with the virgin binder, resulting in an effective binder modulus that is softer than the fully blended condition. Therefore, the back calculated |G*| values for a mixture containing highly aged RAP may be softer than those for a mixture containing moderately aged RAP due to a greater percentage of “black rock” and less blending between the virgin and RAP binders.

Figure 3.14 shows a comparison of the back calculated |G*| curves for the different RAP mixtures. There is not a trend with respect to RAP content. The recovered |G*| curves for all four mixtures are shown in Figure 3.15; clearly, the recovered (fully blended) |G*| increases with increasing RAP content, as would be expected.

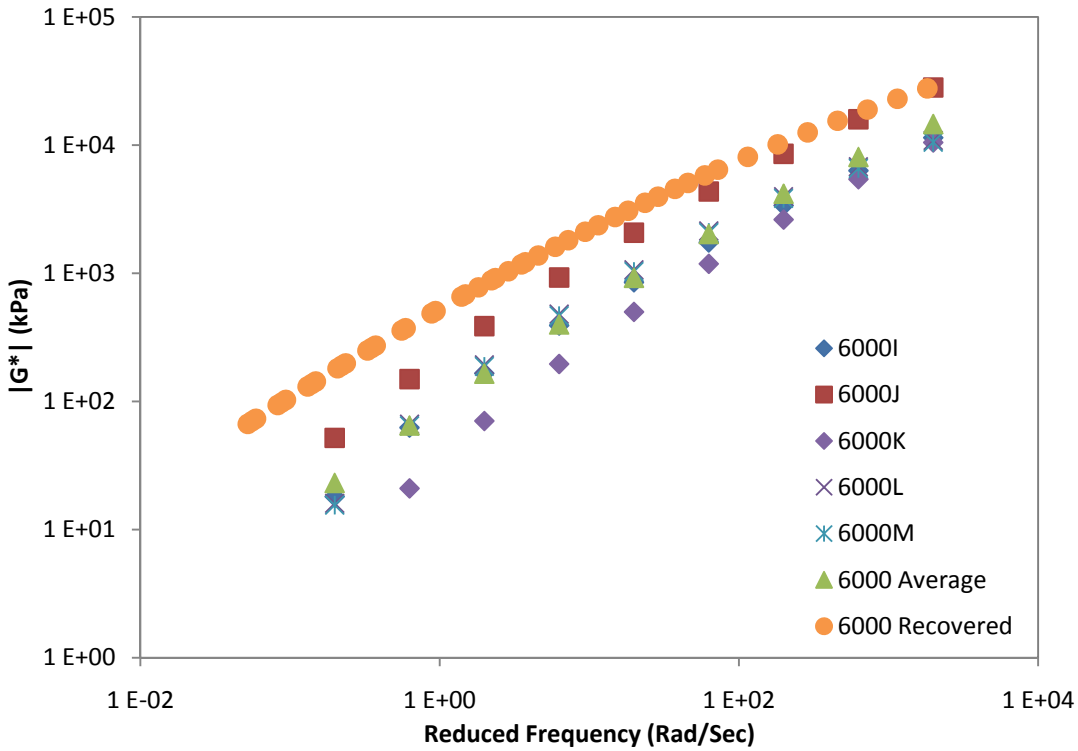

Figure 3.10 Control Mixture Binder Modulus Curves

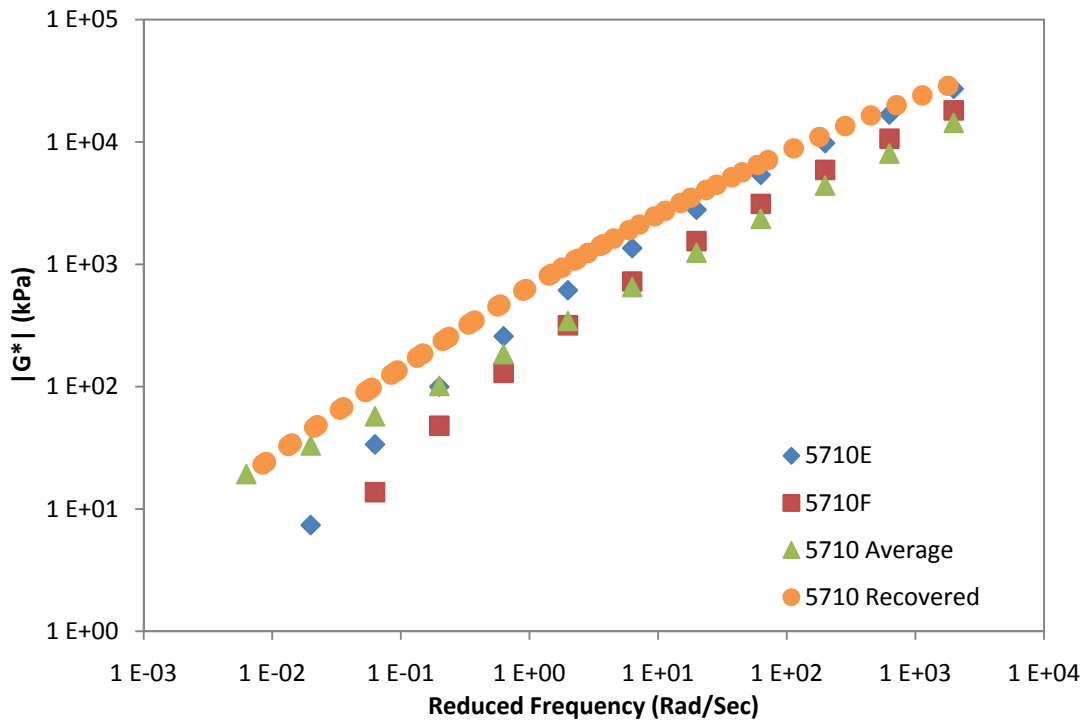

Figure 3.11 10% RAP Mixture Binder Modulus Curves

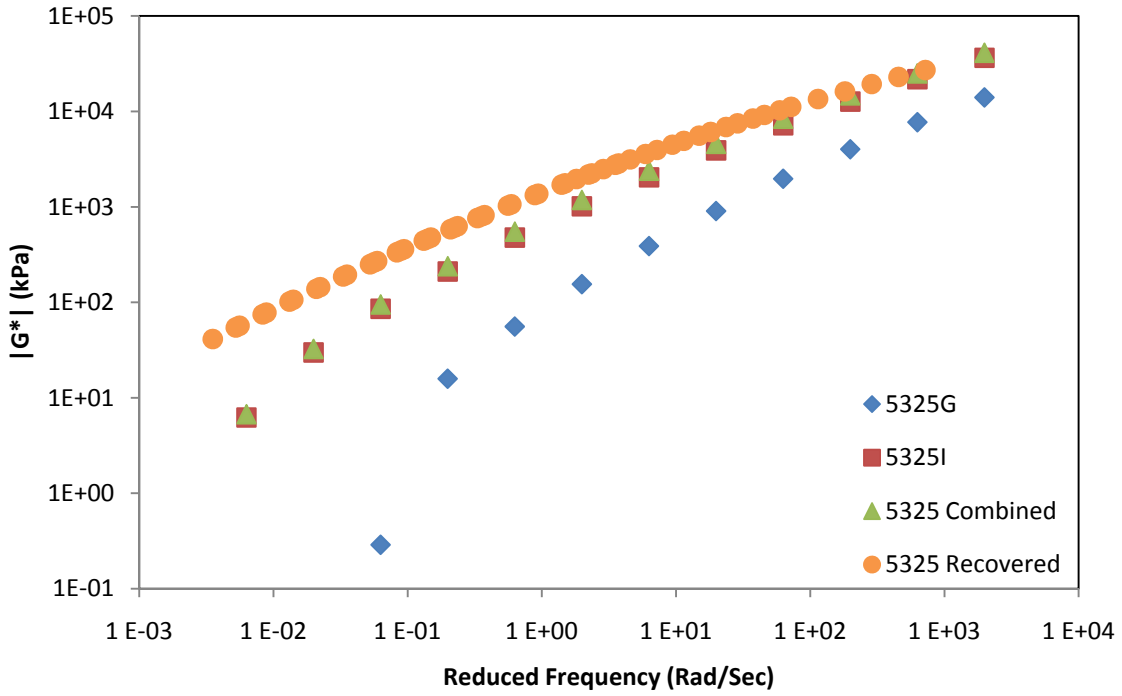

Figure 3.12 25% RAP Mixture Binder Modulus Curves

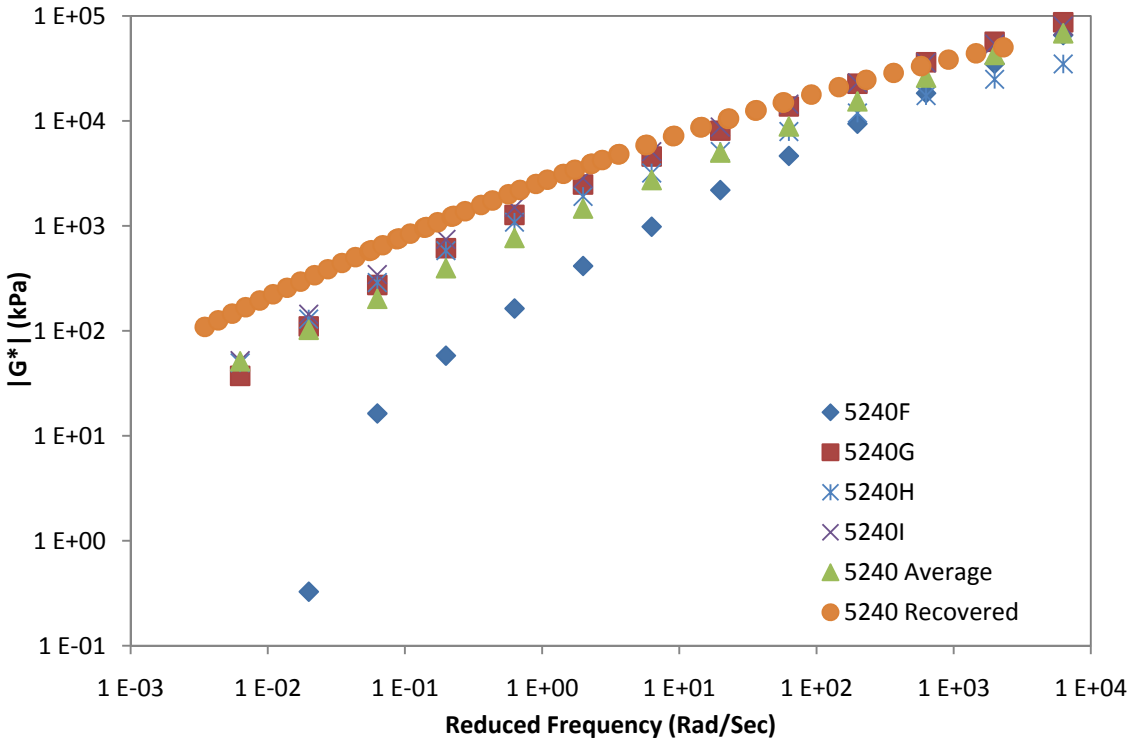

Figure 3.13 40% RAP Mixture Binder Modulus Curves

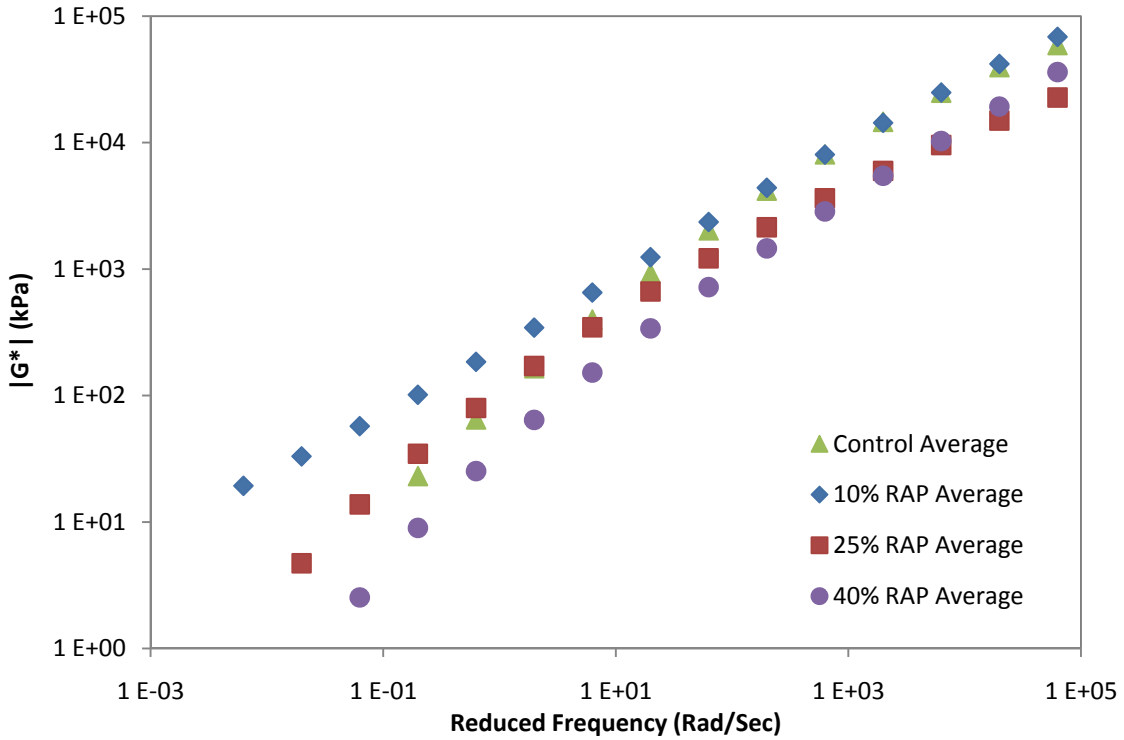

Figure 3.14 Average Binder Modulus Curves for All RAP Mixtures

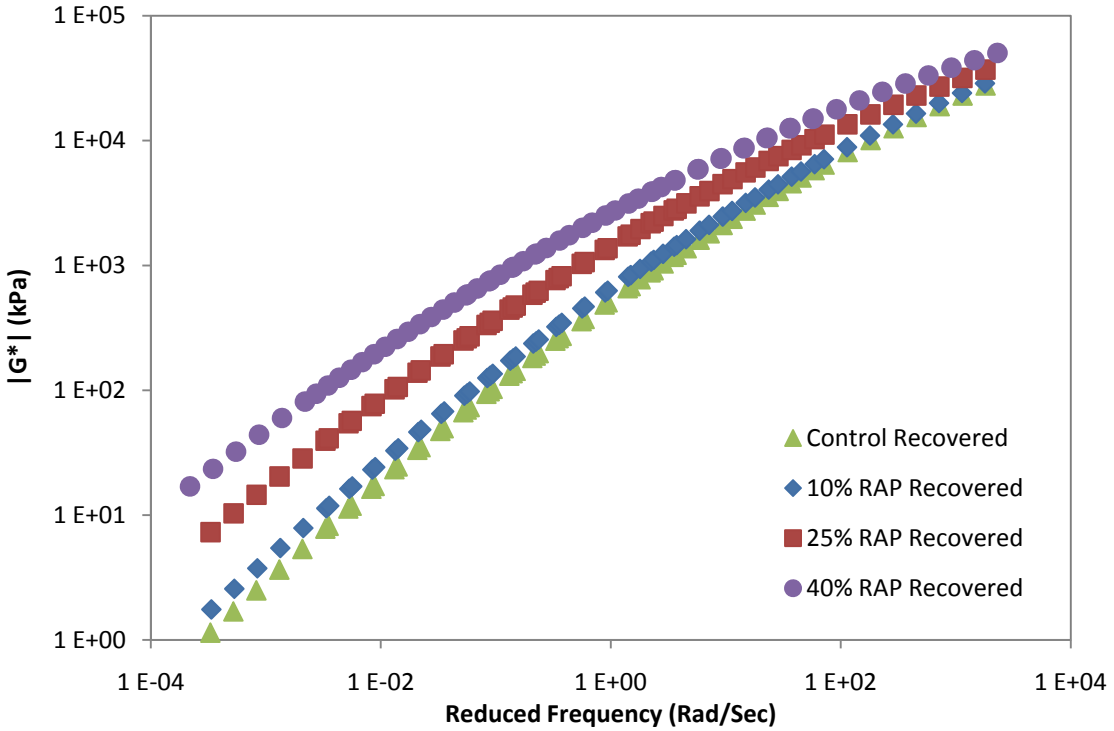

Figure 3.15 Recovered Binder Modulus Curves for All RAP Mixtures

Statistical Analysis

The binder modulus results were compared using a two-tailed t-test to evaluate significant differences between the mixtures. The results are shown in Table 3.3. The control mixture does not have values at the low frequency so there are no results for comparison. The control and 40% RAP mixtures are significantly different over the middle frequency range. All other mixtures are not statistically different.

Table 3.3 Binder Modulus T-Test Results for RAP Mixtures

Comparison	Reduced Frequency (rad/sec)				
	0.01	**1**	**100**	**10000**	**1000000**
Control-10% RAP	n/a	0.28	0.24	0.25	0.99
Control-25% RAP	n/a	0.52	0.48	0.42	0.45
Control-40% RAP	n/a	0.04	0.03	0.04	0.24
10% RAP-25% RAP	0.73	0.87	0.91	0.62	0.46
10% RAP-40% RAP	0.06	0.07	0.09	0.09	0.24
25% RAP-40% RAP	0.09	0.16	0.29	0.41	0.45

The extracted PG binder grade, representing a fully blended condition, was determined for each mixture and is summarized in Table 3.4 below. The control mixture experiences a change in PG grade just through the mixing and short term aging process that happens in the laboratory. The increase in RAP content results in an increase in both the high and low temperature PG grades.

Table 3.4 Extracted PG Grade of RAP Mixtures

Mixture	Extracted PG Grade	
	Continuous	**Standard**
Control	72.0-27.4	70-22
10% RAP	75.4-28.8	70-28
25% RAP	85.0-26.7	82-22
40% RAP	99.3-19.9	94-16

3.2.2 Different PG Binder Grades

The asphalt binder |G*| curves back calculated from the mixture dynamic modulus for the various PG grade mixtures are shown in Figures 3.16 through 3.18. The data for the PG 64-28 mixture is shown in Figure 3.10 above. Figure 3.19 shows a comparison of the average curves for each mixture and Table 3.5 provides the statistical analysis. The PG 64-28 mixture has the softest back calculated binder modulus, but there are not significant differences between the mixtures.

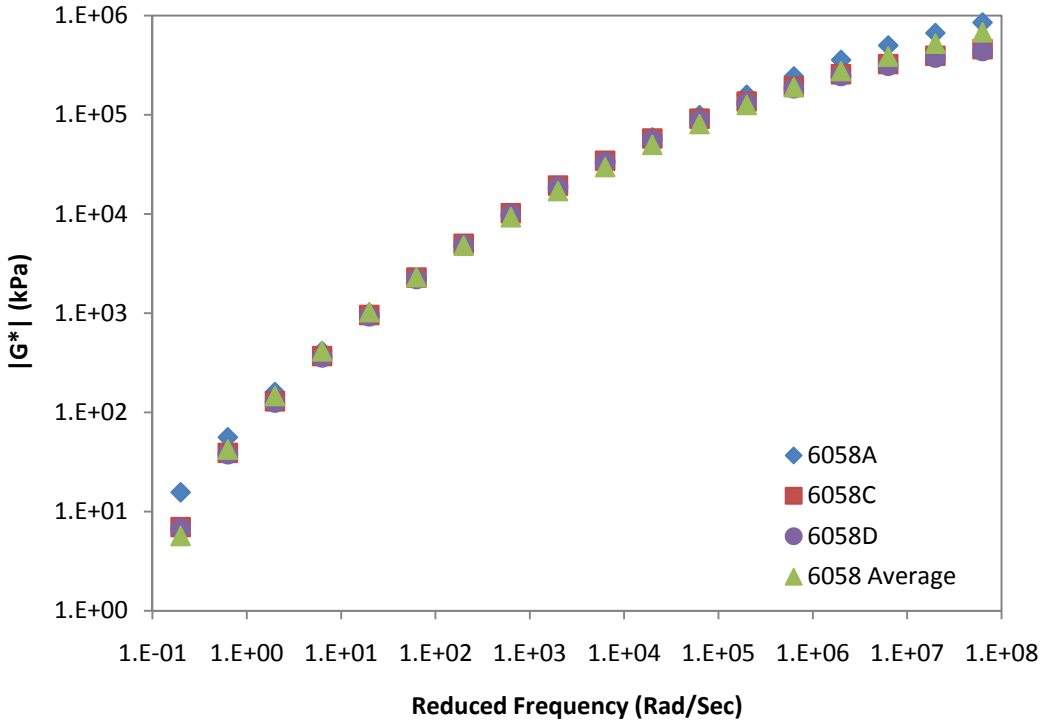

Figure 3.16 PG 58-28 Mixture Binder Modulus Curves

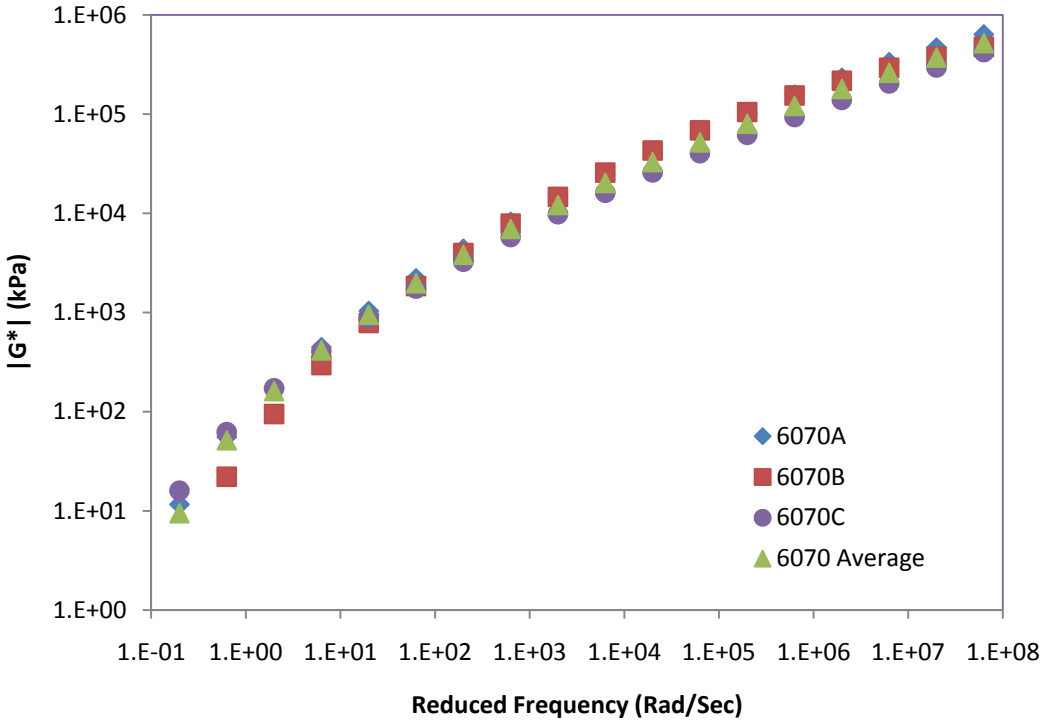

Figure 3.17 PG 70-22 Mixture Binder Modulus Curves

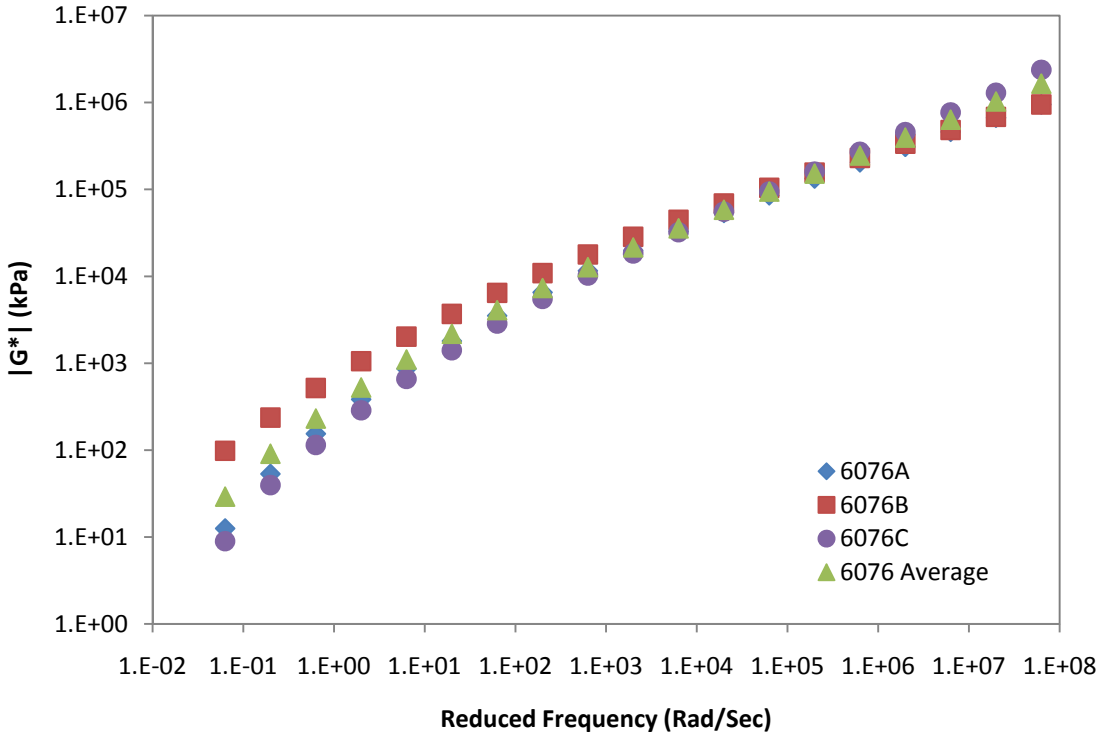

Figure 3.18 PG 76-22 Mixture Binder Modulus Curves

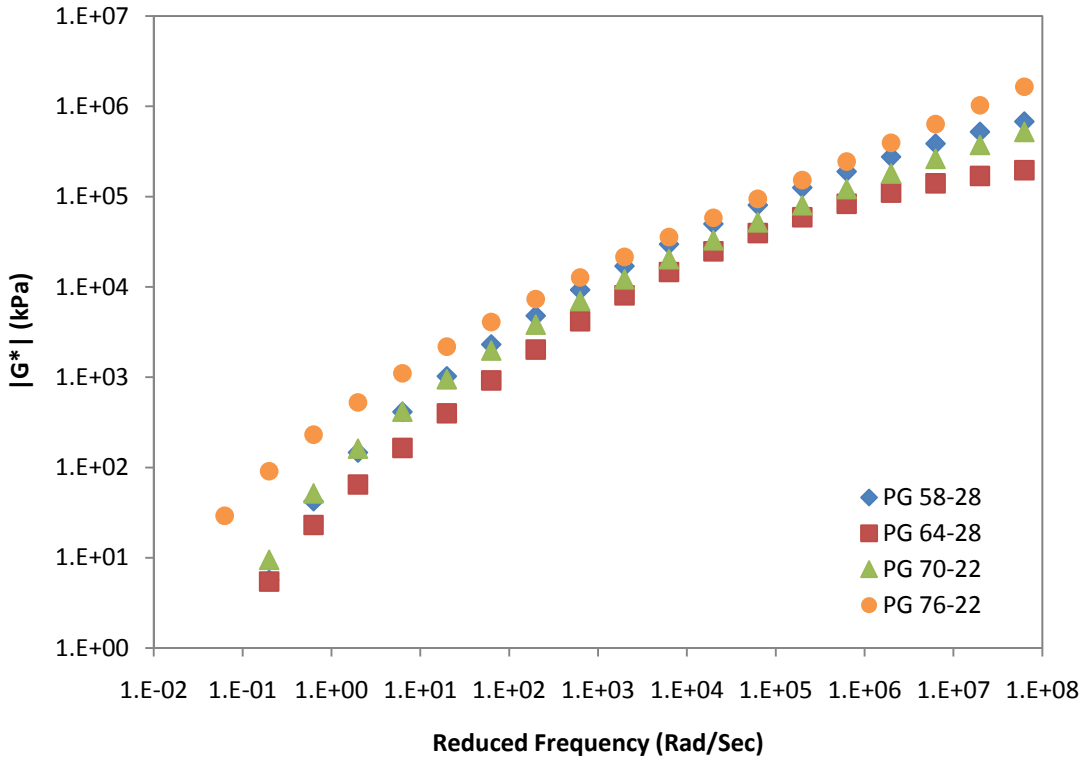

Figure 3.19 Average PG Mixture Binder Modulus Curves

Table 3.5 Binder Modulus T-Test Results for PG Mixtures

Comparison	Frequency			
	1	100	10000	1000000
PG 64-PG 58	0.41	0.42	0.10	0.45
PG 64- PG 70	0.43	0.68	0.98	0.99
PG 64-PG 76	0.24	0.17	0.09	0.10
PG 58-PG 70	0.97	0.07	0.05	0.24
PG 58-PG 76	0.20	0.30	0.77	0.19
PG 70-PG 76	0.20	0.12	0.04	0.08

3.3 Creep Compliance

The creep compliance master curves and individual data points for the control, 10%, 25% and 40% RAP are shown in Figures 3.20 through 3.23, respectively. Figure 3.24 shows a comparison among the average master curves for all four mixtures. The control and 25% RAP mixtures have more specimen to specimen variability than the 10% and 40% mixtures. The average response for the different mixtures is very similar; the control mixture has an overall softer response, but there is no trend with respect to the different RAP contents.

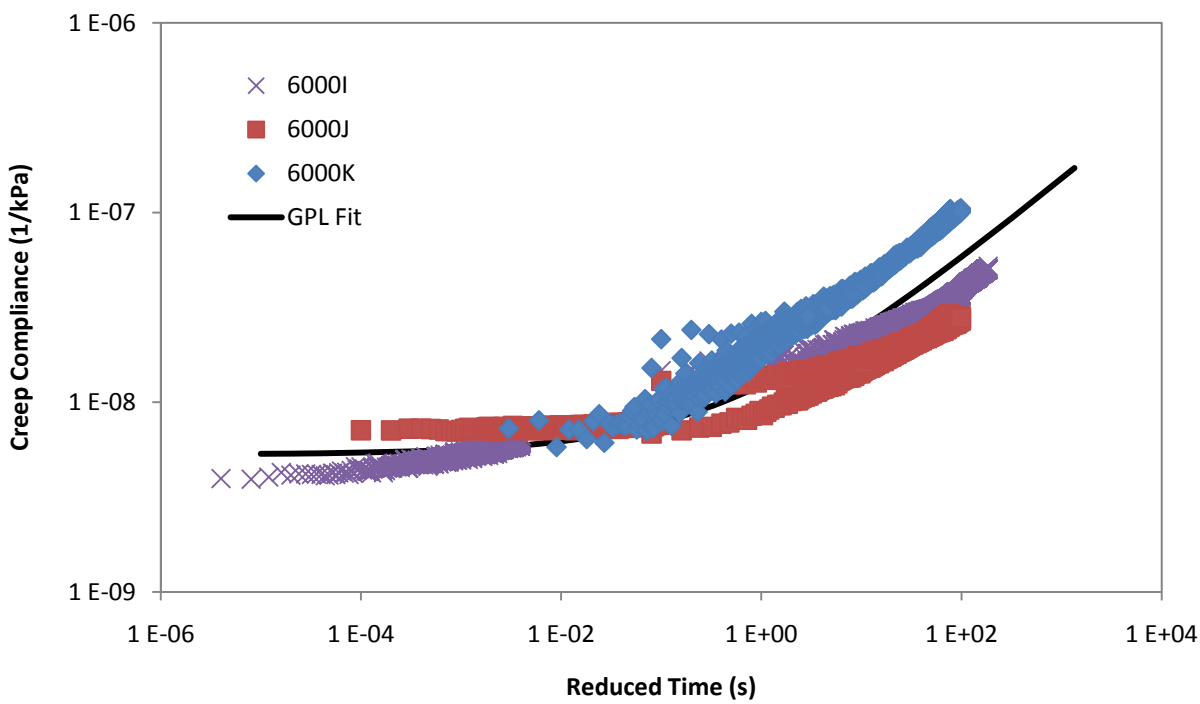

Figure 3.20 Control Mixture Creep Compliance Master Curve

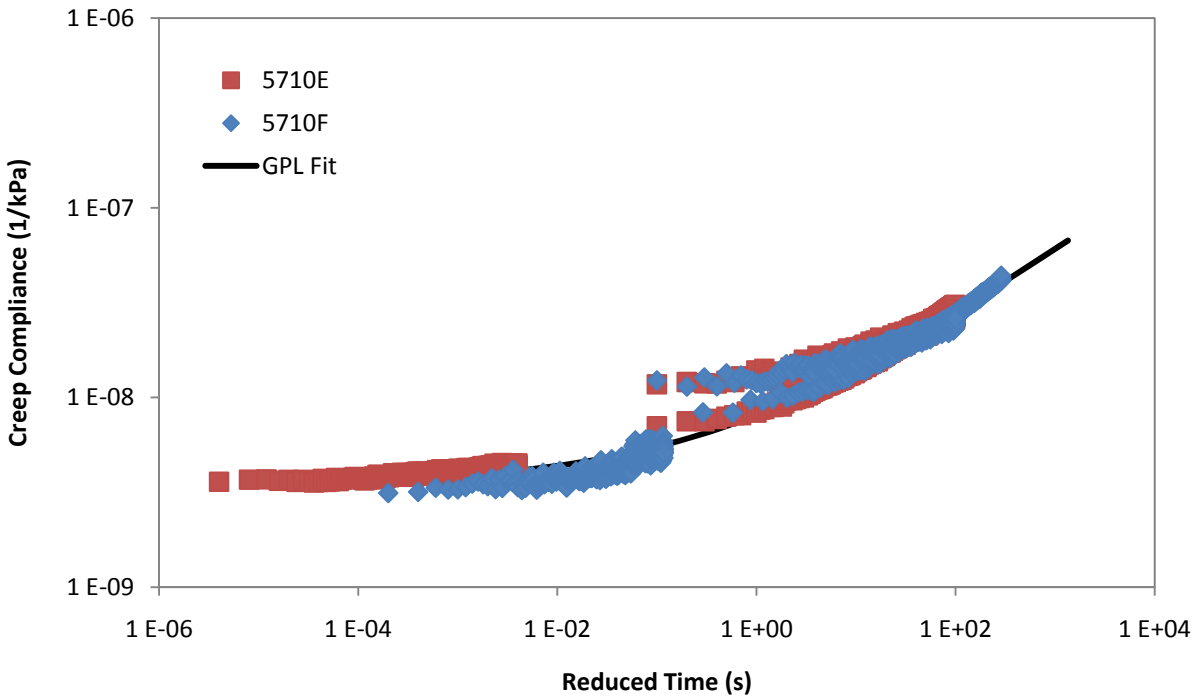

Figure 3.21 10% RAP Mixture Creep Compliance Master Curve

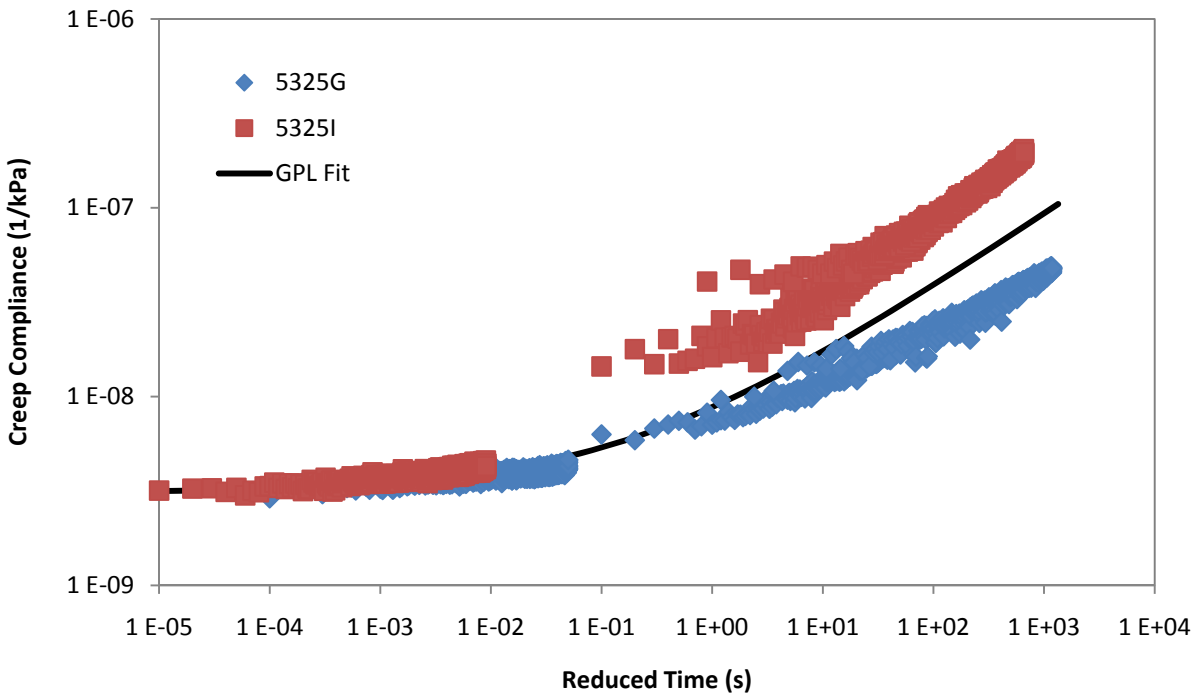

Figure 3.22 25% RAP Mixture Creep Compliance Master Curve

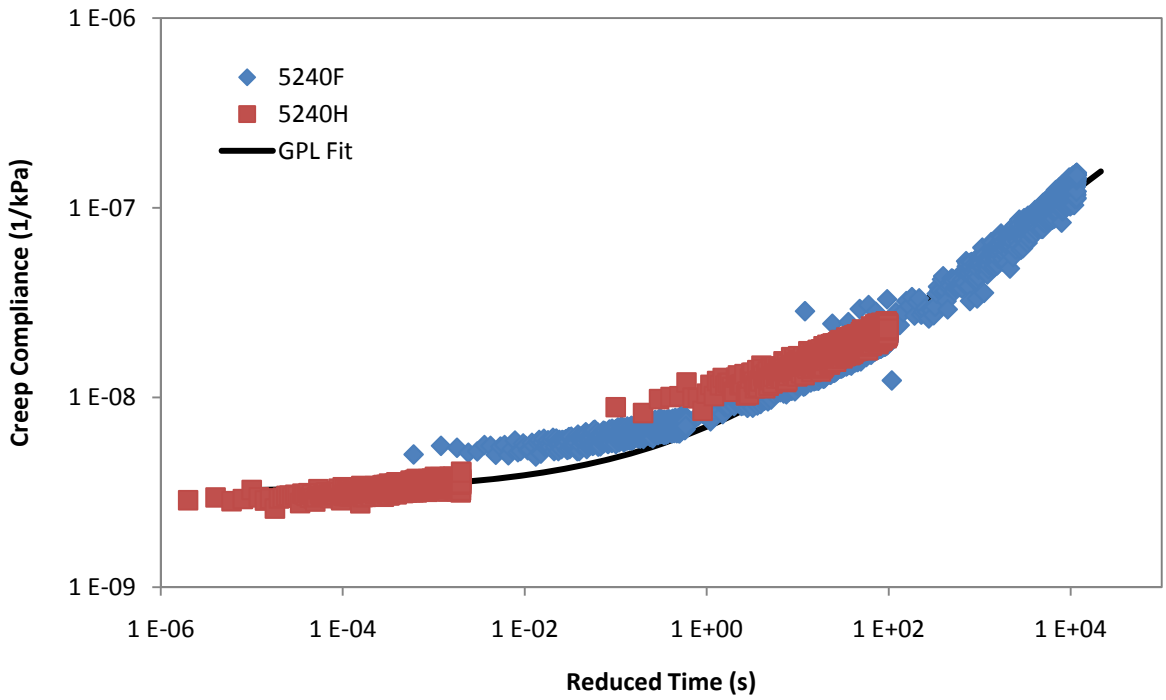

Figure 3.23 40% RAP Mixture Creep Compliance Master Curve

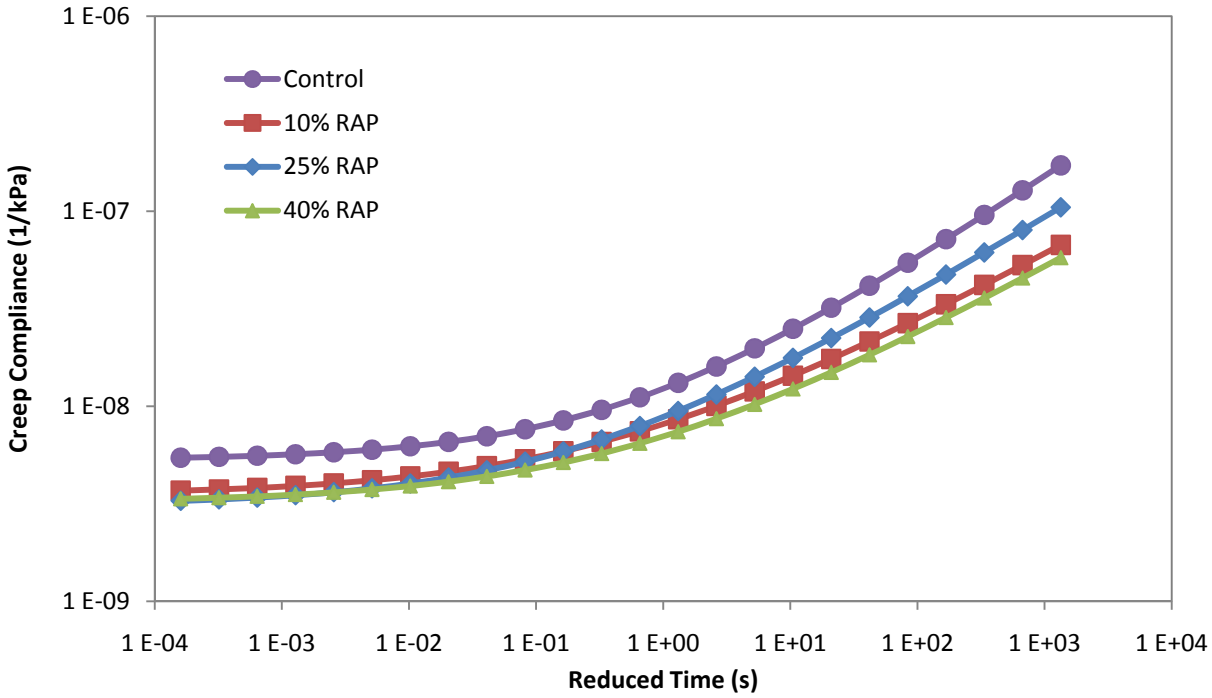

Figure 3.24 Average Mixture Creep Compliance Master Curves

3.4 Indirect Tensile Strength

The tensile strengths at -10°C for the individual specimens and averages for each mixture type are summarized in Table 3.6. Figures 3.25 through 3.27 show the results graphically for the RAP and PG Mixtures. The statistical comparisons of the various mixtures are summarized in Tables 3.7 and 3.8. The average strength for the RAP mixtures does not change significantly from the 0% to the 10% level, but then is significantly different at 25% and 40% RAP. There is a decrease in average strength shown from the 25% RAP mixture to the 40% RAP mixture. The different PG grade mixtures show consistent average strength for the PG 58, PG 64, and PG 70 mixtures. The PG 76 mixture has a significant increase in strength over the other mixtures. There is an increase in average strength from the PG-28 to the PG-22 mixtures, but the difference is not significant (p value = 0.10).

Table 3.6 Summary of Indirect Tensile Strengths

Mix Type	Sample ID	Strength (kPa)	Average Strength (kPa)	Standard Deviation
Control PG 64-28	6000I	3894.4	3807.2	344.5
	6000J	3288.3		
	6000K	3654.7		
	6000L	4054.5		
	6000M	4144.2		
10% RAP	5710E	3495.9	3503.7	11.1
	5710F	3511.6		
25% RAP	5325E	4429.5	4507.7	348.4
	5325F	4999.1		
	5325G	4176.2		
	5325I	4426.1		
40% RAP	5240E	4102.1	4106.5	365.1
	5240F	3634.5		
	5240G	4657.3		
	5240H	4022.8		
	5240I	4115.6		
Field Core	FC 3	3825.8	3389.4	617.2
	FC 5	2952.9		
PG 58-28	6058A	4013.7	3925.7	373.3
	6058B	3680.3		
	6058C	3593.4		
	6058D	4415.3		
PG 70-22	6070A	3464.7	3796.7	566.7
	6070B	4533.3		
	6070C	3256.2		
	6070D	3932.4		
PG 76-22	6076A	5276.9	5005.5	264.5
	6076B	4977.1		
	6076C	4653.9		
	6076D	5114.0		

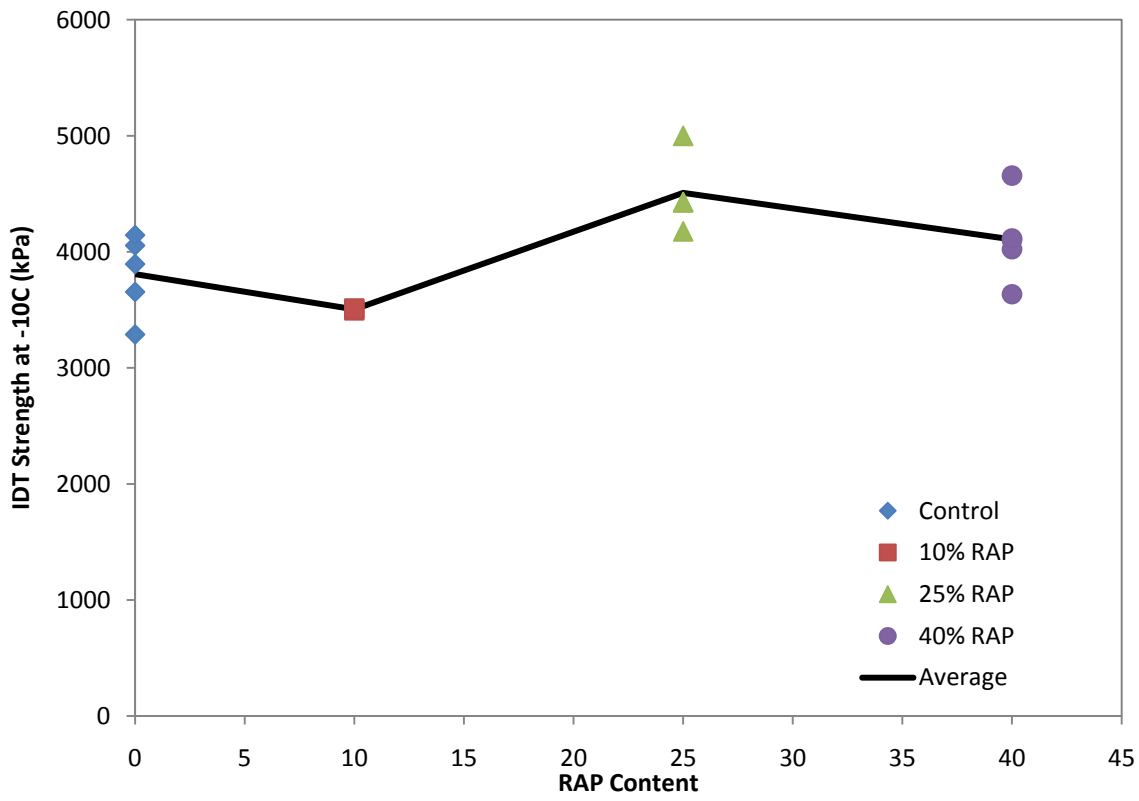

Figure 3.25 Indirect Tensile Strengths for RAP Mixtures

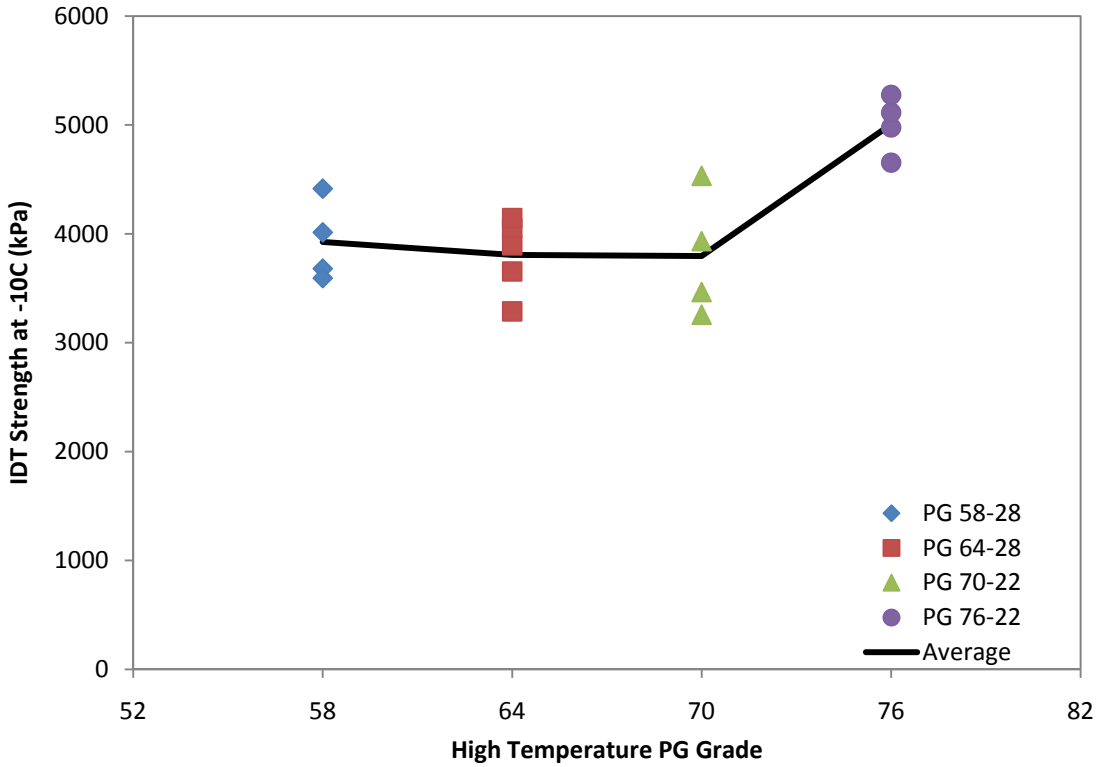

Figure 3.26 Indirect Tensile Strengths for PG Mixtures by High Grade

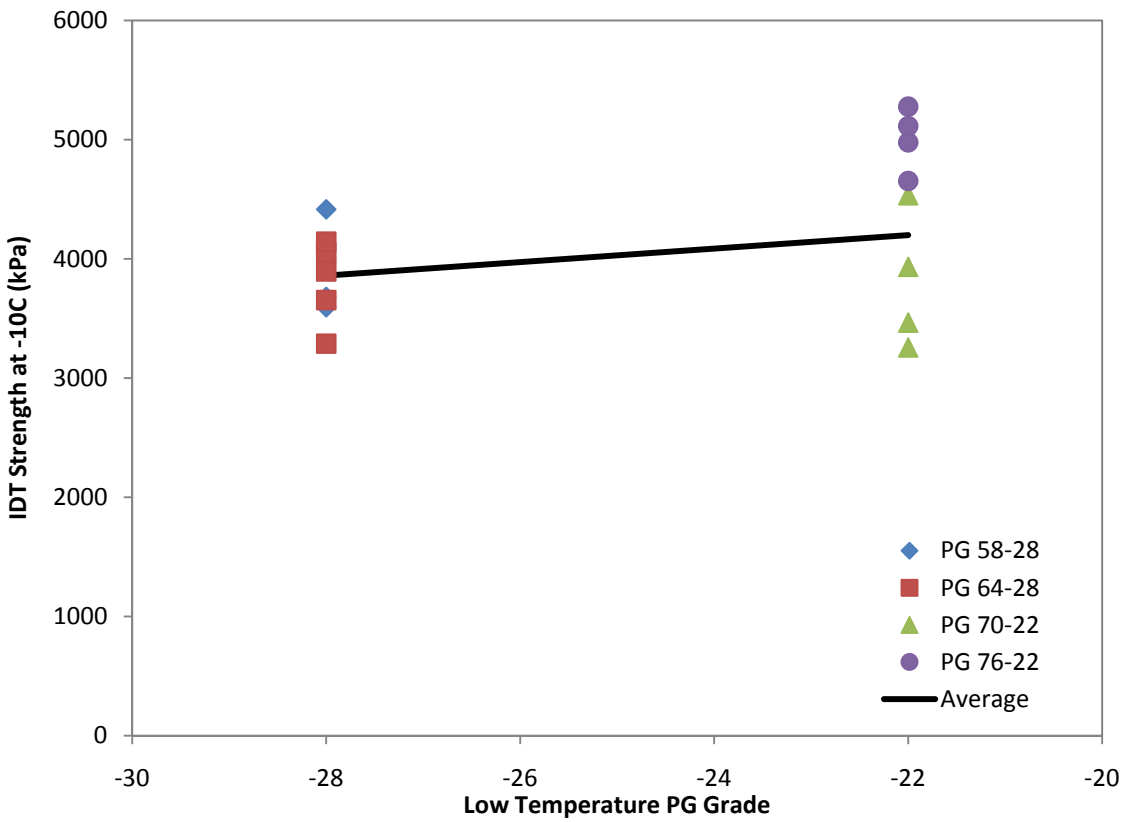

Figure 3.27 Indirect Tensile Strengths for PG Mixtures by Low Grade

Table 3.7 IDT T-Test Results for RAP Mixtures

	Control	10% RAP	25% RAP	40% RAP
10% RAP	0.12	-	-	-
25% RAP	0.02	0.01	-	-
40% RAP	0.22	0.02	0.14	-
Field Cores	0.51	0.84	0.20	0.32

Table 3.8 IDT T-Test Results for PG Mixtures

	PG 64	PG 58	PG 70
PG 58	0.64	-	-
PG 70	0.98	0.72	-
PG 76	0.00	0.00	0.02

4.0 ESTIMATING EFFECTIVE PG GRADE

This chapter will present the methods examined in this study for estimating the effective PG grade of the binder in a RAP mixture.

4.1 High Temperature Grade

4.1.1 Linear Blending Prediction

A simple linear blending calculation can be done using the PG grade of the virgin binder and the extracted PG grade of the RAP material. The percent binder replacement in the resulting RAP mixture can be calculated using Equation 4.1:

$$\%\ binder\ replacement = \frac{\%\ ac\ in\ RAP \times \%\ RAP\ in\ mix}{\%\ ac\ in\ mix} \tag{4.1}$$

Assuming that 100% of the RAP binder blends with the virgin binder, the high temperature PG grade can be estimated by using Equation 4.2:

$$Estimated\ PG\ grade = \frac{\%\ RAP}{100} \times RAP\ PG + \left(1 - \frac{\%\ RAP}{100}\right) \times virgin\ PG \tag{4.2}$$

These equations were used to estimate the PG grade of the RAP mixtures in this study; the results are summarized in Table 4.1 below.

Table 4.1 Estimated High PG Grade Using Linear Blending

Mixture	% binder replacement	Estimated High PG grade
10% RAP	8.5	67.1
25% RAP	22.9	72.2
40% RAP	37.3	77.4

The advantage of this method is that it is a very simple and straightforward calculation if the PG grade of the RAP binder is known. However, it assumes full blending of the binders, which is known not to be the case in the field. It also does not take into account aging of the binder during the mixing and compaction process and the interaction of binder and aggregate.

4.1.2 Empirical Method Using Measured Mixture Properties

In this method, the indirect tensile strength data from the different PG grade binders was used to establish a relationship between a material property and the high temperature PG grade. Based on the data gathered in this research project, there are two different approaches to determining this relationship. The statistical analysis of the indirect strength test data indicates that there is no significant difference between the PG 58, PG 64, and PG 70 mixtures. Therefore, a bi-linear fit can be used to represent the relationship. The average strength for all the PG 58, PG 64, and PG 70 specimens is used for the flat portion of the curve and a linear fit is performed from the average value to the PG 76 data over the PG 70 to PG 76 range. Alternatively, a polynomial form can be used to create a continuous function for the relationship; both forms are

shown in Figure 4.1. The functional forms of the two relationships are shown in Equations 4.3 and 4.4.

Bi-Linear: $$Strength\ (kPa) = 3840.5\ \ (for\ PG < 70) \qquad (4.3)$$
$$Strength\ (kPa) = 194.2(PG) - 9752\ (for\ PG > 70)$$

Polynomial: $$Strength\ (kPa) = 0.148(PG)^3 - 24.5(PG)^2 + 1335(PG) - 20007 \qquad (4.4)$$

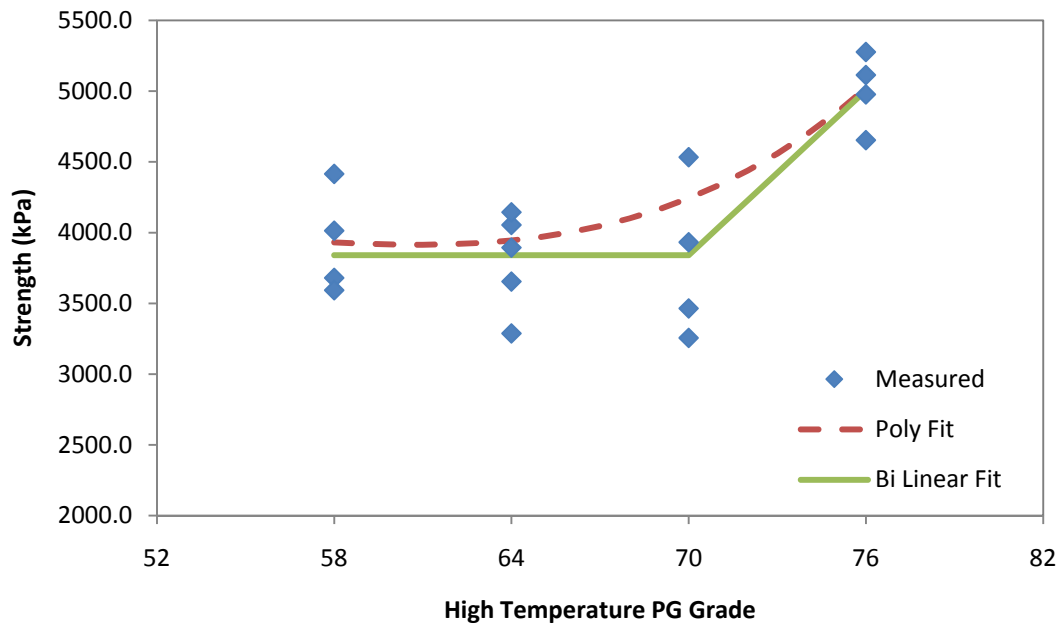

Figure 4.1 Relationship Between High Temperature PG Grade and IDT Strength

The estimated high temperature PG grade for each RAP mixture is then determined by inputting the measured strength into the equation and calculating the estimated PG grade. This can be done graphically as well. The estimated PG grades determined from the polynomial and bi-linear relationships for the RAP mixtures are summarized in Table 4.2. The average strength for the 10% RAP mixture was 3504 kPa; this is below the average value for the control mixture and also below the fit lines for either method, so it is assumed that the effective PG grade of the binder in the 10% RAP mixture is the same as that for the control mixture.

Table 4.2 Estimated Effective High PG Binder Grades from Empirical Analysis

	25% RAP	40% RAP
Polynomial Fit	72.6	68.1
Bi Linear Fit	73.4	71.4

The main advantage of this method is that it considers the mixture properties and does not rely on extracted binder data. The major disadvantage is the amount of testing that is required to establish the relationship between material properties and the PG grade of the binder. The relationship has to be established for each type of mixture (gradation, density) and may also vary with the test temperature. The strength testing in this project was performed at -10°C, so

may not be representative of the differences in strength at temperatures closer to the high PG grades. Also, the four different PG grade binders were not from the same source and could have very different chemical compositions, which would change the relationships between behavior at different temperatures. The PG 70-22 and PG 76-22 binders were modified, which will also influence the behavior and make it more difficult to interpolate between the various mixtures.

4.1.3 Method Using the Hirsch Model

The Hirsch Model (Eq 2.3) was used to back calculate the binder |G*| values from the measured mixture dynamic modulus curves. The back calculated |G*| values from the mixture can be compared with the recovered |G*| values measured on the extracted binder to evaluate the amount of blending that is happening between the virgin and RAP binders. If the two curves overlap, that indicates a significant amount of blending occurs. These graphs at 20°Cfor the RAP mixtures in this study are shown in Figures 3.11 through 3.13 and indicate that full blending is not occurring.

The percent difference between the back calculated |G*| and the recovered |G*| was calculated at 20°C for several frequencies for each mixture. These values are summarized in Figures 4.2 through4.4. The difference between the back calculated and recovered |G*| values decreases as the reduced frequency increases, meaning the difference is more pronounced at the slow loading range (which also corresponds to high temperature). There is significant specimen to specimen variability in this comparison, so it is not possible to determine a trend with respect to the amount of RAP in the mixture.

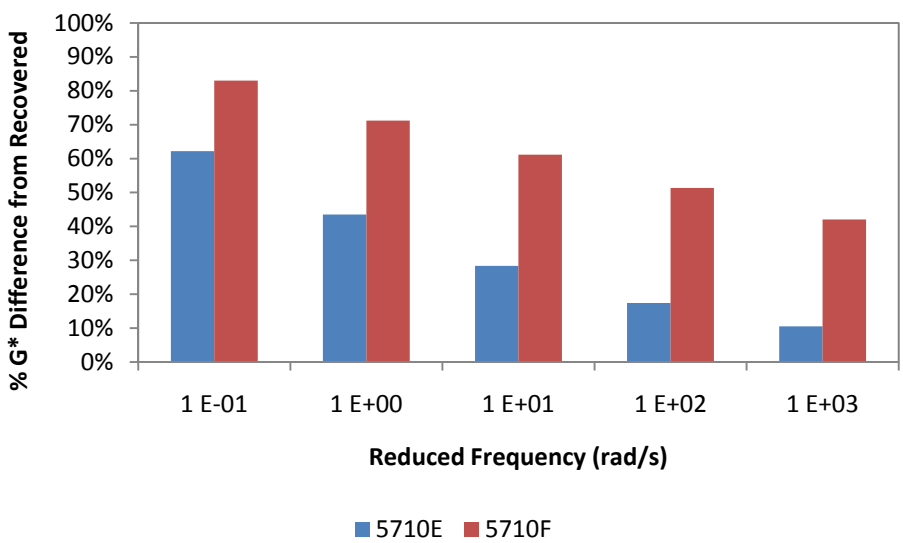

Figure 4.2 Percent Difference in G* values for 10% RAP Mixture

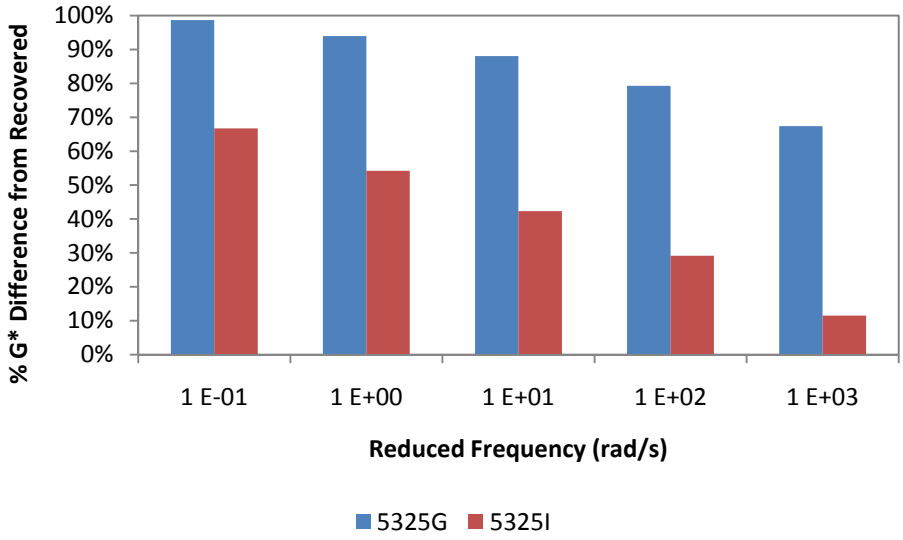

Figure 4.3 Percent Difference in G* values for 25% RAP Mixture

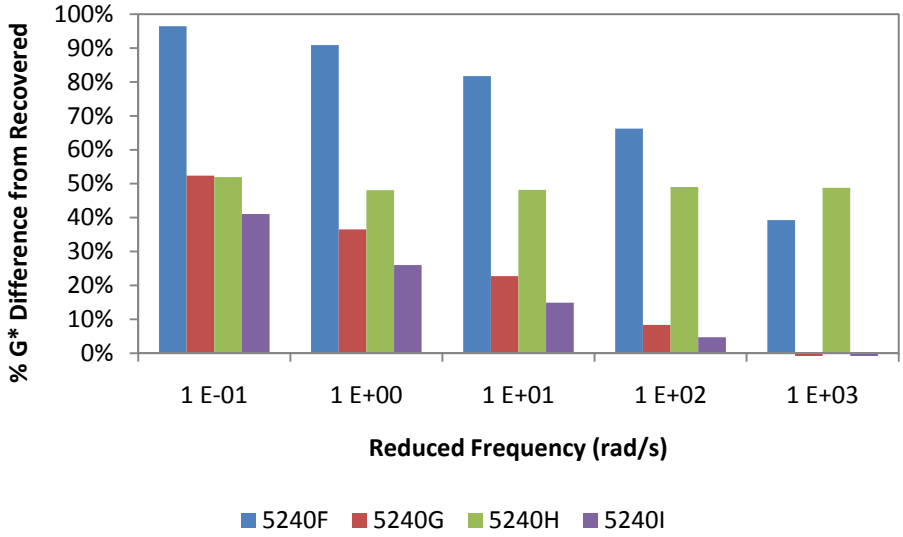

Figure 4.4 Percent Difference in G* values for 40% RAP Mixture

The back calculated and recovered |G*| values for a particular RAP mixture can also be compared with the back calculated |G*| values from the different PG grade mixtures. This is done at 20°C and a frequency of 10 radians/sec for the three RAP mixtures and is shown in Figures 4.5 through 4.7. From this information, and knowing the grade of the recovered binder (Table 3.4), the effective grade of the mixture can be interpolated. Taking the 25% RAP mixture as an example: The average |G*| for the 25% RAP mixture falls between the values for the PG 76-22 mix and the recovered binder |G*|. Assuming a linear relationship exists, the effective grade for the 25% RAP mixture is calculated to be 82.7. The estimated values for all three RAP mixtures are summarized in Table 4.3.

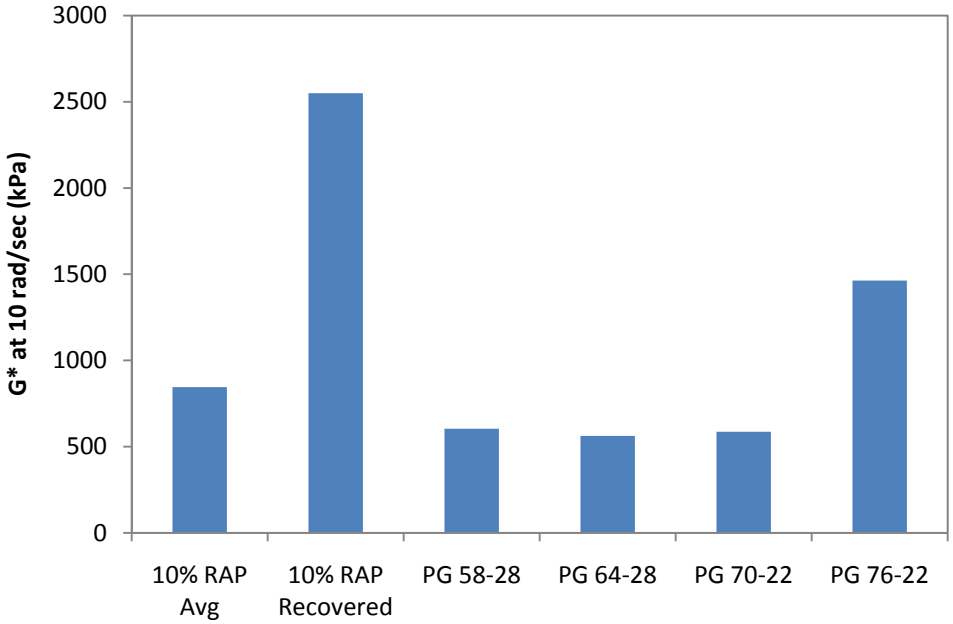

Figure 4.5 Comparison of 10% RAP Mixture with PG Mixtures

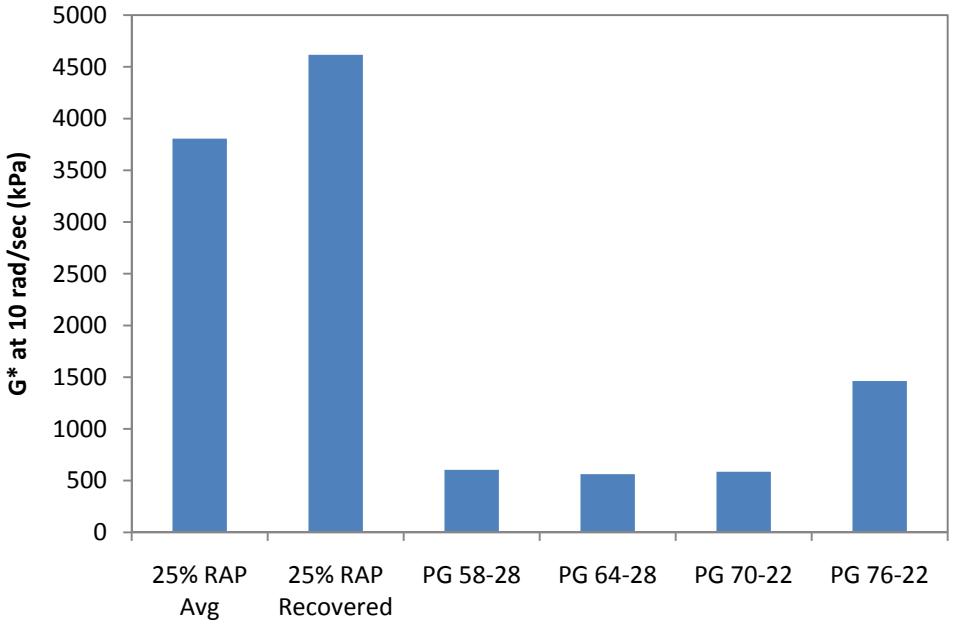

Figure 4.6 Comparison of 25% RAP Mixture with PG Mixtures

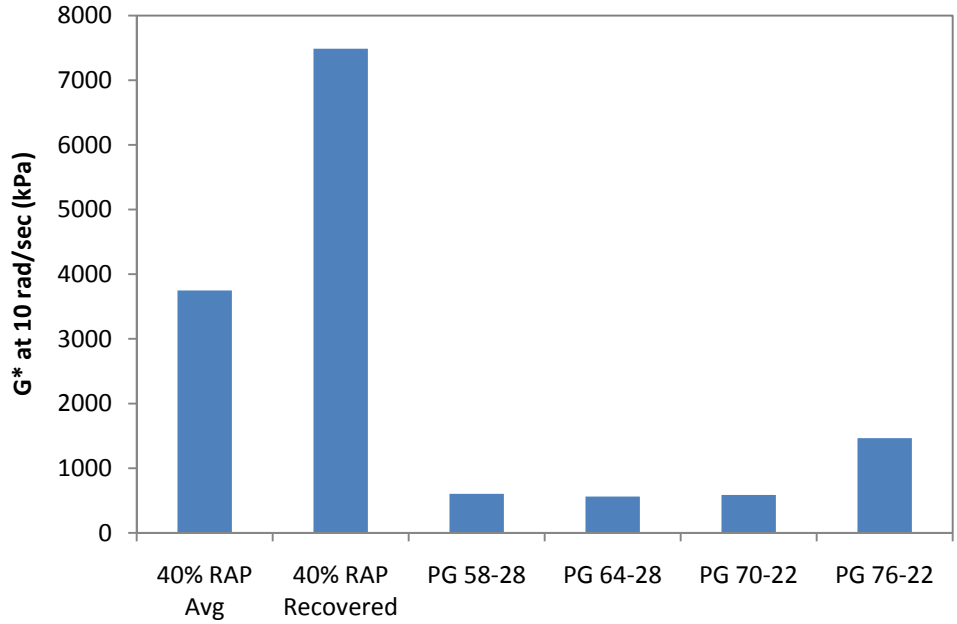

Figure 4.7 Comparison of 40% RAP Mixture with PG Mixtures

Table 4.3 Estimated High PG Grade Using Hirsch Model

Mixture	Estimated High PG grade
10% RAP	71.8
25% RAP	82.7
40% RAP	84.8

The advantage of this method is that it relies on measured properties of the mixture and is compared to the fully blended recovered binder. The comparison performed for this project was done at a frequency of 10 radians/sec, which corresponds to the frequency used to grade binders. The temperature is 20°C however, so the estimated PG grade may be different if other temperatures are evaluated. It is not possible to test mixtures at the high PG grade temperatures, so the measured mixture properties would have to be shifted to higher temperatures using the time-temperature superposition principle. The shift factors for the high PG grade temperatures would have to be established through more extensive (larger temperature range) binder testing.

The estimated binder grade using this method is determined using interpolation between the recovered binder |G*| and back calculated |G*| from mixtures with different PG grade binders. The various binders likely have different chemical compositions because they were obtained from different sources and some are modified. The different chemical compositions may cause drastically different behaviors at other temperatures, so linear interpolation may not be appropriate. It is recommended that the virgin binder properties be measured and used for comparison to avoid this issue.

The Hirsch method only considers the |G*| value and not the phase angle. However, both properties are needed to determine the PG grade. It is not possible to back calculate the binder phase angle from the mixture properties using the Hirsch model. There are methods of estimating the phase angle from the |G*| master curve (Rowe et al. [19]). As with the |G*| master

curves, difficulties exist in shifting the phase angle values to the high PG grade temperatures at which they would be useful.

4.2 Low Temperature Grade

4.2.1 Linear Blending Prediction

The same linear blending calculation that was done for the high PG grade can also be done for the low PG grade. Equations 4.1 and 4.2 are used again to estimate the low PG grade of the RAP mixtures in this study shown in Table 4.4. As discussed for the high PG grade estimation, this method is simple and straight forward, but does not represent what happens in the field with the mixture.

Table 4.4 Estimated Low PG Grade Using Linear Blending

Mixture	Estimated Low PG grade
10% RAP	-26.0
25% RAP	-22.5
40% RAP	-19.0

4.2.2 Empirical Method Using Measured Mixture Properties

In this method, the indirect tensile strength data from the different PG grade binders was used to establish a relationship between a material property and the high temperature PG grade. The PG xx-28 and PG xx-22 mixtures were pooled together and a linear fit was used to represent the relationship, as shown in Figure 4.8. Statistically, the two sets of data are not significantly different (p value of 0.10), however, estimated low PG grades for the different RAP mixtures were calculated and are summarized in Table 4.5 below. The 10% RAP mixture had a strength below the average value for the PG xx-28 mixtures, so it was assumed that the effective low PG grade of the binder in the 10% RAP mixture was the same as that for the control mixture. The advantages and disadvantages of this method are the same as those discussed for the empirical estimation of the high temperature PG grade.

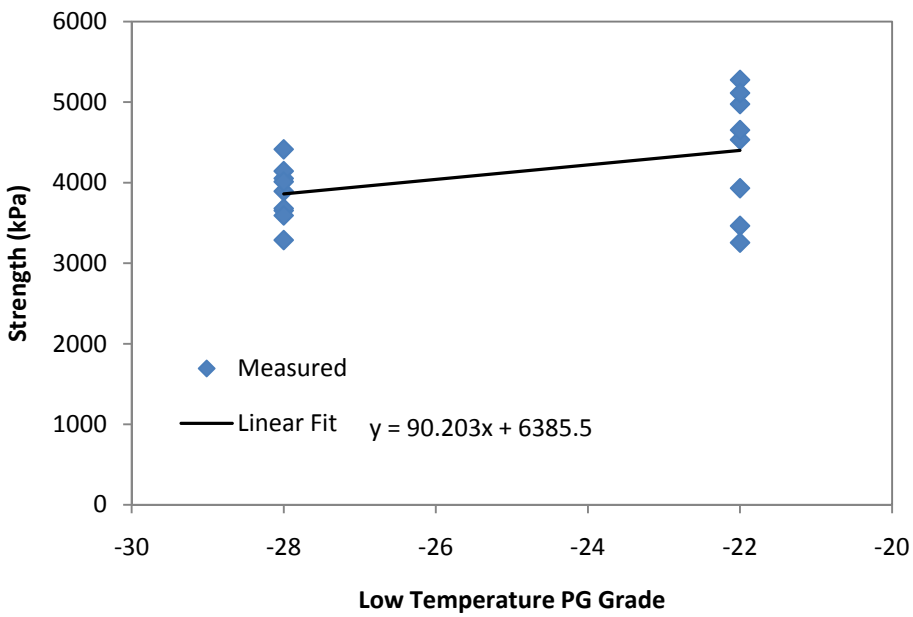

Figure 4.8 Relationship Between Low Temperature PG Grade and IDT Strength

Table 4.5 Estimated Effective Low PG Binder Grades from Empirical Analysis

Mix	Est Low PG
10% RAP	-28
25% RAP	-20.8
40% RAP	-25.3

4.2.3 Method Using the Hirsch Model

The |G*| values back calculated using the Hirsch Model can also be used to estimate the low PG grade that provides resistance to fatigue cracking. Similar to what was done to estimate the high temperature PG grade, linear interpolation between the back calculated mixture |G*| values and the recovered |G*| and the PG mix |G*| values was performed. The estimated low PG grades from this analysis are summarized in Table 4.6 below. The temperature at which |G*| is measured for low temperature (fatigue) grading is close to 20°C, so the data obtained in this project does not require shifting to significantly different test temperatures. The shift factors obtained from the original dynamic modulus testing of the mixture could be used. Also, the phase angle values for the binder could be estimated from the back calculated |G*| using Rowe's procedure (19). If this is done, then the temperature at which |G*| sinδ = 5000 kPa could be determined directly.

Table 4.6 Estimated Low PG Grade Using Hirsch Model

Mixture	Estimated Low PG Grade
10% RAP	-22.0
25% RAP	-25.5
40% RAP	-21.2

4.2.4 Method Using Creep Compliance

The theoretical procedure used to estimate the low temperature PG grades from measured creep compliance follows a method suggested by Zofka (20). The low temperature creep compliance measurements for each specimen were first converted to creep stiffness by taking the inverse of the creep compliance; a typical creep stiffness curve is shown in Figure 4.9. The Hirsch model relationship was then used to back calculate the binder stiffness from the mixture stiffness. The form of the Hirsch model necessitates the use of an error minimization technique to back calculate the binder stiffness; this must be done for each individual data point. A more efficient approach is to establish the binder-mixture stiffness relationship for a particular mixture using assumed binder stiffness values and a forward calculation of the Hirsch model. A power law equation fit to this relationship can be used to estimate the binder stiffness from any mixture stiffness value using the functional relationship. This makes it much easier to manipulate the data in a spreadsheet. The binder-mixture stiffness relationships for the RAP mixtures evaluated in this study are shown in Figure 4.10 and the power law coefficients are shown in Table 4.7. The Hirsch Model requires English units, so the creep stiffness and resulting binder-stiffness relationships are in psi. Once the binder stiffness is determined, it was converted to MPa for further analysis.

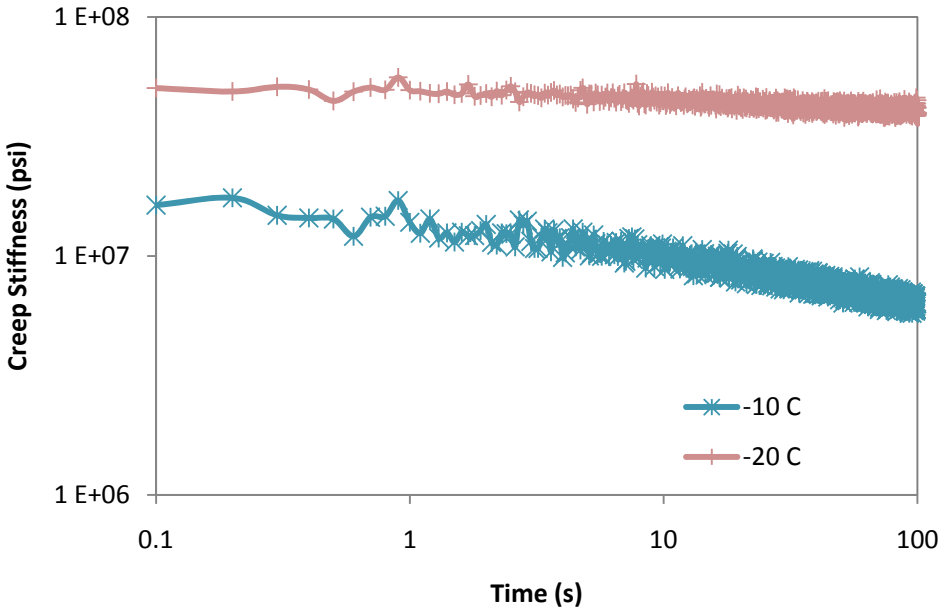

Figure 4.9 Typical Creep Stiffness Curve

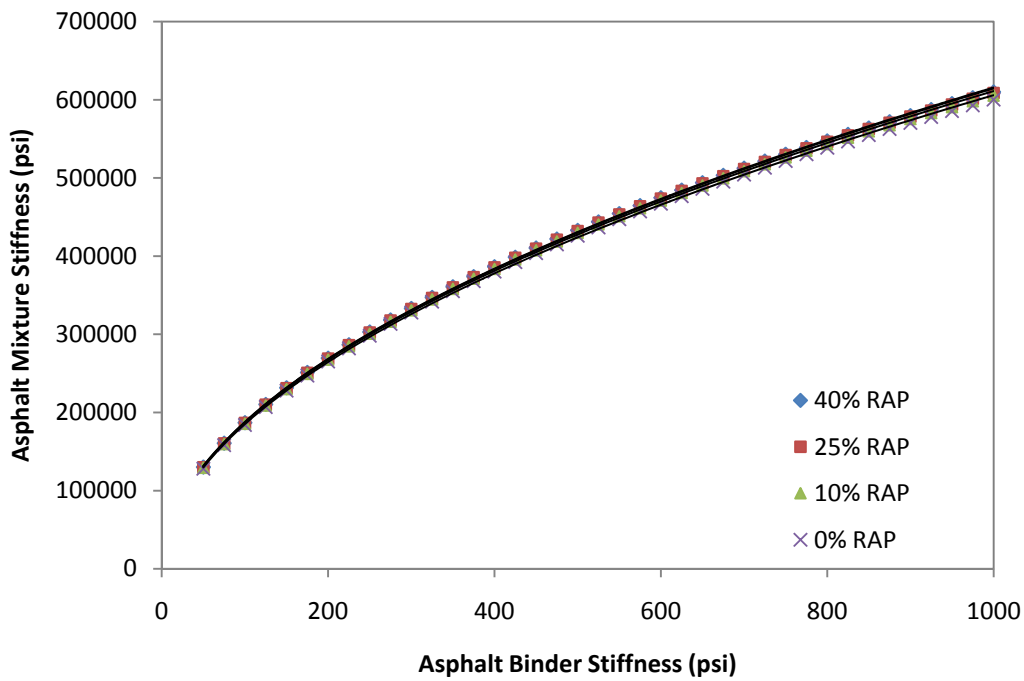

Figure 4.10 Binder-Mixture Stiffness Relationships Using Hirsch Model

Table 4.7 Power Law Coefficients for Binder-Mixture Stiffness Relationships

Mixture	A	n
0% RAP	17276	0.5150
10% RAP	17420	0.5150
25% RAP	17513	0.5150
40% RAP	17546	0.5151

The binder stiffness as a function of time was plotted on logarithmic scale to determine the S value and m-value for the mixture at a time of 60 seconds, as shown schematically in Figure 4.11. Practically, the measured data contains noise, so the binder stiffness data from 55 to 65 seconds was fit using a power law; the value of stiffness at 60 seconds was calculated and the exponential coefficient is the m-value. The values calculated for each specimen and temperature are summarized in Table 4.8. The S-values and m-values are plotted versus temperature in Figures 4.12 and 4.13, respectively. The Superpave criteria for these parameters are also shown in the figures.

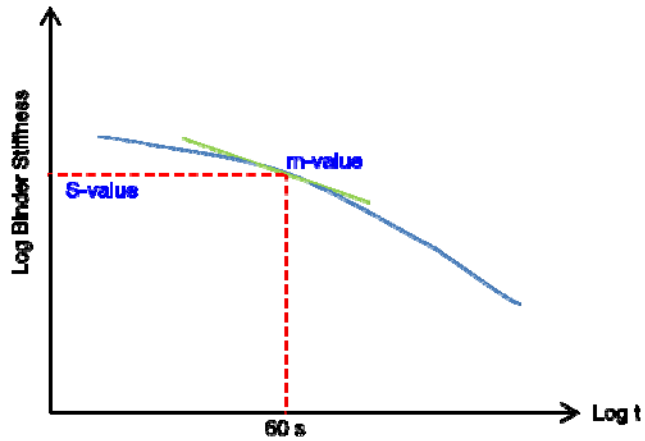

Figure 4.11 Determination of S-value and m-value

Table 4.8 S-values and m-values Determined from Binder Stiffness Curves

% RAP	Specimen	S-value (MPa)			m-value		
		-20°C	-10°C	0°C	-20°C	-10°C	0°C
0	6000I	9510	342	203	0.231	0.558	0.867
	6000J	5518	588	628	0.122	0.477	0.735
	6000K	600	54	57	0.417	0.624	1.015
10	5710E	16609	586	549	0.057	0.451	0.742
	5710F	11016	679	299	0.400	0.627	0.822
25	5325G	18958	213	851	0.096	0.376	0.779
	5325I	17571	12	81	0.498	0.855	0.704
40	5240F	24466	785	n/a	-0.042	0.630	n/a
	5240H	6312	1298	1060	0.140	0.638	0.454

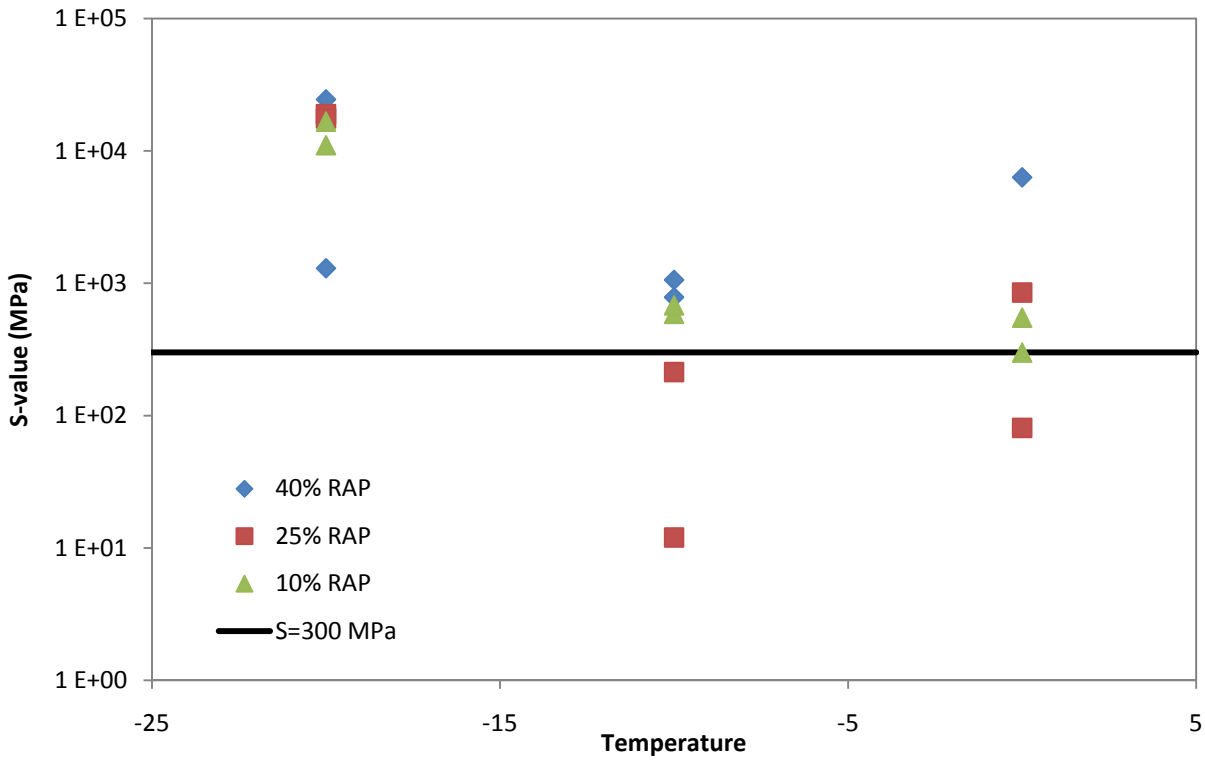

Figure 4.12 Calculated S-values for RAP Mixtures

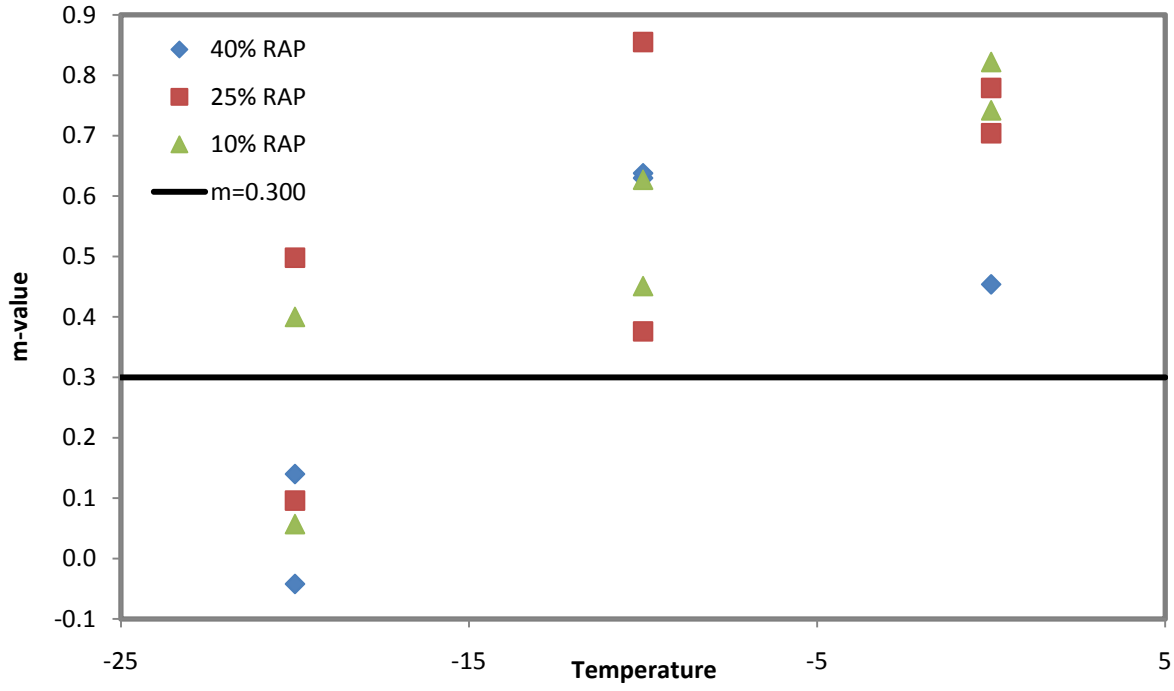

Figure 4.13 Calculated m-values for RAP Mixtures

The stiffness values should decrease as the temperature increases. However, the data for this study show a decrease from -20°C to -10°C and then an increase in stiffness to 0°C. The explanation for this is experimental issues in testing at the -10°C and 0°C temperatures. The m-values show a reasonable trend with respect to temperature for the 10% RAP and 25% RAP mixtures despite the testing issues. There was significant specimen to specimen variability, but a linear fit can be applied to the m-value data and the temperature at which m=0.300 calculated. These values and the corresponding estimated low temperature PG grade are summarized in Table 4.9.

Table 4.9 Estimated Low PG Grade from m-value

Mixture	Temp where m=0.300	Estimated Low PG grade
10% RAP	-17.8	-27.8
25% RAP	-21.3	-31.3
40% RAP	-14.5	-24.5

The advantage of this method is that it does not require any binder testing; it relies solely on properties that are measured from the mixture. In this project, creep compliance was measured on IDT specimens at low temperatures. Both the low temperatures and IDT setup require a significant technician skill and can easily result in high specimen to specimen variability. An alternative method would be to measure the complex modulus of a uniaxial specimen and use linear viscoelastic theory to convert complex modulus to creep compliance. This testing could be done using the Asphalt Mixture Performance Test (AMPT) equipment developed for mixture performance testing and would result in lower variability in the data.

5.0 SUMMARY AND RECOMMENDATIONS

5.1 Summary

The objective of this research project was to develop a method to determine or estimate the binder grade in mixtures designed with RAP from the properties of the mixture itself. Three different RAP percentages (10%, 25%, 40%) were evaluated for a 12.5 mm Superpave mixture. A PG 64-28 virgin binder was used. Additionally, testing was done on virgin mixtures with PG 58-28, PG 70-22, and PG 76-22 binders. Dynamic modulus, creep compliance, and strength tests were run in the indirect tensile mode for the various mixtures. The Hirsch model was used to back calculate the binder |G*| values from the measured mixture dynamic modulus values. Partial |G*| master curves were measured on the extracted binder from each mixture and the recovered binder was also PG graded.

Several methods of estimating the effective PG grade of the binder were evaluated. Empirically based methods of interpolating values of measured mixture properties are straightforward, but require an extensive amount of testing in the laboratory. The relationship between material properties and PG grade must be established for each type of mixture (gradation, asphalt content).

The most promising methods for determining the effective PG grade of the mixture use the Hirsch model to back calculate binder |G*| from the measured mixture dynamic modulus. Some difficulties exist in determining the high temperature PG grade because of the large difference in temperatures between the dynamic modulus testing and PG grading temperatures. However, recovered and virgin binder information can be used to compare with the back calculated |G*| from the mix to estimate the effective high temperature PG grade. The low temperature PG grade can be estimated from mixture testing only because the range of temperatures for PG grading corresponds to the dynamic modulus testing temperatures.

5.2 Recommended Procedure for Estimating PG Grade

Based on the results of the research conducted in this project, the research team recommends the following procedure for estimating the PG grade of mixtures containing RAP:

1. Perform complex modulus testing on at least three replicate specimens. Recommend that temperatures from -20°C to 30°C be used to develop master curves and obtain desired shift factors. This may require modification of current AMPT devices to test at lower temperatures.
2. To estimate high temperature PG grade:
    a. Obtain |G*| master curve for virgin binder
    b. Obtain |G*| master curve for extracted and recovered mixture binder
    c. Back calculate |G*| using the measured dynamic modulus and the Hirsch model
    d. Compare back calculated |G*| to virgin and recovered values to estimate the effective high temperature PG grade
3. To estimate low temperature PG grade for fatigue:
    a. Back calculate |G*| using the measured dynamic modulus and the Hirsch model
    b. Use the Rowe method to determine the phase angles from the back calculated |G*| master curve

   c. Shift master curves to determine temperature at which $|G^*| \sin\delta = 5000$ kPa
4. To estimate low temperature PG grade for thermal cracking:
   a. Use linear viscoelastic theory to convert complex modulus to creep compliance
   b. Calculate creep stiffness of mixture
   c. Use Hirsch relationship to calculate creep stiffness of binder
   d. Calculate S-value and m-value for each mixture as a function of temperature
   e. Calculate temperature at which S=300 MPa and m=0.300
   f. Determine effective low temperature PG grade

5.3 Recommendations for Further Research

Further research is required on different types of RAP mixtures and different virgin PG grades to verify and refine the procedures developed as part of this research project. In particular, it is important to perform testing on plant produced mixtures to capture what truly happens to these mixtures in the field. Future testing should focus on the low to intermediate temperature testing as this is the biggest concern with the addition of aged RAP binder in the mix.

6.0 REFERENCES

1. FHWA RAP Expert Task Group Website: http://www.morerap.us/

2. Lee, K.W., A Shukla, S. Vankatram, N. Soupharath "Evaluation of Permanent Deformation and Fatigue Cracking Resistance Characteristics of Recycled Pavement Binder" Final Research Report to Rhode Island DOT, 1998.

3. McDaniel, R., and R.M. Anderson. "Recommended Use of Reclaimed Asphalt Pavement in the Superpave Mix Design Method: Technician's Manual", NCHRP Report 452, Transportation Research Board- National Research Council, National Academy Press, Washington, D.C., 2001.

4. McDaniel, Rebecca and R.M. Anderson. "Recommended Use of Reclaimed Asphalt Pavement in the Superpave Mix Design Method: Guidelines". NCHRP Research Results Digest, Number 253, 2001.

5. McDaniel, Rebecca S., H. Soleymani, R.M. Anderson, P. Turner, R. Peterson. "Recommended Use of Reclaimed Asphalt Pavement in the Superpave Mix Design Method". Contractor's Final Report, NCHRP Web Document 30 (Project D9-12), 2000.

6. Soleymani, H., M. Anderson, R. McDaniel, and M. Abdelrahman "Investigation of the Black Rock Issue for Recycled Asphalt Mixtures", Journal of the Association of Asphalt Paving Technologists, Vol. 69, p. 366-390, 2000.

7. Stephens, J., J. Mahoney, and C.Dippold "Determination of the PG Binder Grade to Use in a RAP Mix", Final Report JHR 00-278, Project 99-1, Connecticut Department of Transportation, 2001.

8. Stroup-Gardiner, M., and C. Wagner "Use of Reclaimed Asphalt Pavement in Superpave Hot-Mix Asphalt Applications", Transportation Research Record 1681, 1999.

9. National Cooperative Highway Research Program Synthesis of Highway Practice. "Recycling Materials for Highways". 1978.

10. Harrington, Jason. "Recycled Roadways". FHWA Public Roadways. 2005 Website: http://www.tfhrc.gov/pubrds/05jan/02.htm

11. McDaniel, Rebecca S, H. Soleymani, Shah, A. "Use of Reclaimed Asphalt Pavement Under Superpave Specifications". Contractors Final Report, FHWA/IN/JTRP-2002/6 May 2002. Website: http://rebar.ecn.purdue.edu/JTRP_Completed_Project_Documents/SPR_2143/FinalReport/spr_2143_final.pdf

12. Abdulshafi, Osama, B. Kedzierski, M.G. Fitch. "Determination of Recycled Asphalt Pavement Content in Asphalt Mixes Based on Expected Durability". Ohio Department of

Transpotation December 2002 Website:
http://www.dot.state.oh.us/research/2002/Materials/14734-FR.pdf

13. Sondag, Michael S., B. Chadbourn, Drescher A. "Investigation of Recycled Asphalt Pavement". Contractor's Final Report for the Minnesota DOT. February 2002 Website: http://www.lrrb.org/pdf/200215.pdf

14. Thompson, Gary. "Determining Asphalt Content for Recycled Asphalt Pavement Materials". Asphalt Pavement Association of Oregon. July 2003 Website: www.oregon.gov/ODOT/TD/TP_RES/ docs/Reports/DetAsphConRAP.pdf

15. Christensen, Donald W., R.F. Bonaquist. "VMA: One Key to Mixture Performance". North Central Superpave Center News. Spring 2005

16. Daniel, J.S., and A. Lachance, “Mechanistic and Volumetric Properties of Asphalt Mixtures with RAP”, Transportation Research Record: Journal of the Transportation Research Board, No.1929, Transportation Research Board of the National Academies, Washington, D.C., 2005, pp. 28-36.

17. Kim, Y.R., Y. Seo, M. King, and M. Momen “Dynamic Modulus Testing of Asphalt Concrete in Indirect Tension Mode”. Transportation Research Board, 2004.

18. Christensen, D.W., T. Pellinen, R. Bonaquist “Hirsch Model for Estimating the Modulus of Asphalt Concrete”, Journal of the Association of Asphalt Paving Technologists, Vol. 72, pp. 97-121, 2003.

19. Rowe, G.M., “Phase angle determination and interrelationships within bituminous materials,” Proceedings of the 7th Int. RILEM Symposium on Advanced Testing and Characterization of Bituminous Materials, Rhodes, Greece, (Book 1, Edited by Loizos, Partl, Scapas & Al-Qadi), May 27 to 29, 2009. pp. 43-52.

20. Zofka, A., M. Marasteanu, X. Li, T. Clyne, and J. McGraw. “Simple Method to Obtain Asphalt Binders Low Temperature Properties from Asphalt Mixtures Properties”, Journal of the Association of Asphalt Paving Technologists, Vol. 74, pp. 255-282, 2005.

7.0 APPENDICES

APPENDIX A: MIXTURE DESIGN DATA

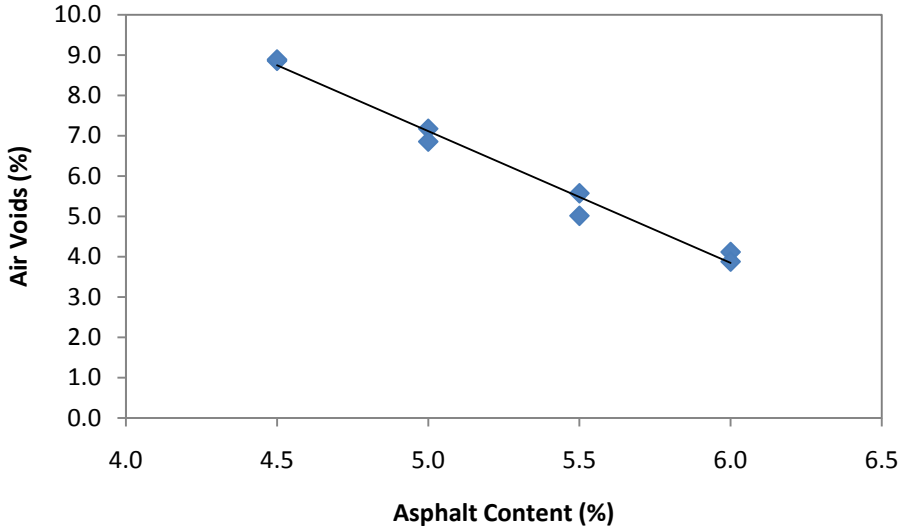

Figure A.1 Air Voids versus Asphalt Content for Control Mixture

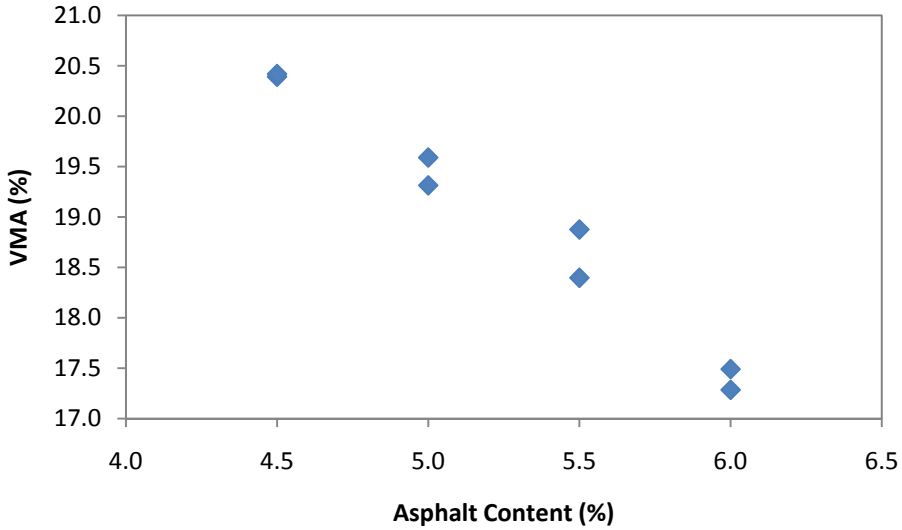

Figure A.2 VMA versus Asphalt Content for Control Mixture

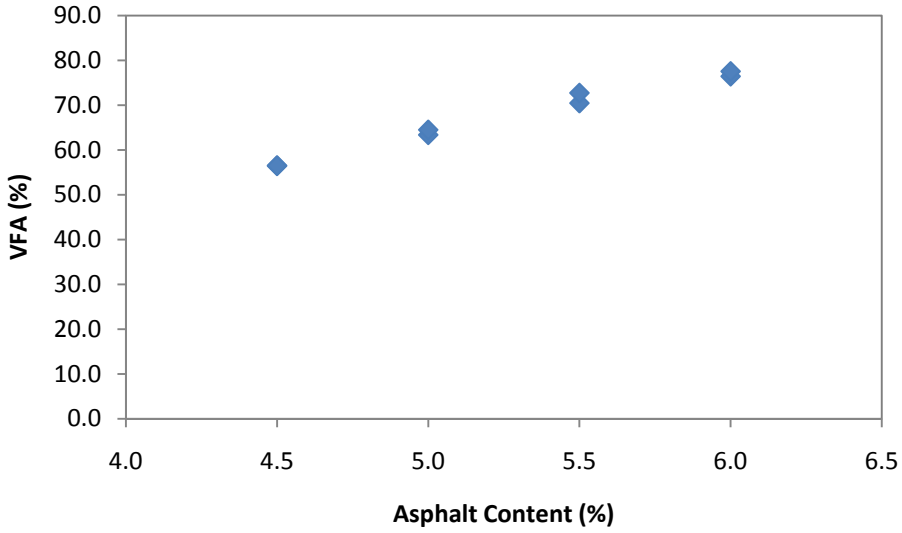

Figure A.3 VFA versus Asphalt Content for Control Mixture

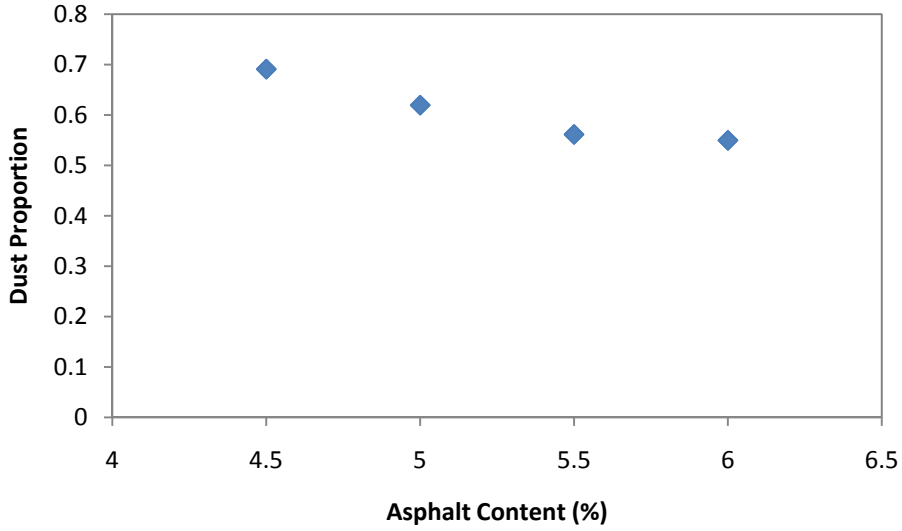

Figure A.4 Dust Proportion versus Asphalt Content for Control Mixture

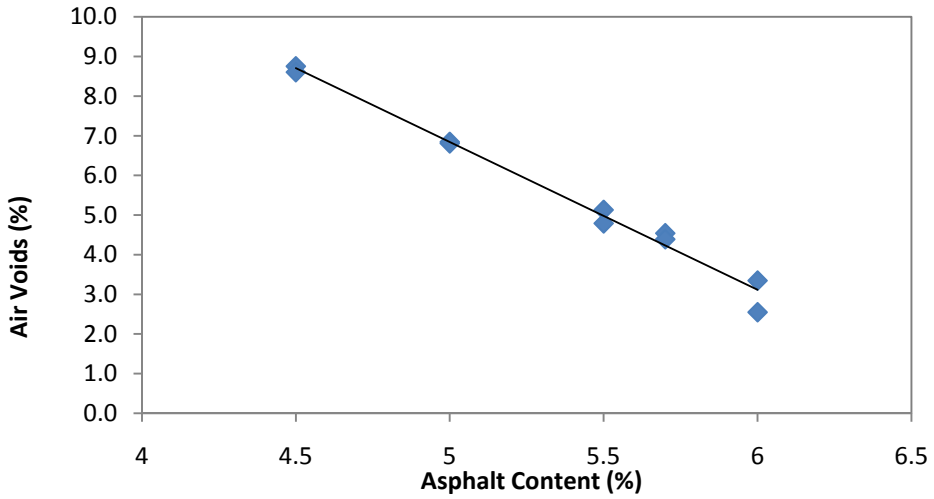

Figure A.5 Air Voids versus Asphalt Content for 10% RAP Mixture

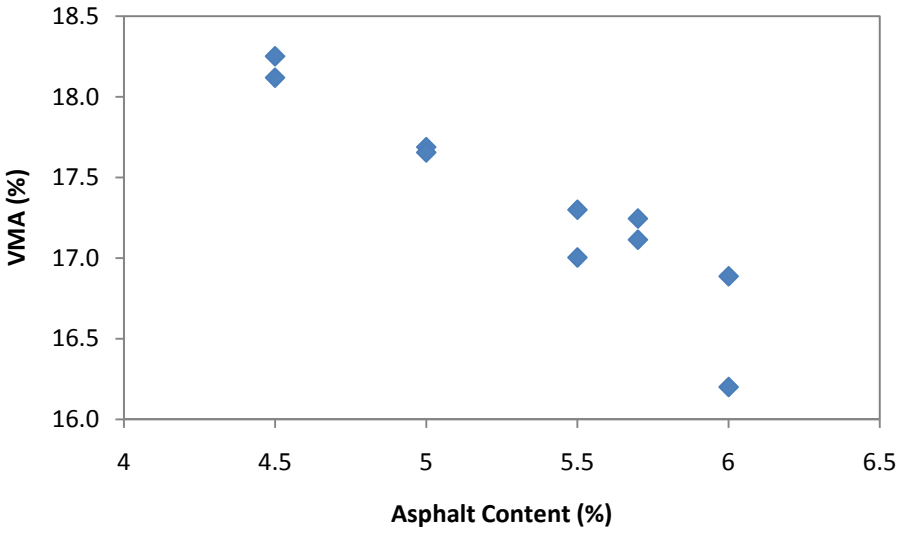

Figure A.6 VMA versus Asphalt Content for 10% RAP Mixture

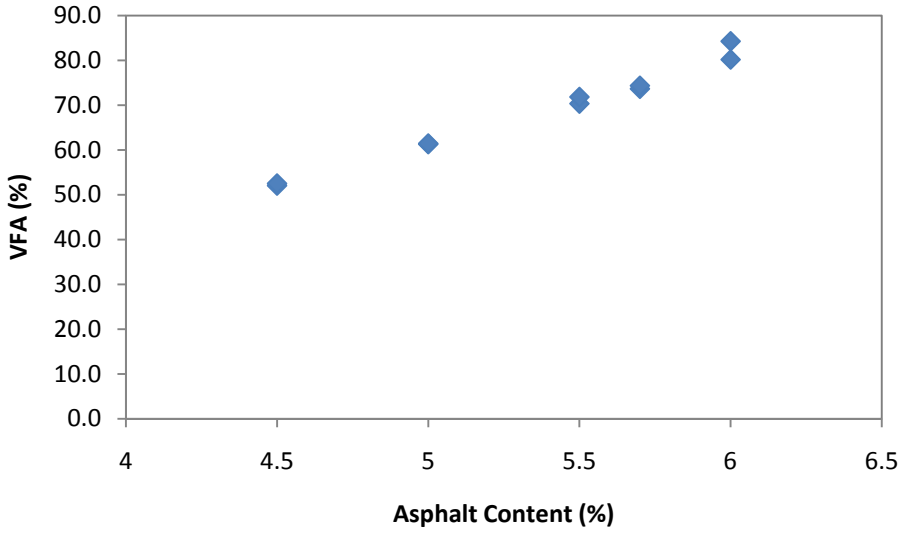

Figure A.7 VFA versus Asphalt Content for 10% RAP Mixture

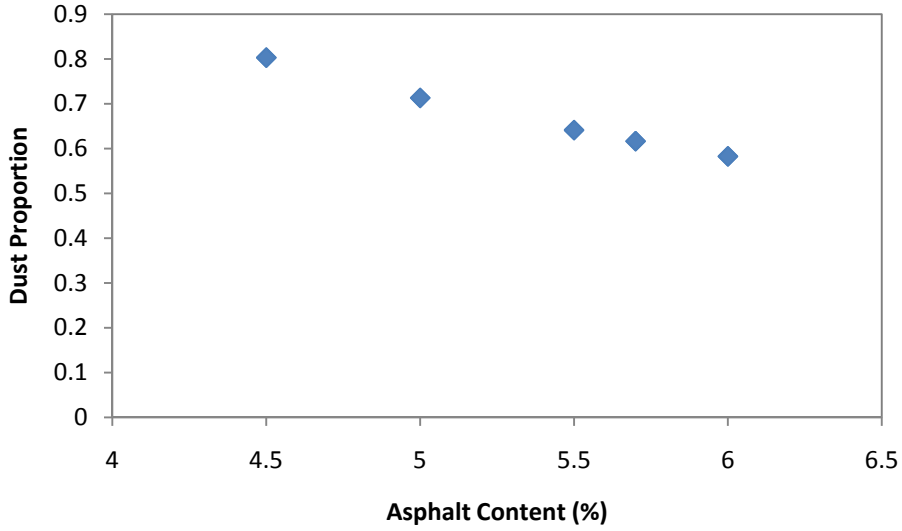

Figure A.8 Dust Proportion versus Asphalt Content for 10% RAP Mixture

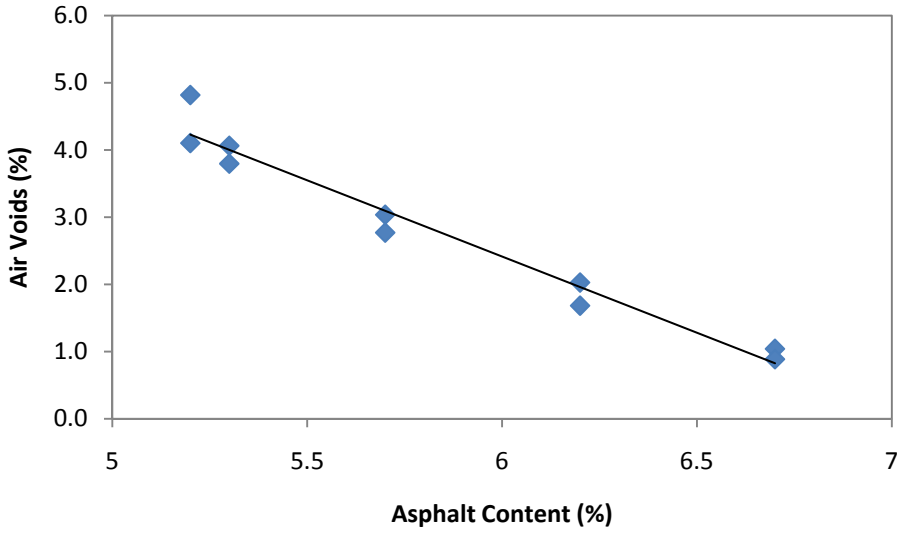

Figure A.9 Air Voids versus Asphalt Content for 25% RAP Mixture

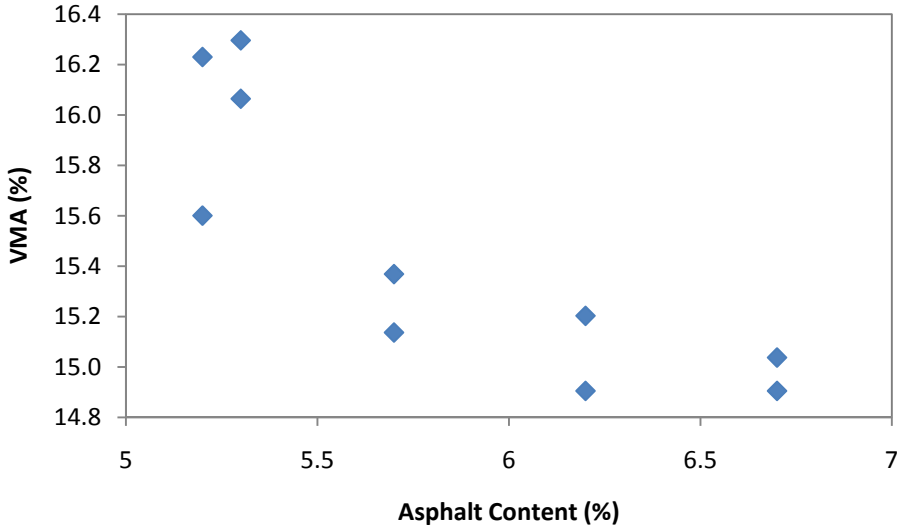

Figure A.10 VMA versus Asphalt Content for 25% RAP Mixture

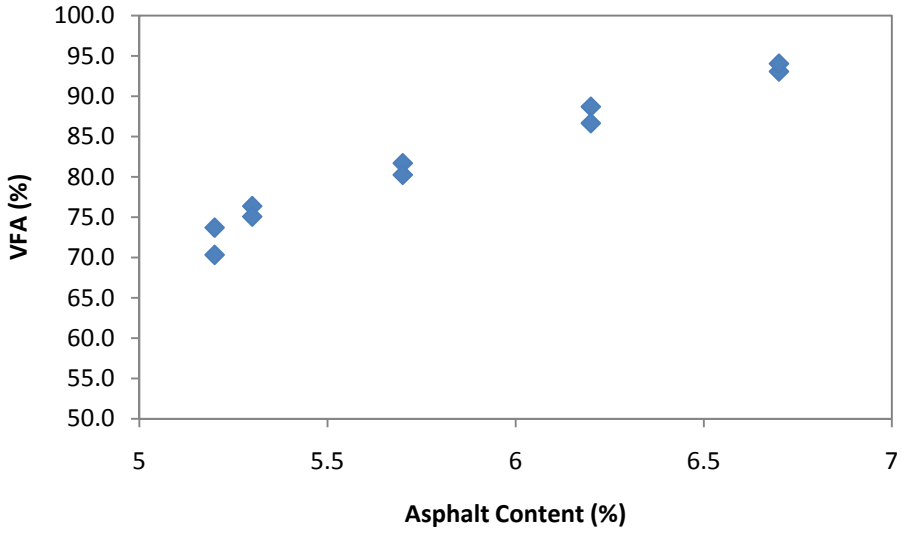

Figure A.11 VFA versus Asphalt Content for 25% RAP Mixture

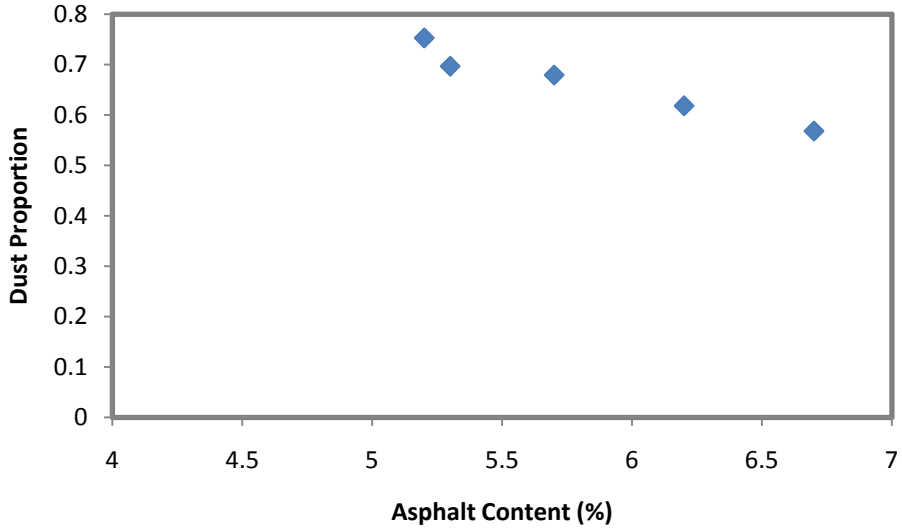

Figure A.12 Dust Proportion versus Asphalt Content for 25% RAP Mixture

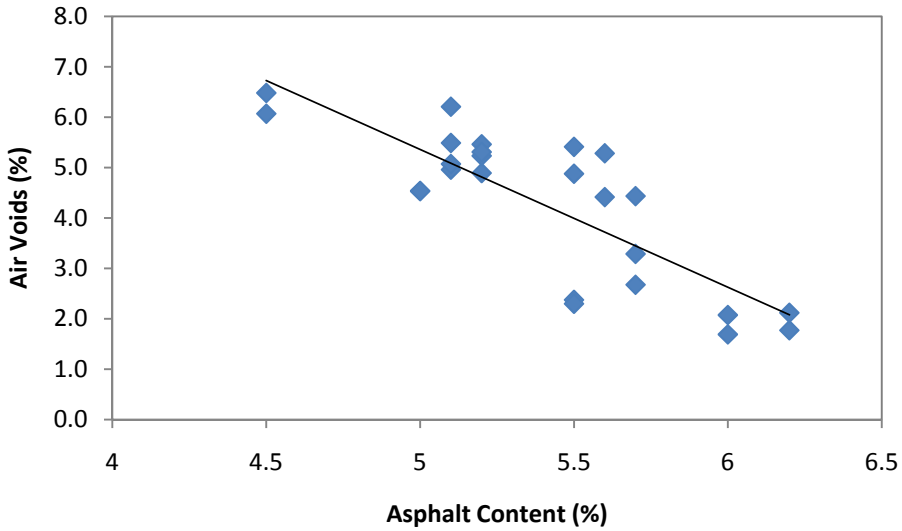

Figure A.13 Air Voids versus Asphalt Content for 40% RAP Mixture

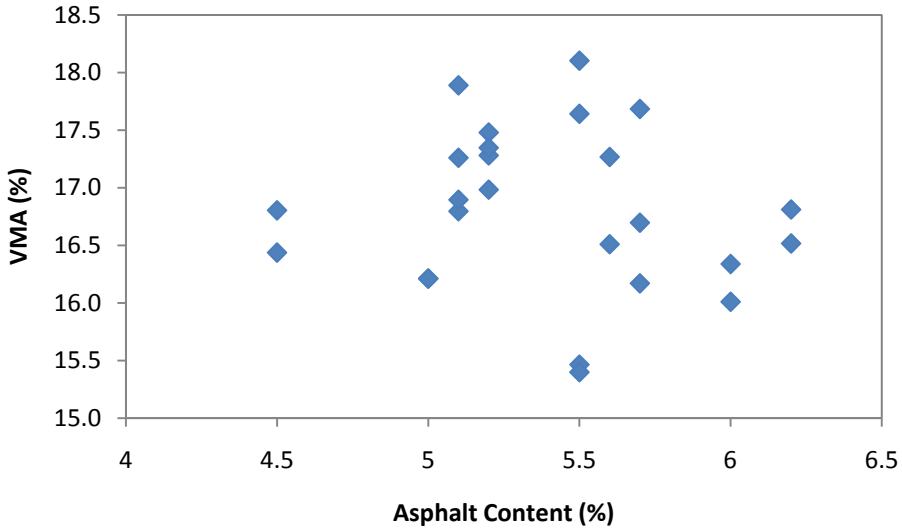

Figure A.14 VMA versus Asphalt Content for 40% RAP Mixture

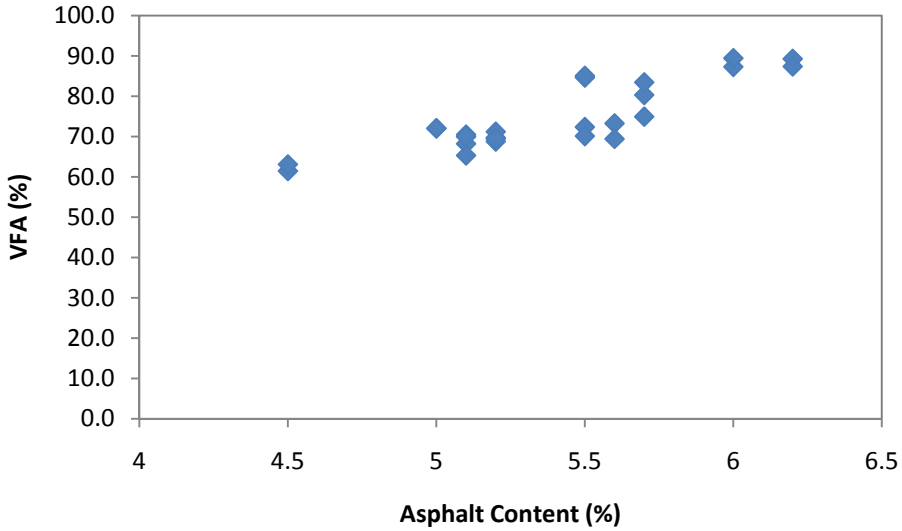

Figure A.15 VFA versus Asphalt Content for 40% RAP Mixture

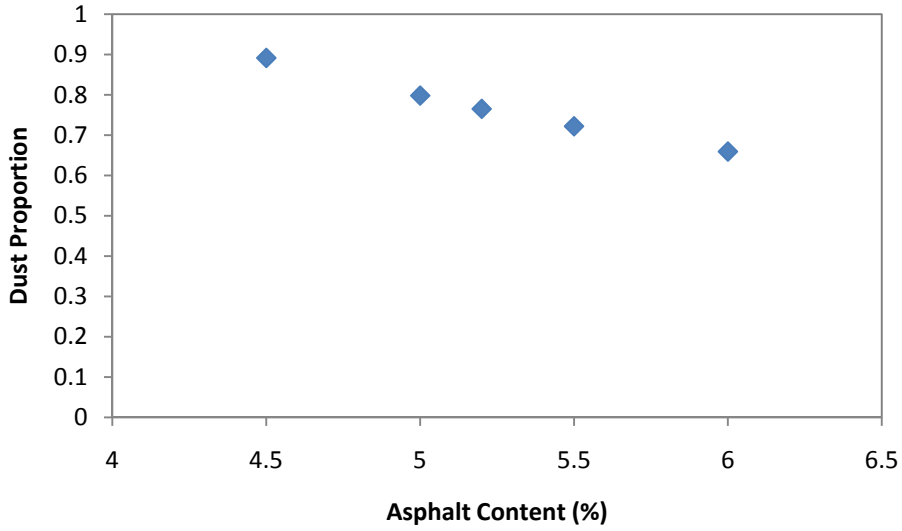

Figure A.16 Dust Proportion versus Asphalt Content for 40% RAP Mixture

APPENDIX B: DYNAMIC MODULUS DATA

Table B.1 Control Specimens Measured Dynamic Modulus

Temp C	Freq Hz	6000I |E*|MPa	6000J |E*|MPa	6000K |E*|MPa
-10	0.1	12827	14698	13018
-10	0.2	21164	15520	13975
-10	0.5	20534	16864	15205
-10	1	16942	17835	15999
-10	2	29305	18577	16873
-10	5	23222	19682	17991
-10	10	24836	20624	18818
-10	20	16985	19664	20735
0	0.1	6769	8909	6808
0	0.2	7753	10084	7730
0	0.5	9107	11504	9151
0	1	10119	12680	10108
0	2	11254	13796	11200
0	5	13014	15167	12624
0	10	14907	16202	14648
0	20	15228	16965	13706
10	0.1	2220	3056	1581
10	0.2	2799	3814	2063
10	0.5	3705	4948	2873
10	1	4532	5976	3620
10	2	5473	6899	4398
10	5	6925	8429	5521
10	10	8243	9536	6384
10	20	9539	10804	7143
20	0.1	663	1027	330
20	0.2	901	1352	484
20	0.5	1283	1938	798
20	1	1695	2542	1129
20	2	2273	3390	1632
20	5	3154	4532	2335
20	10	4008	5637	3028
20	20	2952	6944	3817
30	0.1	209	217	195
30	0.2	264	275	596
30	0.5	412	428	406
30	1	566	588	550
30	2	778	809	767
30	5	1157	1203	1151
30	10	1684	1751	1667
30	20	2323	2415	3265

Table B.2 Control Specimens Measured Dynamic Modulus

Temp C	Freq Hz	6000L |E*|MPa	6000M |E*|MPa
-10	0.1	11974	13188
-10	0.2	12809	14159
-10	0.5	13992	15270
-10	1	14814	16030
-10	2	15502	17128
-10	5	15486	18393
-10	10	14532	19066
0	0.1	7003	6467
0	0.2	7839	7420
0	0.5	9024	8740
0	1	9888	9836
0	2	10846	10928
0	5	11509	12324
0	10	12144	13562
0	20	10500	14759
10	0.1	2145	2164
10	0.2	2763	2683
10	0.5	3632	3515
10	1	4508	4317
10	2	5428	5281
10	5	6574	6578
10	10	7859	7358
10	20	7049	9457
20	0.1	655	536
20	0.2	893	737
20	0.5	1291	1126
20	1	1939	1575
20	2	2203	2082
20	5	3027	2980
20	10	3844	3884
20	20	4745	4888

Table B.3 10% RAP Specimens Measured Dynamic Modulus

Temp C	Freq Hz	5710 E |E*| MPa	5710F |E*| MPa
-10	0.1	14278	14514
-10	0.2	15113	15408
-10	0.5	16259	16537
-10	1	16926	17257
-10	2	17756	17793
-10	5	18748	19034
-10	10	18710	19873
-10	20	18021	18831
0	0.1	9711	7695
0	0.2	10403	8780
0	0.5	11863	10191
0	1	12826	11269
0	2	14033	12472
0	5	14993	13546
0	10	13845	14189
0	20	14250	13141
10	0.1	2912	2949
10	0.2	3626	3483
10	0.5	4792	4487
10	1	5799	5386
10	2	7049	6304
10	5	8815	7534
10	10	11039	8163
10	20	11744	10978
20	0.1	943	940
20	0.2	1223	1237
20	0.5	1693	1695
20	1	2292	2238
20	2	3052	2828
20	5	4250	3777
20	10	5652	4696
20	20	8682	5749
30	0.1	372	315
30	0.2	485	390
30	0.5	711	595
30	1	922	755
30	2	1230	1044
30	5	1772	1514
30	10	2383	2121
30	20	3292	2861

Table B.4 25% RAP Specimens Measured Dynamic Modulus

Temp C	Freq Hz	5325G |E*| MPa	5325I |E*| MPa
-10	0.1	17865	18325
-10	0.2	18148	19135
-10	0.5	19333	19256
-10	1	20226	20883
-10	2	20964	21762
-10	5	21450	22887
-10	10	22552	23317
-10	20	18537	18763
0	0.1	11486	10627
0	0.2	12532	11570
0	0.5	13922	12835
0	1	14869	14122
0	2	16039	14881
0	5	17327	16311
0	10	18788	17257
0	20	20808	14243
10	0.1	6487	5507
10	0.2	6585	6403
10	0.5	7928	7699
10	1	8950	8609
10	2	9688	9755
10	5	11878	11298
10	10	13037	12662
10	20	14020	13908
20	0.1	2187	2026
20	0.2	2765	2310
20	0.5	3589	3201
20	1	4430	4112
20	2	5244	4880
20	5	6668	6060
20	10	7840	6982
20	20	8614	8985
30	0.1	646	668
30	0.2	854	895
30	0.5	1225	1254
30	1	1636	1642
30	2	2176	2062
30	5	3046	3092
30	10	3950	3938
30	20	4853	4008

Table B.5 40% RAP Specimens Measured Dynamic Modulus

Temp C	Freq Hz	5240F |E*|MPa	5240G |E*|MPa	5240H |E*|MPa	5240I |E*|MPa
-10	0.1	13233	17551	17257	18091
-10	0.2	13438	18077	17688	18765
-10	0.5	21584	19153	18930	19599
-10	1	22056	19678	19670	20158
-10	2	24174	20545	19935	20747
-10	5	25055	21127	22034	22134
-10	10	23244	21574	21762	22408
-10	20	19000	21826	14663	23283
0	0.1	9405	12312	12312	12312
0	0.2	10646	13378	12098	12901
0	0.5	12144	14487	13927	13874
0	1	13385	15409	13972	14767
0	2	14564	16401	14906	15455
0	5	16012	17523	14923	16537
0	10	17104	18649	11413	17470
0	20	17909	19666	12964	18485
10	0.1	3227	6690	6285	8769
10	0.2	4026	7706	7103	9636
10	0.5	5223	9005	8264	10845
10	1	6308	9945	9054	11983
10	2	7283	10411	9947	12987
10	5	8898	12393	11244	14417
10	10	10067	13450	12249	15605
10	20	11405	14676	7508	16982
20	0.1	1084	3010	2727	3485
20	0.2	1428	3587	3291	4163
20	0.5	2046	4767	4107	5124
20	1	2684	5619	4929	5846
20	2	3579	6456	5811	6782
20	5	4784	7897	6744	8177
20	10	5951	8751	8453	9313
20	20	7330	7599	6300	10509
30	0.1	229	1160	1086	1281
30	0.2	290	1415	1343	1648
30	0.5	452	2072	1733	2166
30	1	621	2569	2195	2726
30	2	854	3196	2830	3388
30	5	1270	4358	3781	4446
30	10	1848	5351	4608	5320
30	20	2549	5916	3926	6398

Table B.6 PG 58-28 Specimens Measured Dynamic Modulus

Temp C	Freq Hz	6058A |E*| MPa	6058C |E*| MPa	6058D |E*| MPa
-10	0.1	14704	12820	12183
-10	0.2	15839	14188	12637
-10	0.5	17162	15274	14844
-10	1	18603	15908	10735
-10	2	20111	16775	11562
-10	5	20993	17974	18103
-10	10	21060	N/A	19593
0	0.1	7671	6406	5551
0	0.2	7897	7237	6566
0	0.5	9440	8890	7991
0	1	10777	9986	9189
0	2	12145	11023	10608
0	5	13921	12558	12319
0	10	15018	13787	14175
0	20	16112	15113	15178
10	0.1	1941	2154	1948
10	0.2	2591	2783	2408
10	0.5	3592	3710	3253
10	1	5206	4641	4193
10	2	5664	5669	5271
10	5	6990	6973	6476
10	10	8362	8175	7733
10	20	9884	9525	9138
20	0.1	630	504	537
20	0.2	890	648	734
20	0.5	1293	1052	1123
20	1	2117	1451	1572
20	2	2463	1904	2502
20	5	3484	2855	3068
20	10	4529	3725	4619
20	20	5491	4884	5294

Table B.7 PG 70-22 Specimens Measured Dynamic Modulus

Temp C	Freq Hz	6070 A |E*| MPa	6070 B |E*| MPa	6070 C |E*| MPa
-10	0.1	15858	13030	13207
-10	0.2	16587	14072	14208
-10	0.5	17824	15228	15277
-10	1	18590	16051	15877
-10	2	19486	16958	17106
-10	5	20810	18316	18110
-10	10	21466	19500	18718
0	0.1	7329	6147	7743
0	0.2	8447	7047	7251
0	0.5	9729	8330	8387
0	1	10706	9351	9385
0	2	11813	10470	10280
0	5	13444	11998	11732
0	10	14431	13486	12708
0	20	15487	11840	13815
10	0.1	2397	2050	2652
10	0.2	3013	2520	2880
10	0.5	3833	3326	3727
10	1	4707	4133	4530
10	2	5652	5049	5325
10	5	7028	6241	6622
10	10	7933	7296	8580
10	20	9145	8619	6628
20	0.1	632	569	707
20	0.2	908	733	853
20	0.5	1195	1076	1190
20	1	1757	1465	1667
20	2	2376	2051	2160
20	5	3313	2916	2971
20	10	4473	3771	3751
20	20	5437	4861	5320

Table B.8 PG 76-22 Specimens Measured Dynamic Modulus

Temp C	Freq Hz	6076 A |E*| MPa	6076 B |E*| MPa	6076 C |E*| MPa
-10	0.1	14326	14366	17626
-10	0.2	15088	15238	18079
-10	0.5	16212	16190	19688
-10	1	17080	17261	20448
-10	2	17872	18059	21125
-10	5	18976	23114	22188
-10	10	19712	23543	23161
0	0.1	8686	8683	9775
0	0.2	9727	9351	10913
0	0.5	11104	10562	12507
0	1	12151	11550	13705
0	2	13111	12436	14741
0	5	14733	13756	16436
0	10	15901	13791	17856
0	20	17176	10973	19136
10	0.1	3156	3244	3211
10	0.2	3832	3928	3803
10	0.5	4870	4895	4706
10	1	5859	5871	5685
10	2	6826	6796	6803
10	5	8206	8289	8402
10	10	9351	9365	9319
10	20	10626	11065	10600
20	0.1	1047	2142	950
20	0.2	1565	2583	1164
20	0.5	1853	3155	1605
20	1	2430	3769	2238
20	2	3174	4517	2887
20	5	4241	5619	3890
20	10	5219	6509	4848
20	20	6693	8519	5976

APPENDIX C: INDIRECT TENSILE STRENGTH DATA

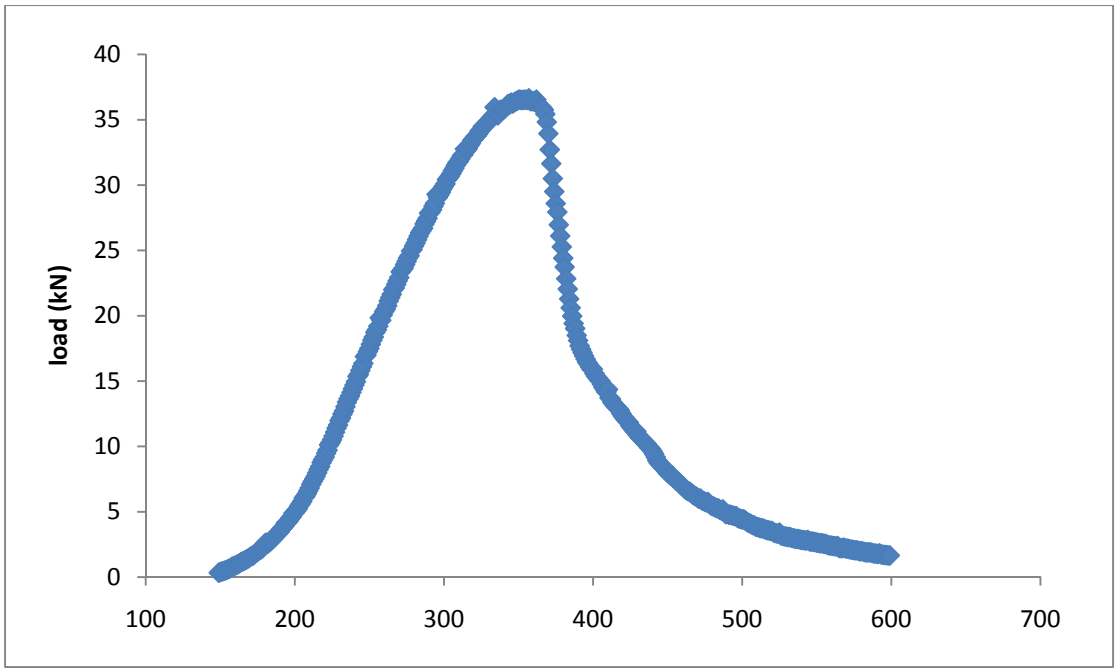

Figure C.1 6000I Strength Curve

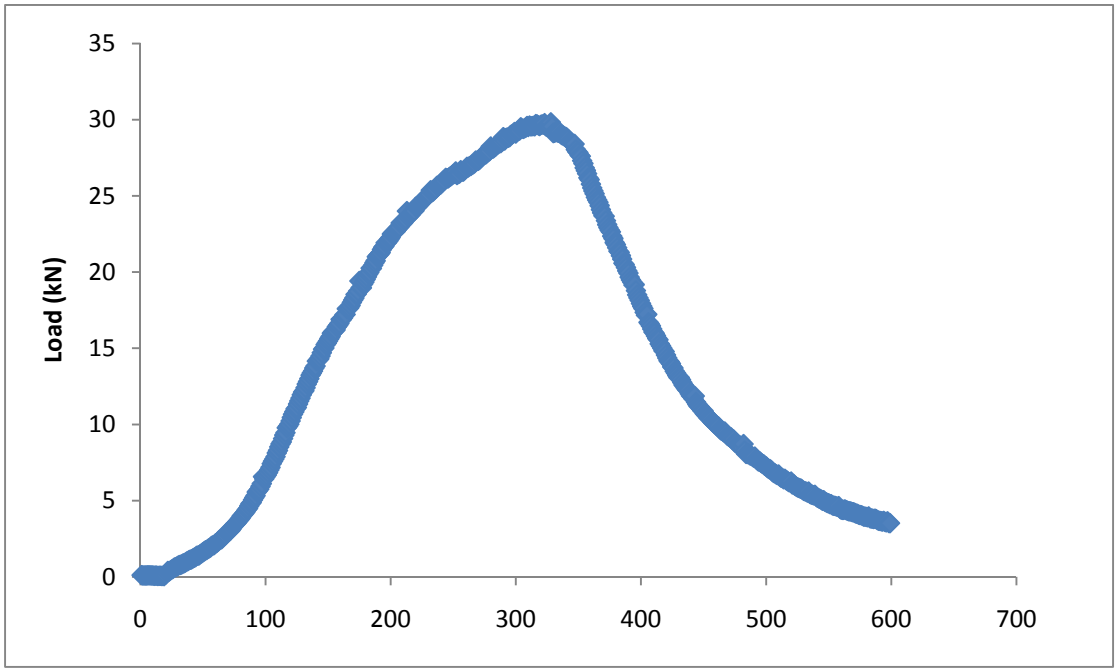

Figure C.2 6000J Strength Curve

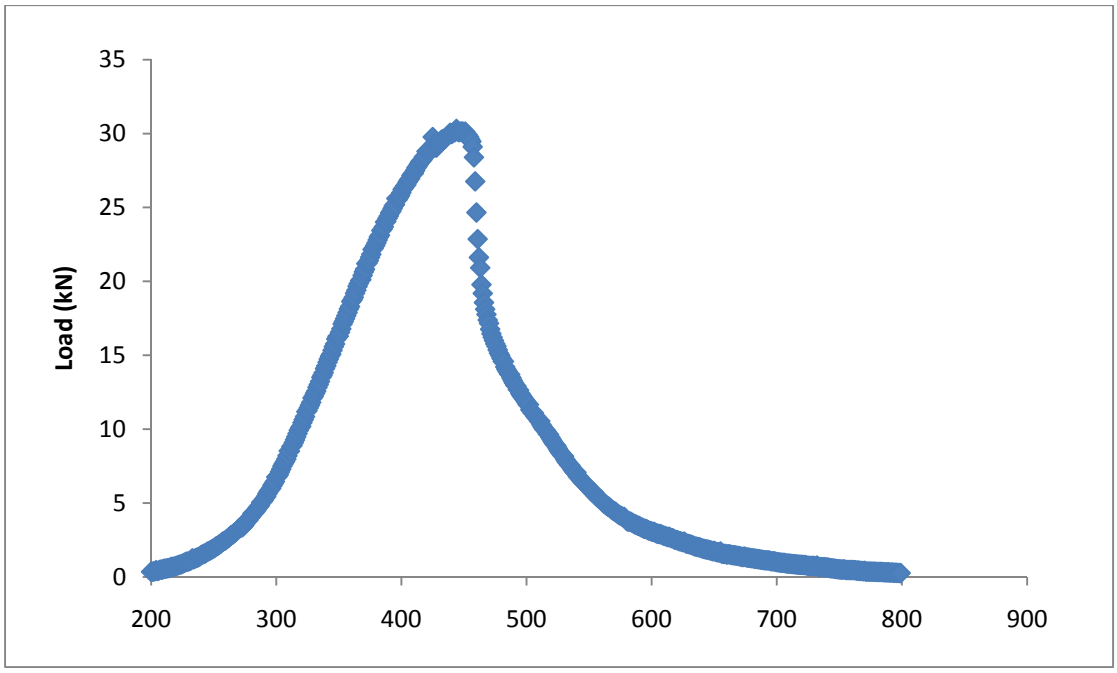

Figure C.3 6000K Strength Curve

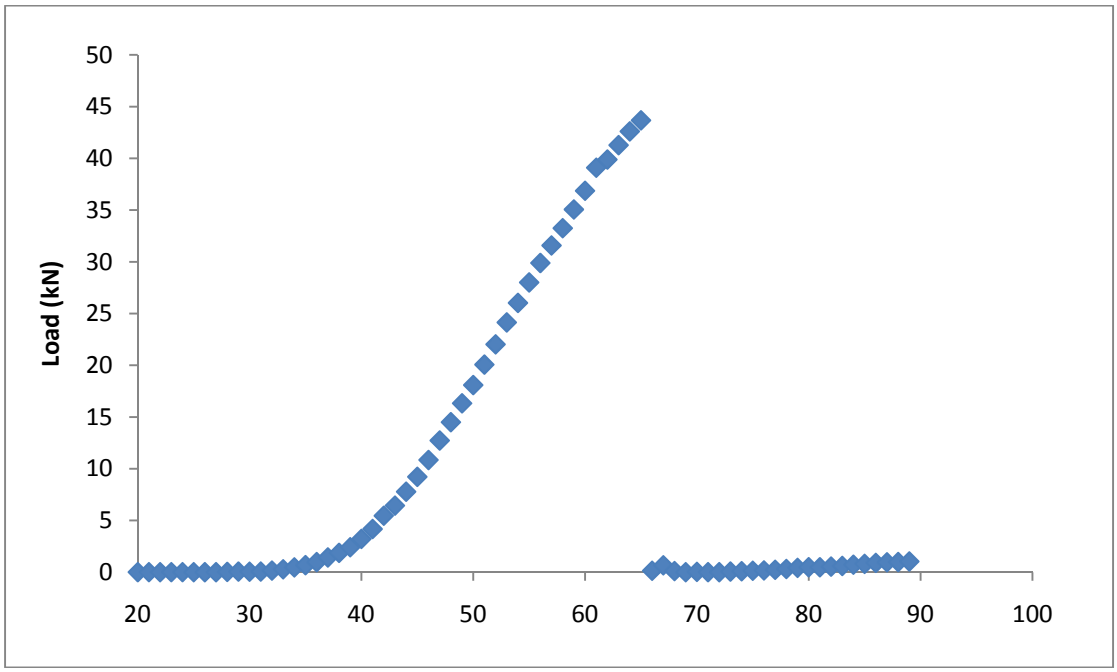

Figure C.4 6000L Strength Curve

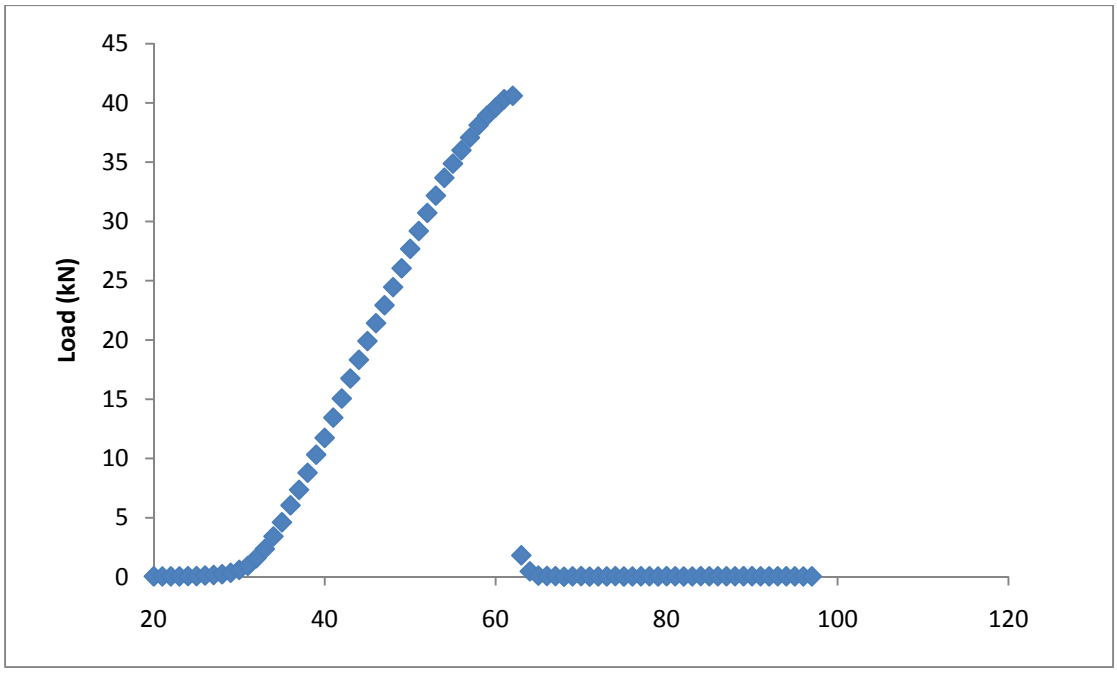

Figure C.5 6000M Strength Curve

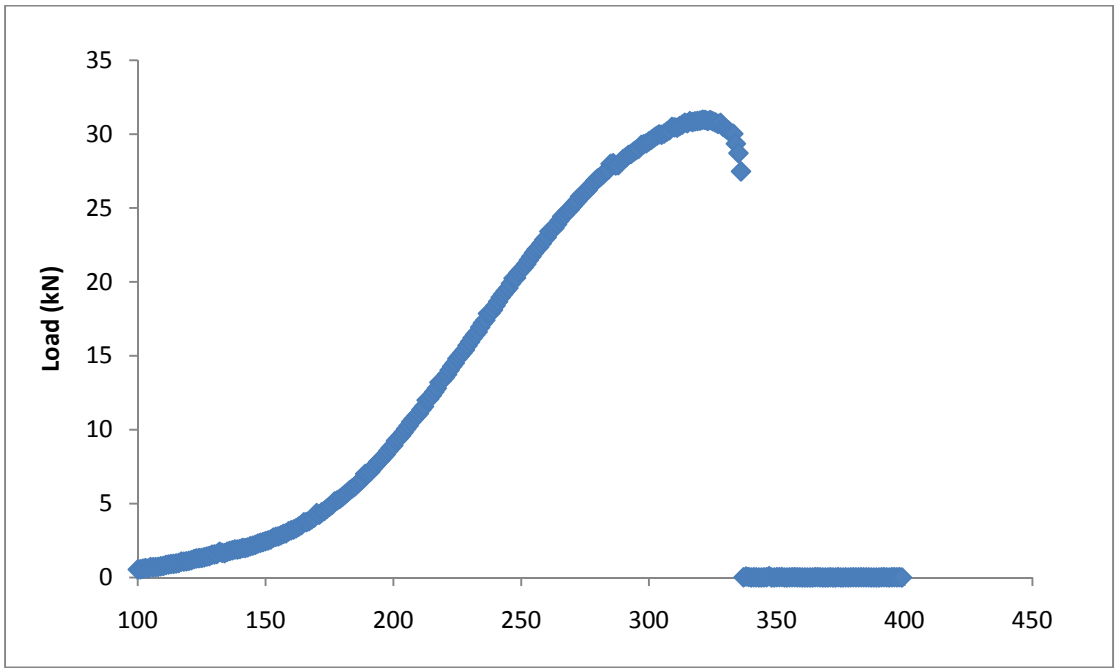

Figure C.6 5710E Strength Curve

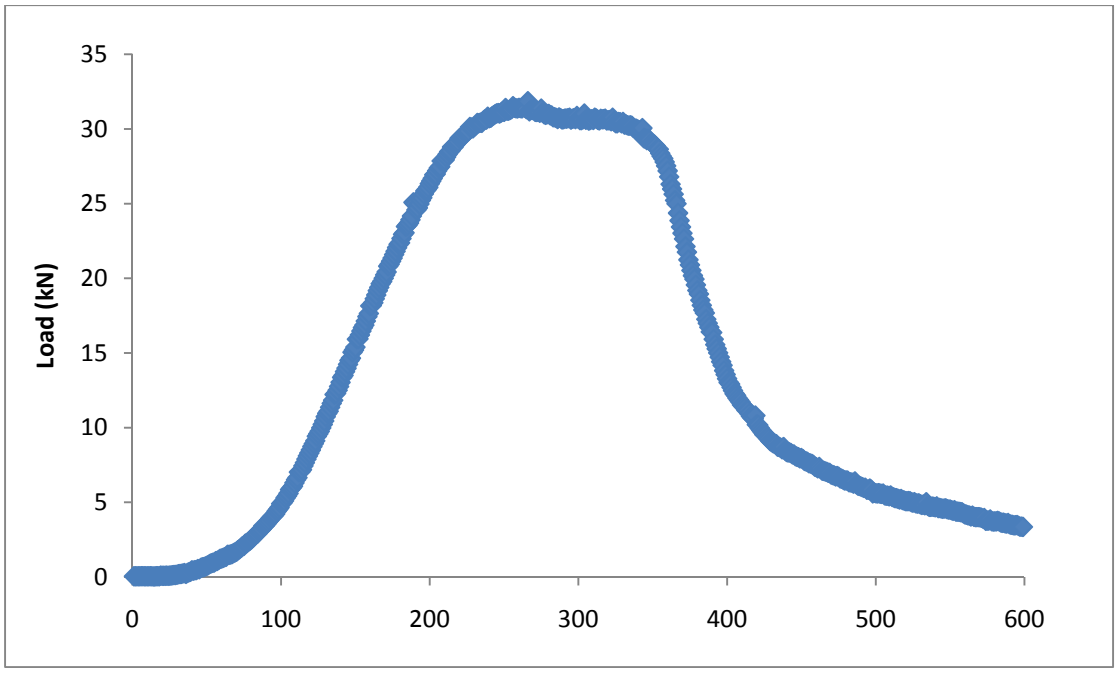

Figure C.7 5710F Strength Curve

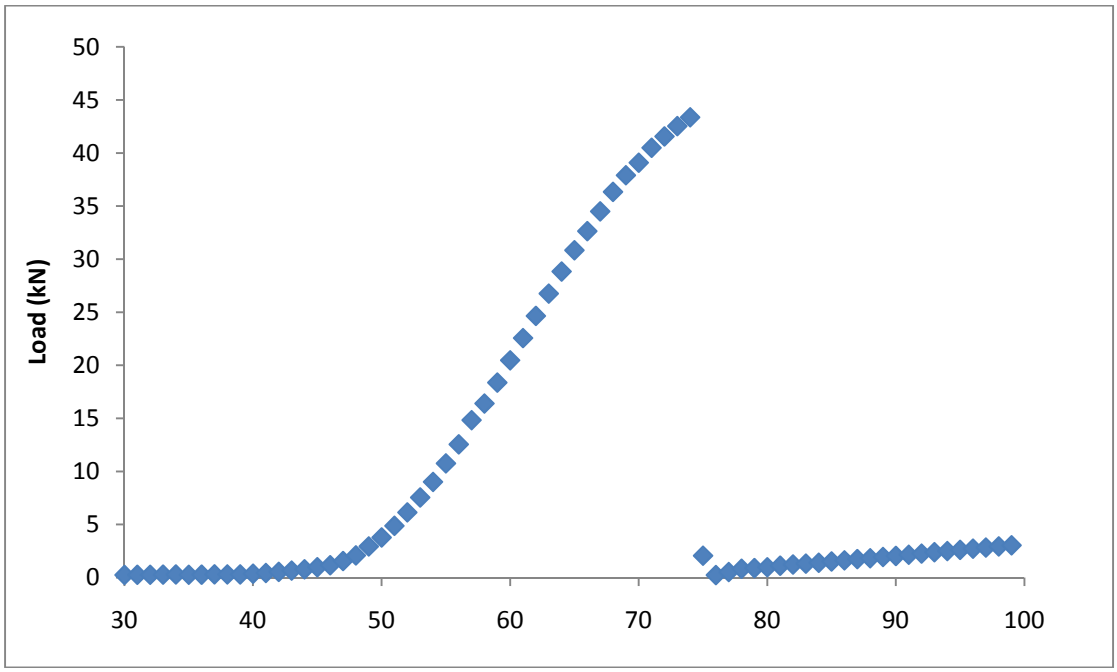

Figure C.8 5710G Strength Curve

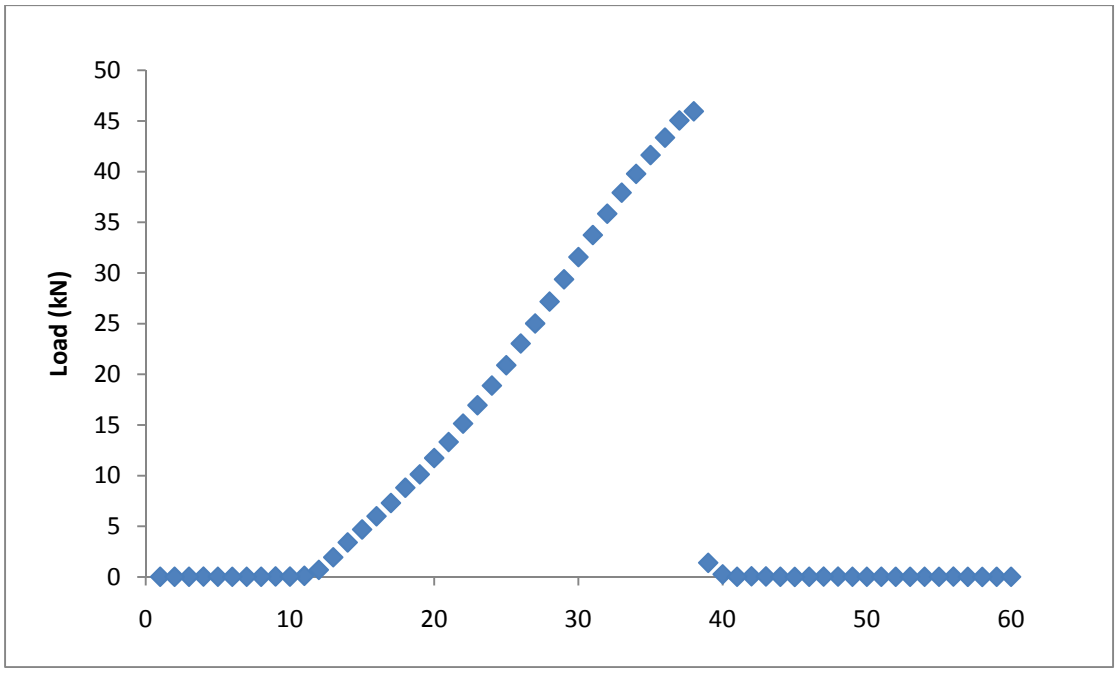

Figure C.9 5710H Strength Curve

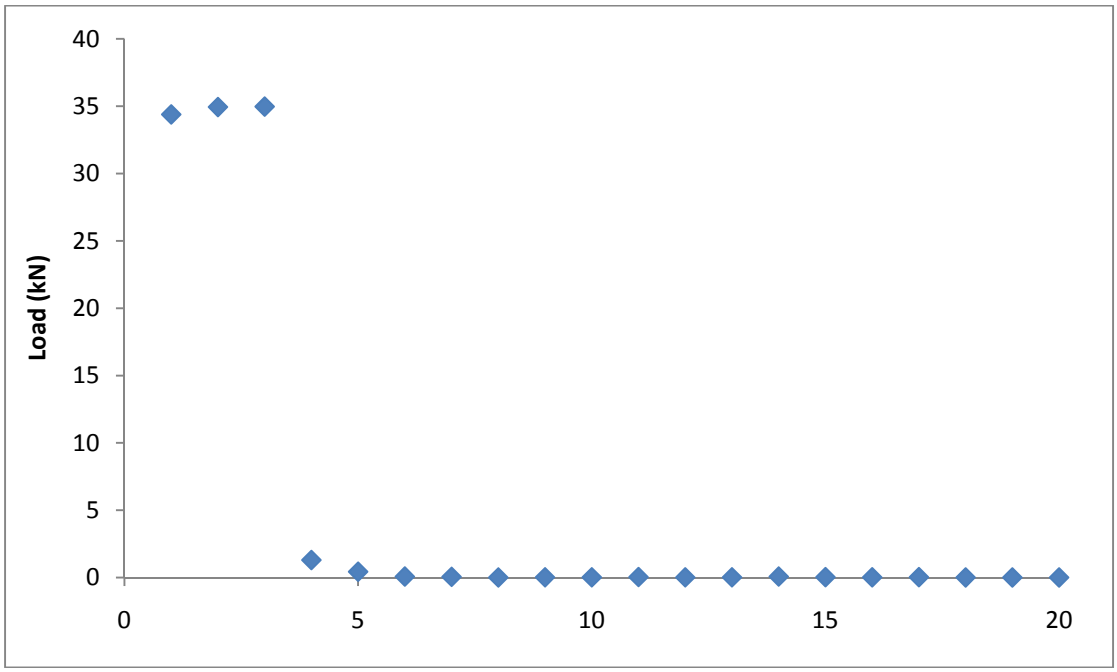

Figure C.10 5325E Strength Curve

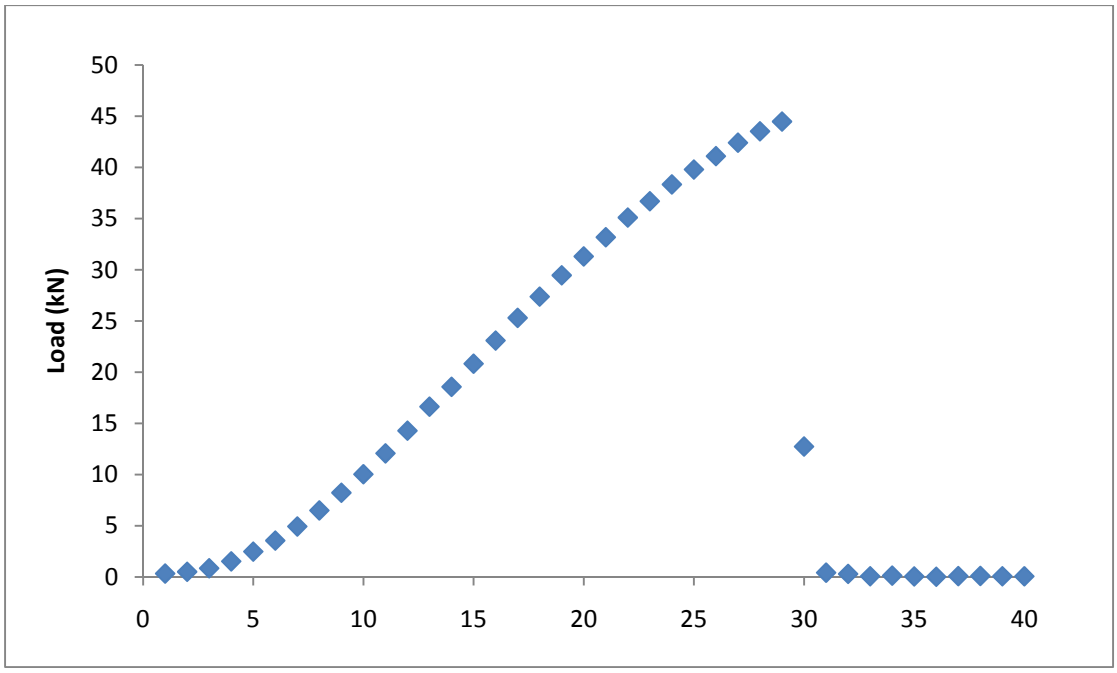

Figure C.11 5325F Strength Curve

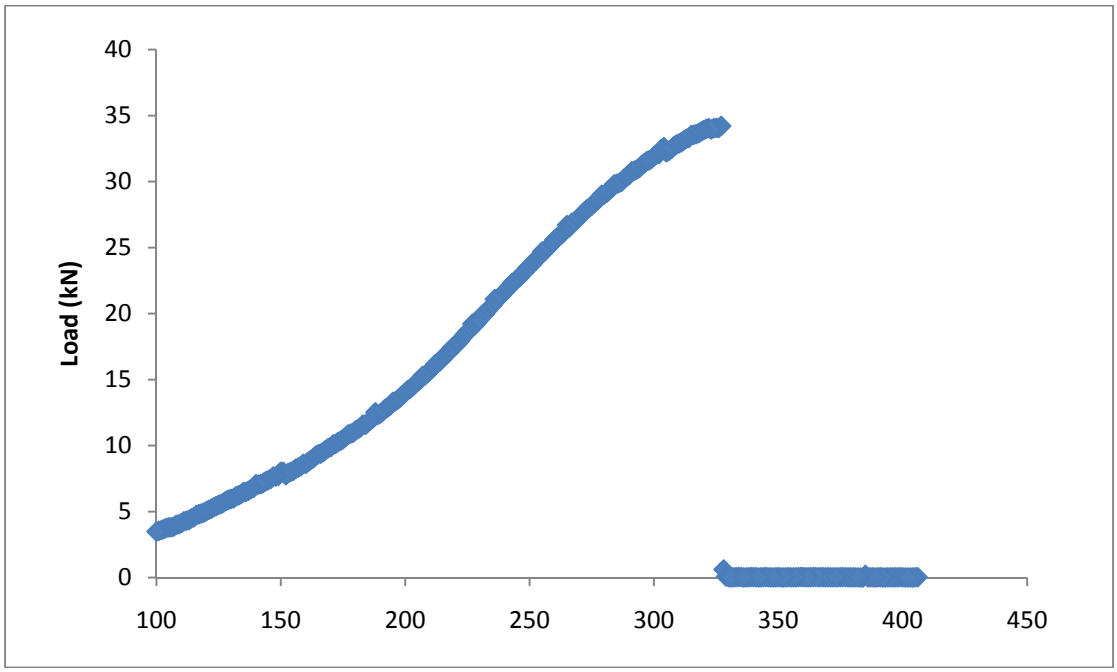

Figure C.12 5325G Strength Curve

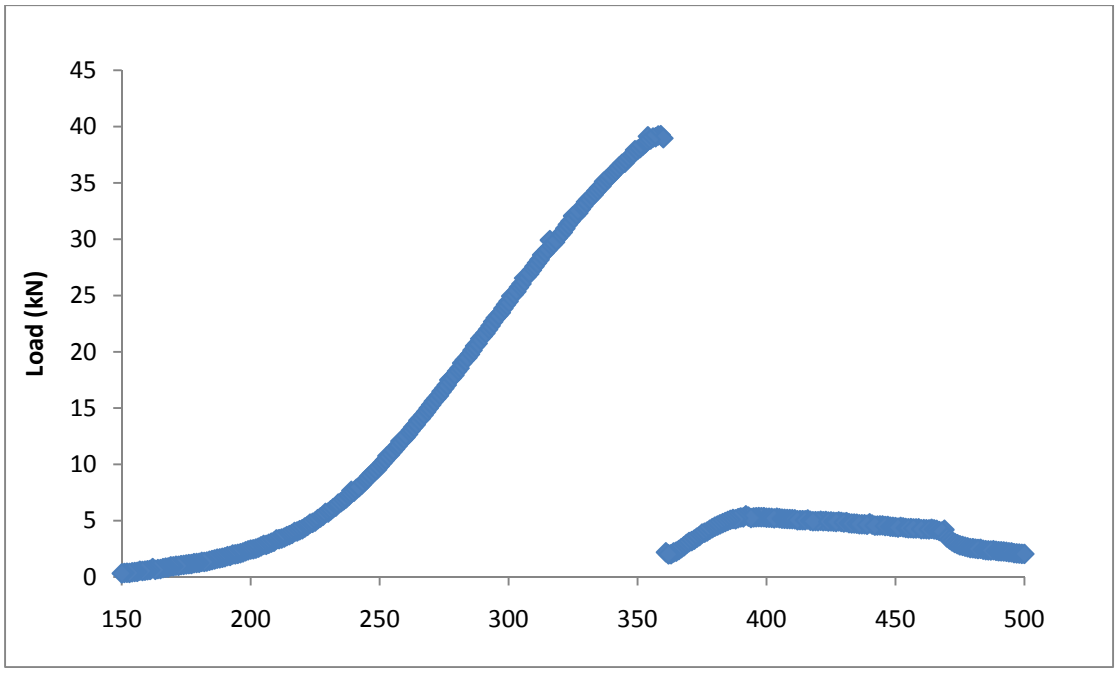

Figure C.13 5325I Strength Curve

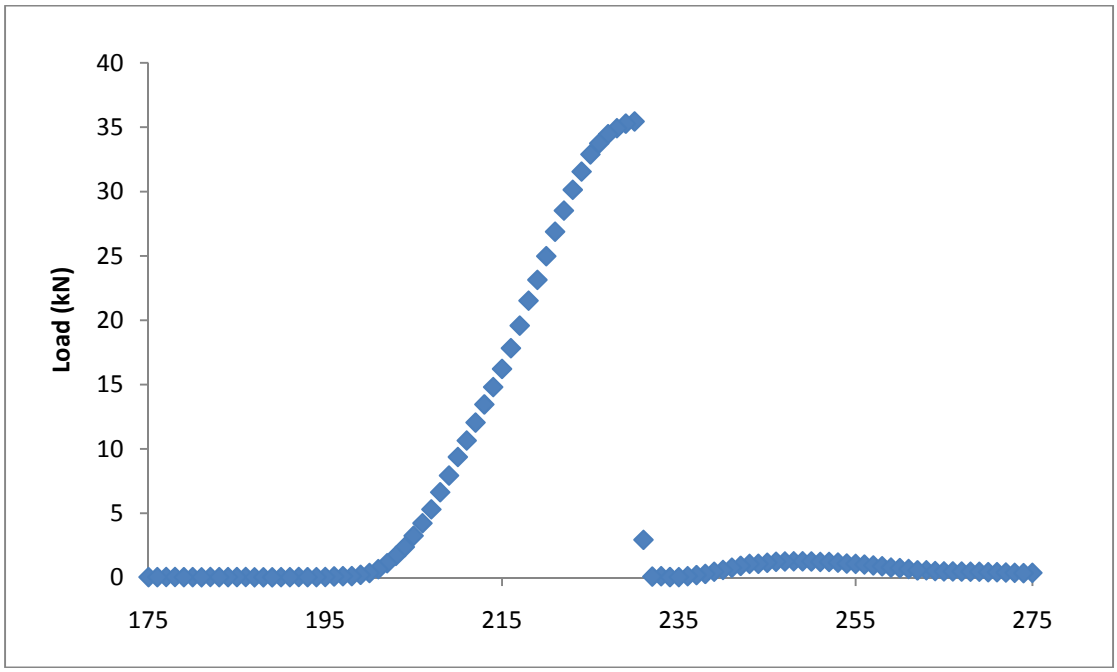

Figure C.14 5240E Strength Curve

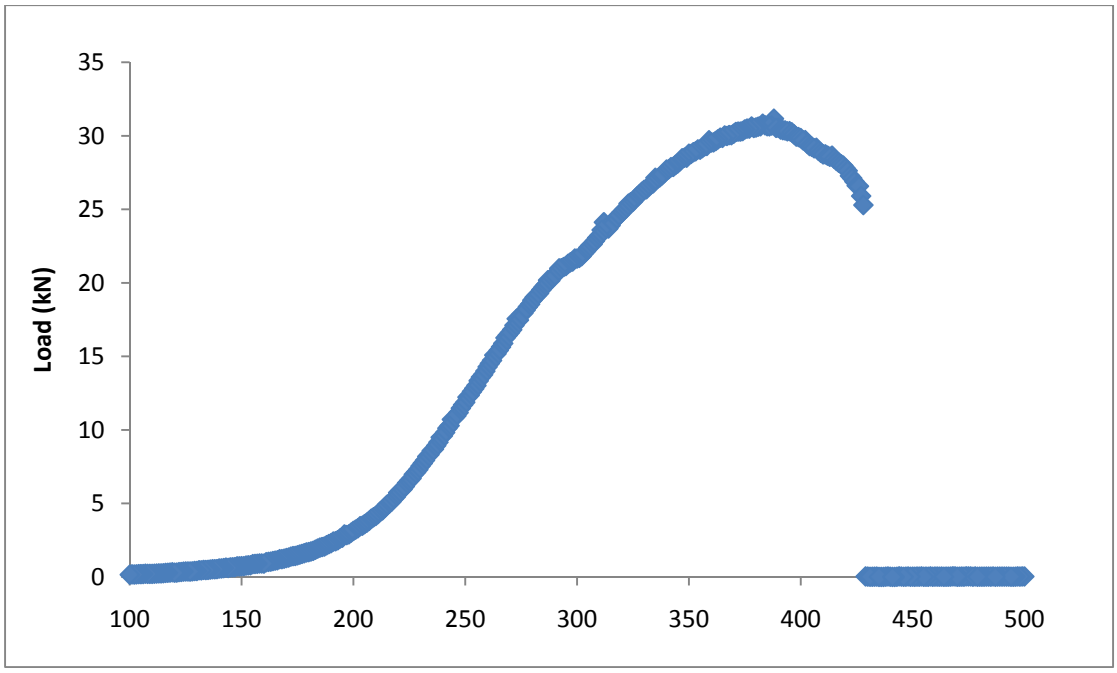

Figure C.15 5240F Strength Curve

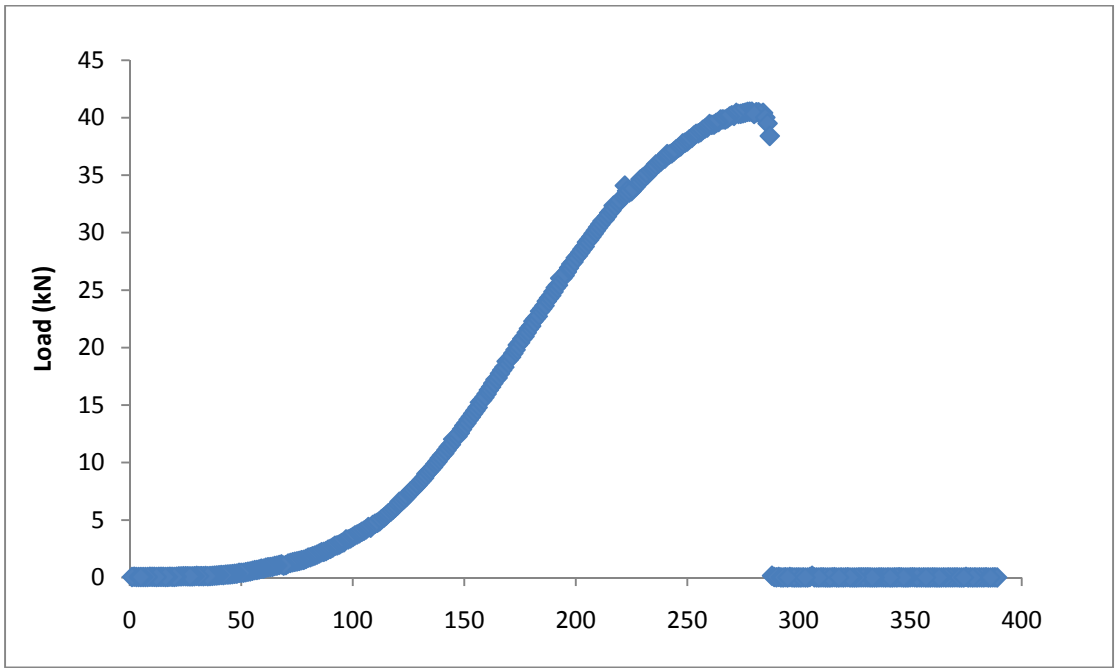

Figure C.16 5240G Strength Curve

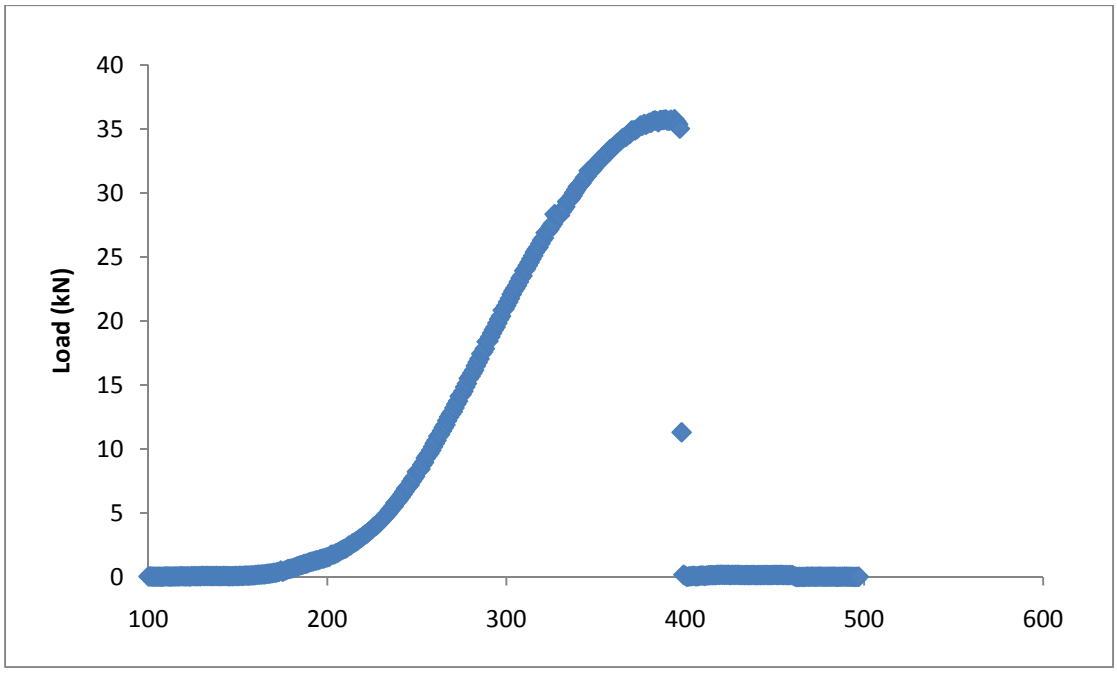

Figure C.17 5240H Strength Curve

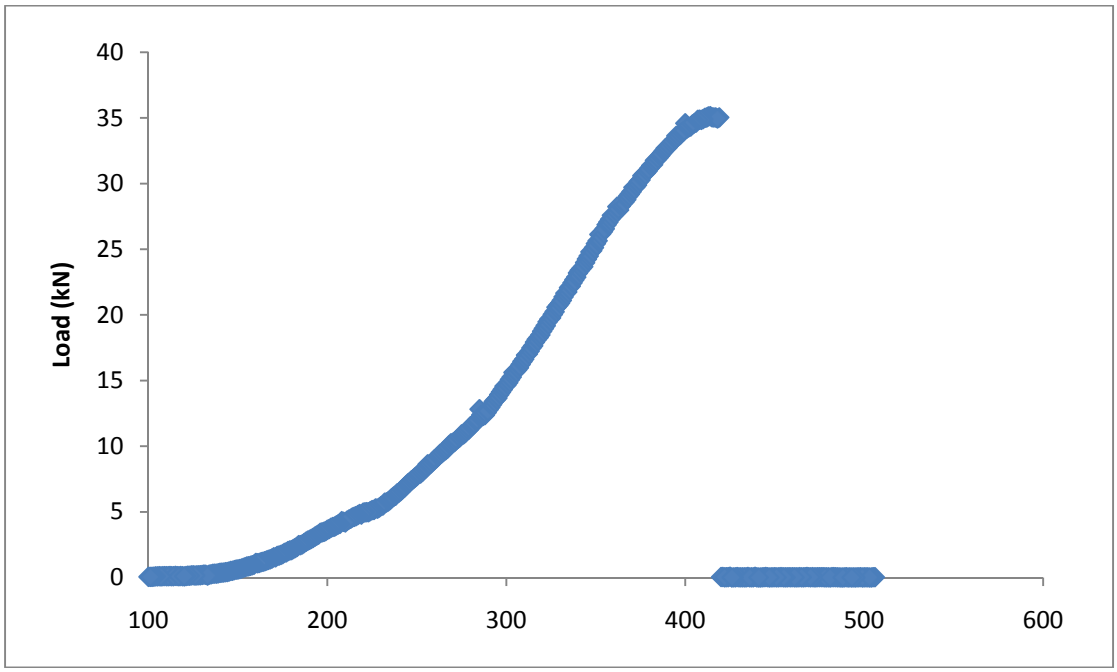

Figure C.18 5240I Strength Curve

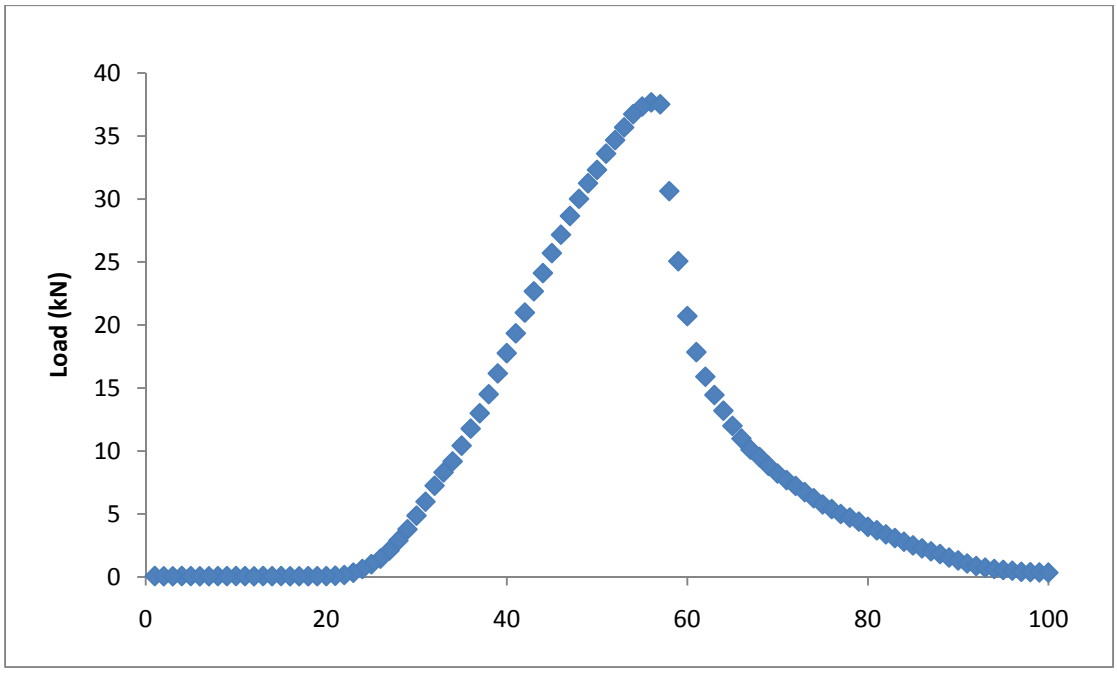

Figure C.19 6058A Strength Curve

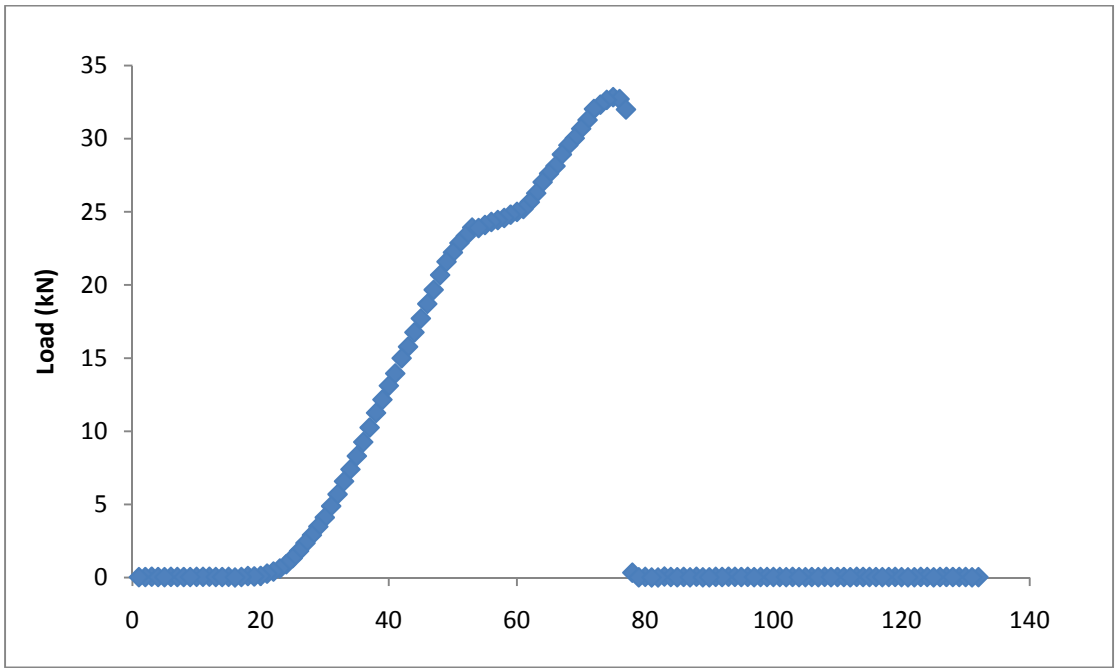

Figure C.20 6058B Strength Curve

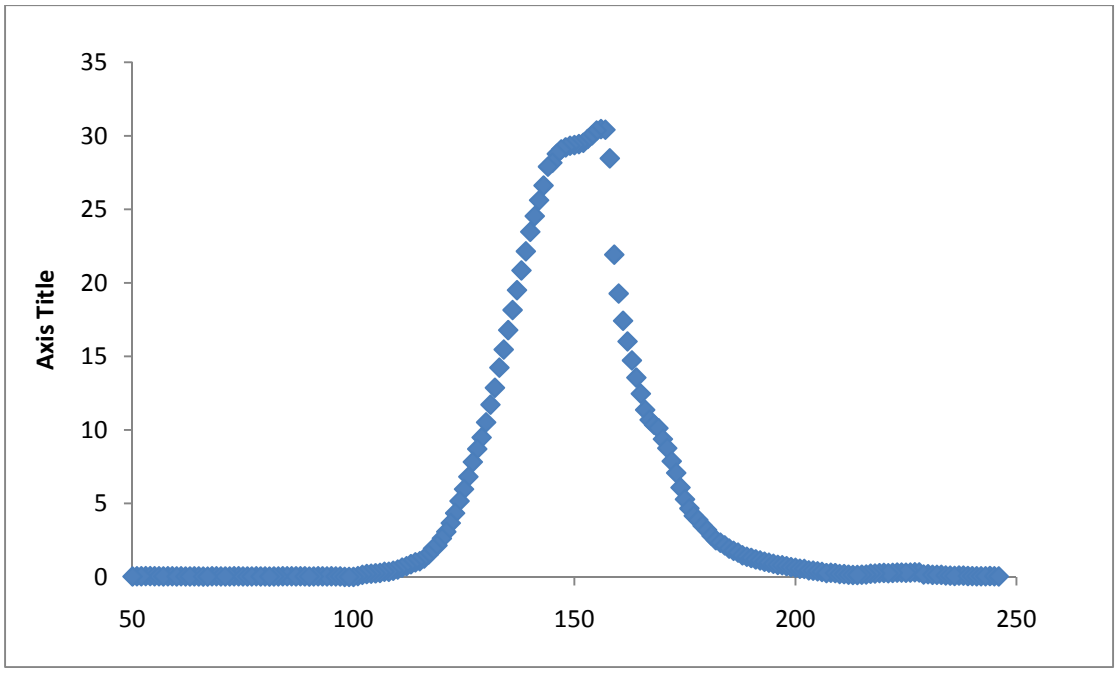

Figure C.21 6058C Strength Curve

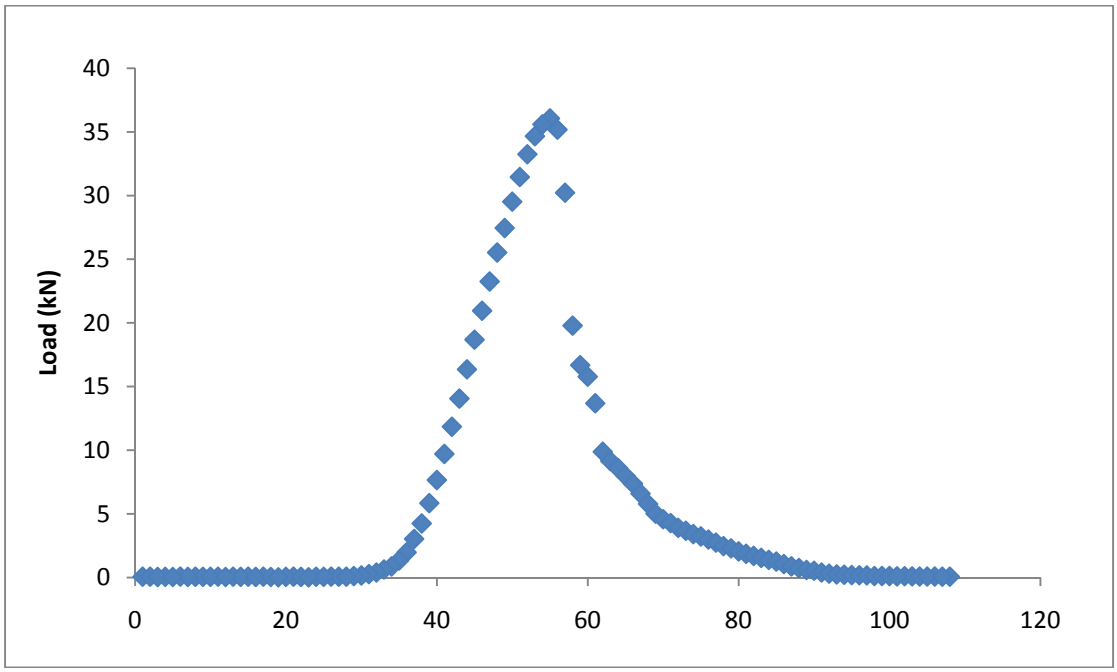

Figure C.22 6058D Strength Curve

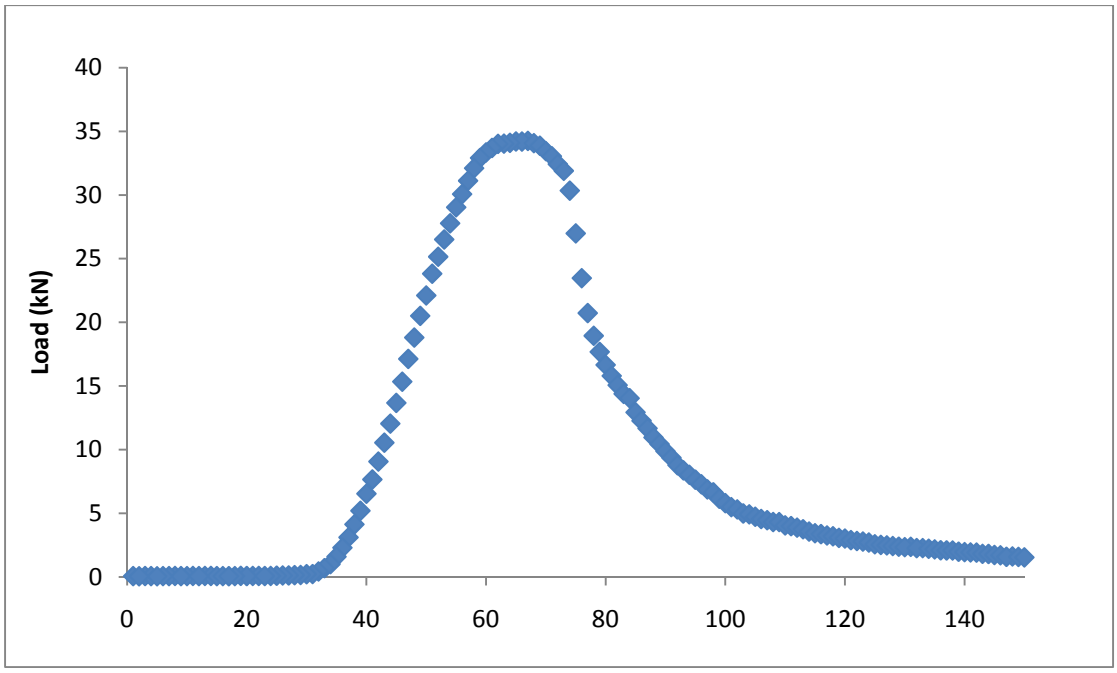

Figure C.23 6070A Strength Curve

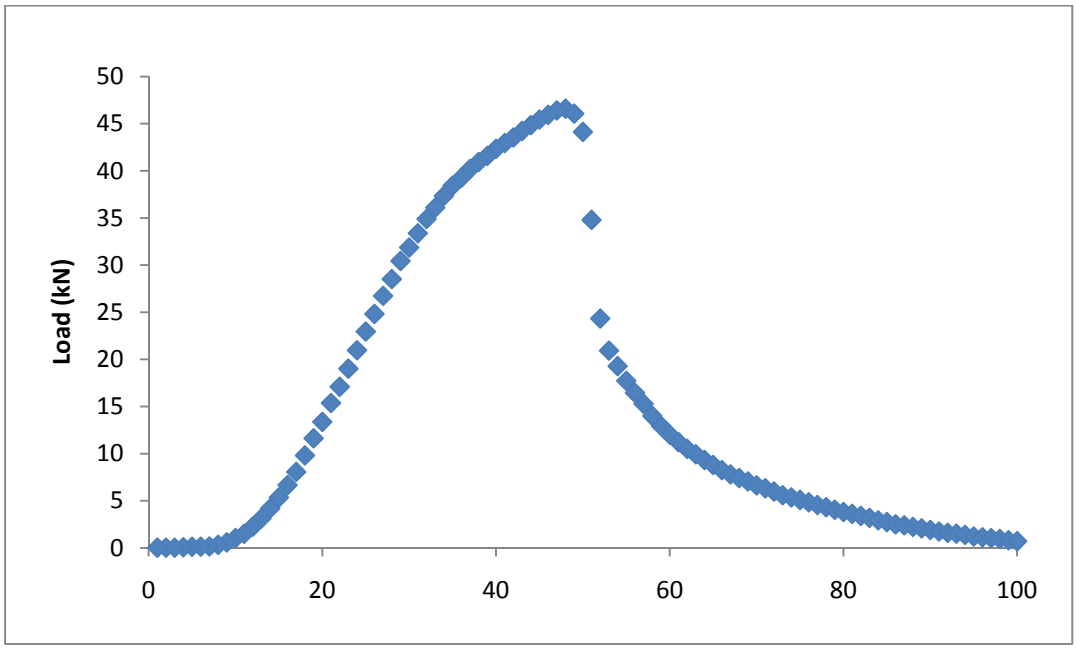

Figure C.24 6070B Strength Curve

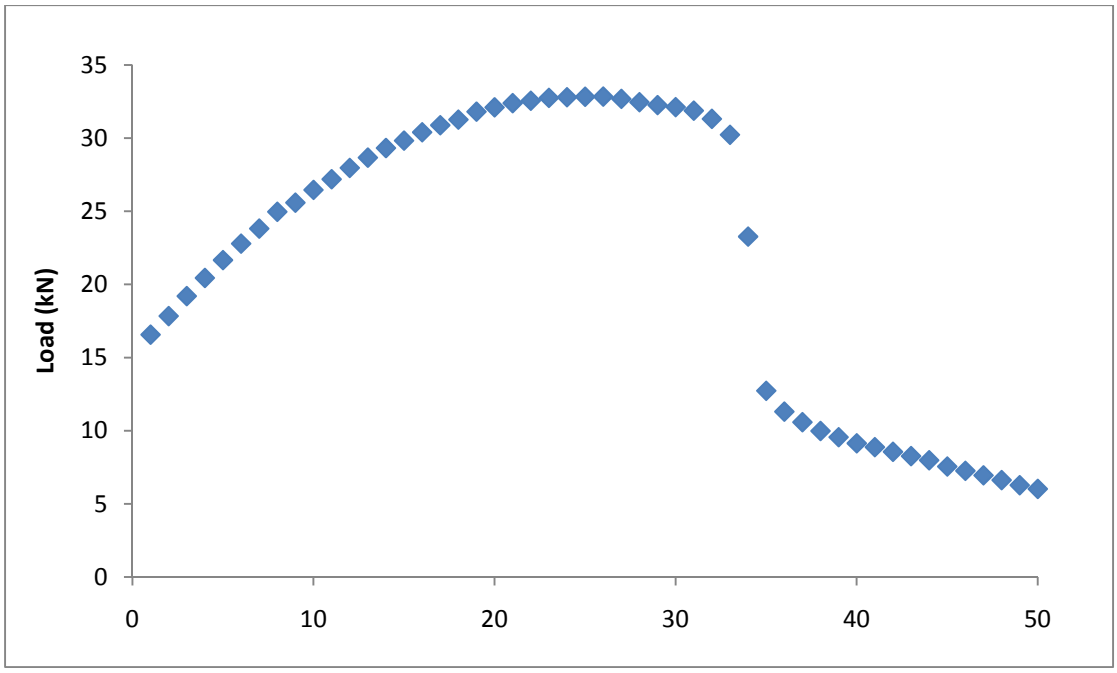

Figure C.25 6070C Strength Curve

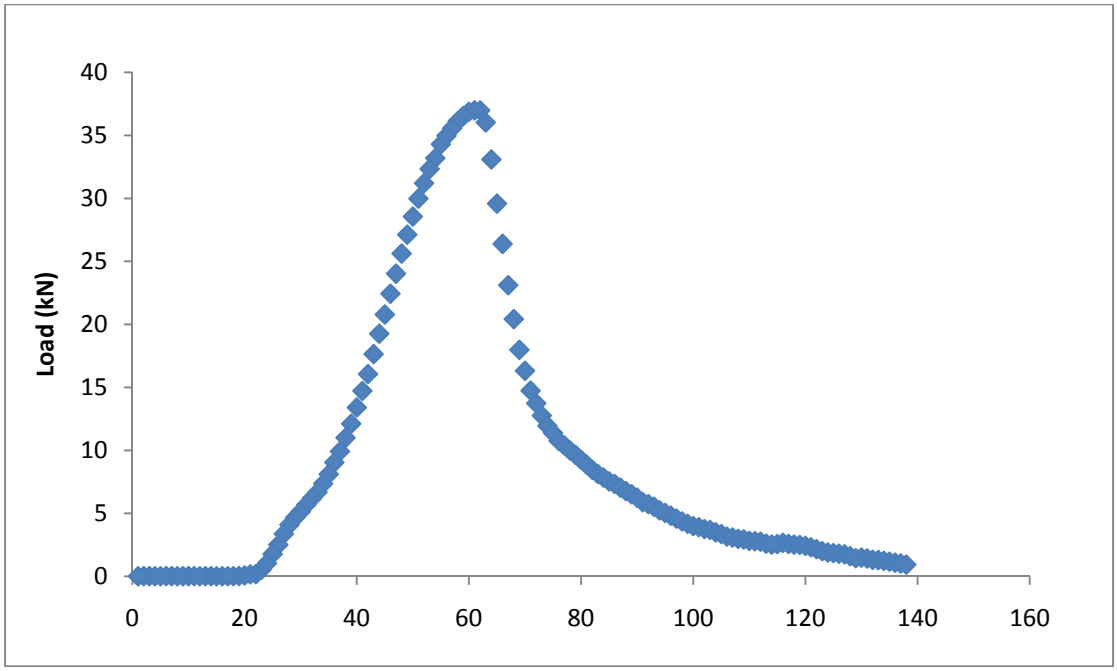

Figure C.26 6070D Strength Curve

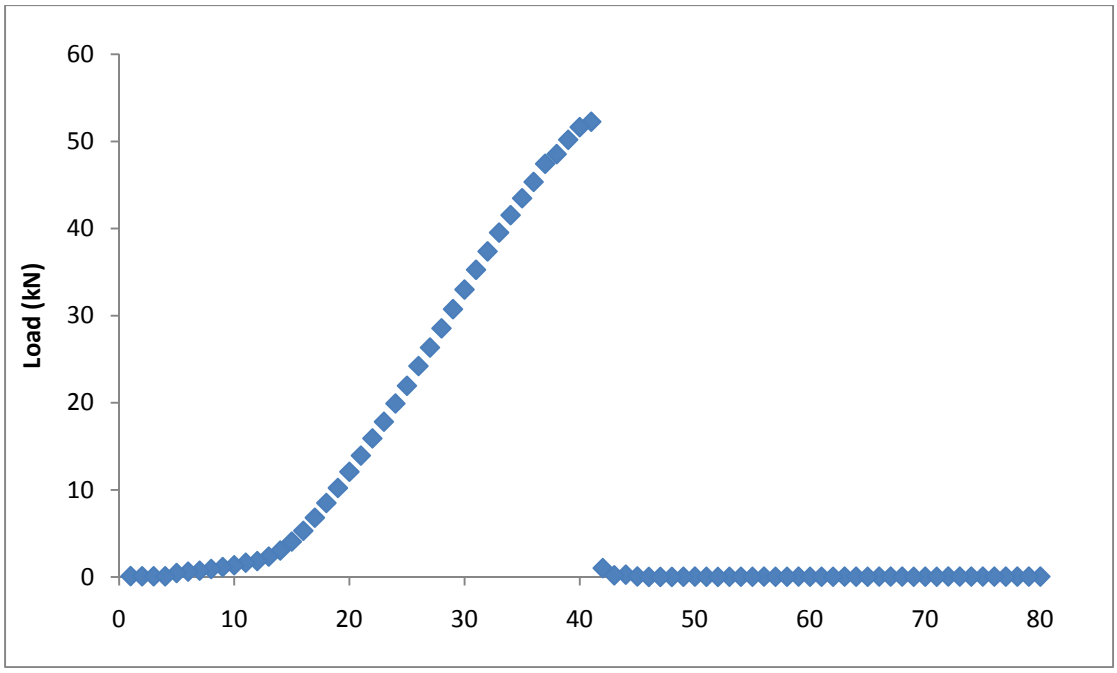

Figure C.27 6076A Strength Curve

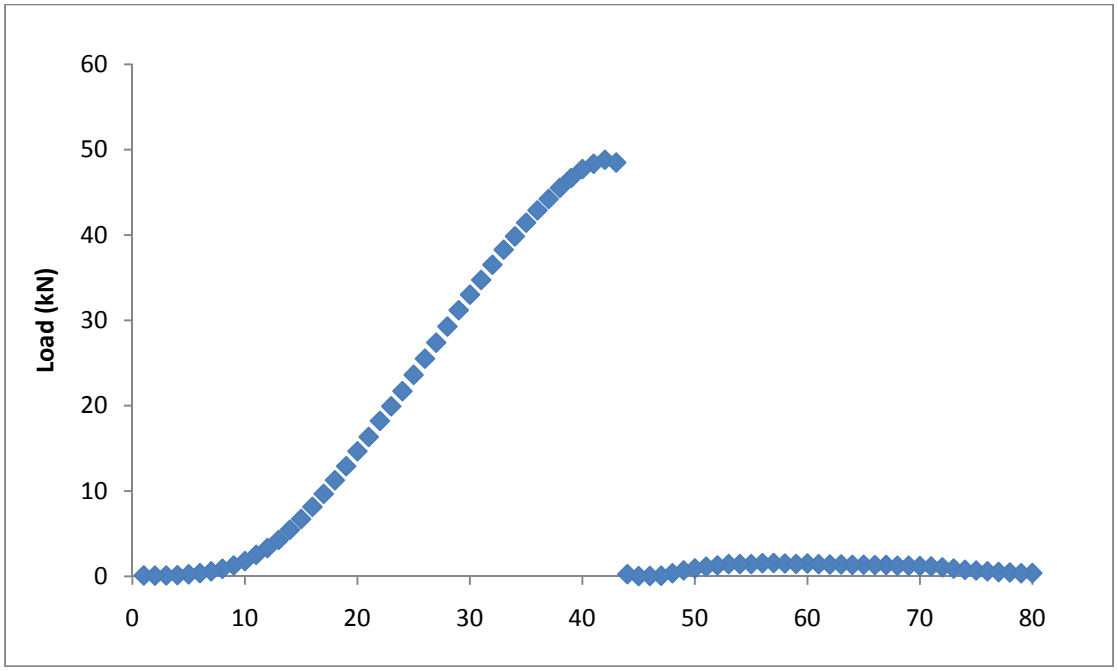

Figure C.28 6076B Strength Curve

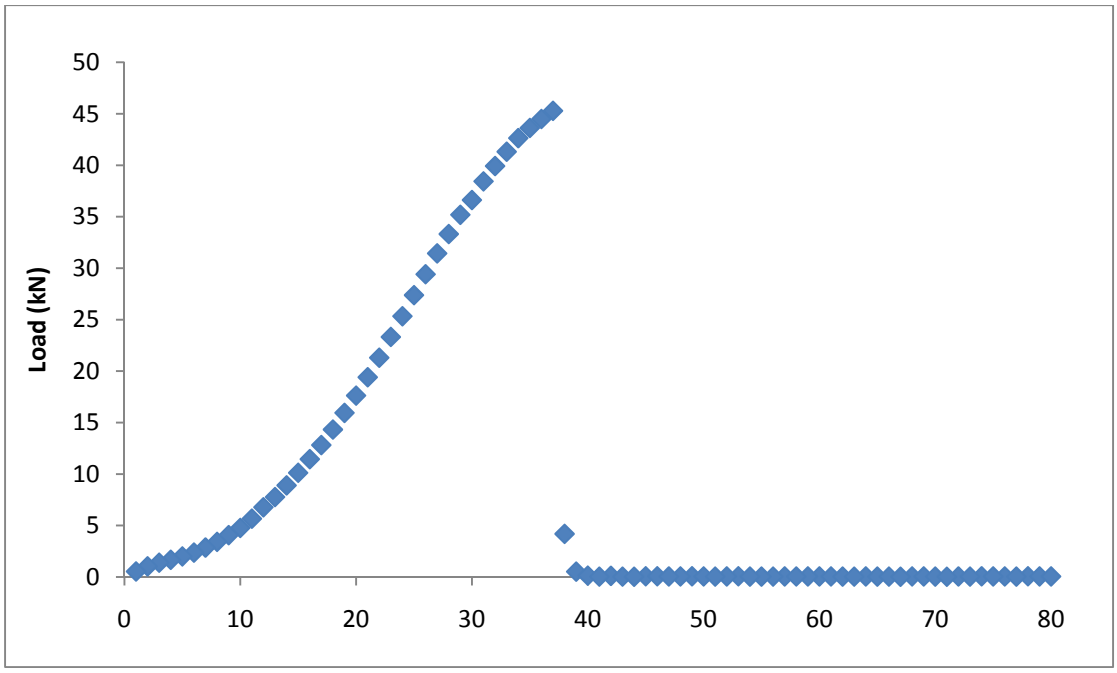

Figure C.29 6076C Strength Curve

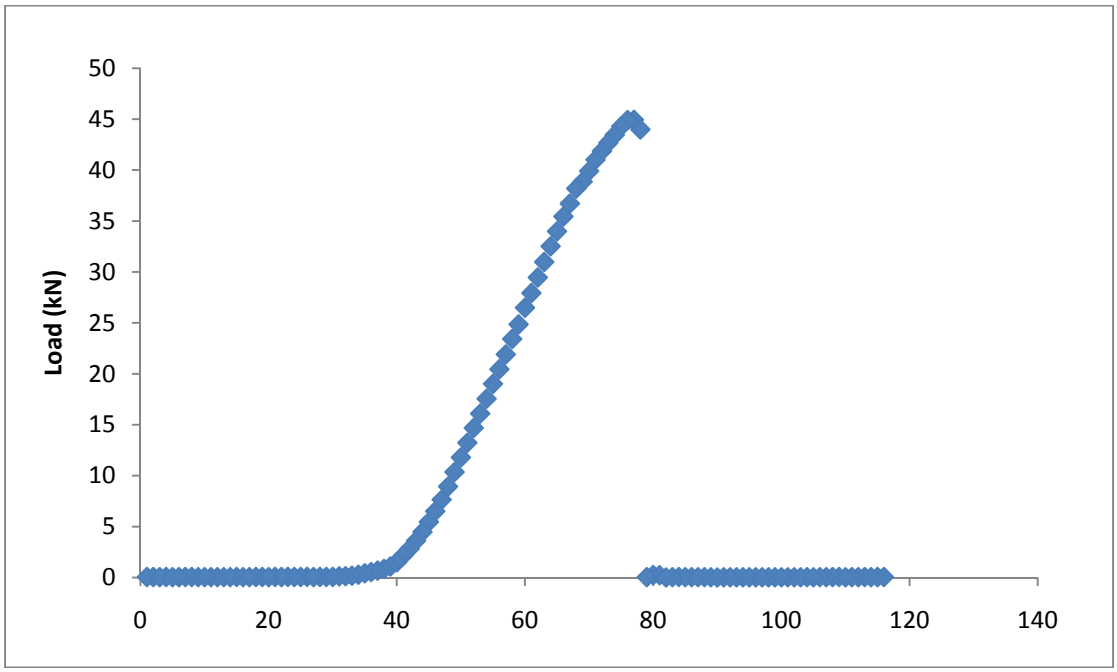

Figure C.30 6706D Strength Curve